USGS
science for a changing world

Prepared in cooperation with the Upper Colorado River Endangered Fish Recovery Program, Bureau of Reclamation, U.S. Fish and Wildlife Service, Argonne National Laboratory, Western Area Power Administration, and Wyoming State Engineer's Office

Application of Sediment Characteristics and Transport Conditions to Resource Management in Selected Main-Stem Reaches of the Upper Colorado River, Colorado and Utah, 1965–2007

Scientific Investigations Report 2012–5195

U.S. Department of the Interior
U.S. Geological Survey

Application of Sediment Characteristics and Transport Conditions to Resource Management in Selected Main-Stem Reaches of the Upper Colorado River, Colorado and Utah, 1965–2007

By Cory A. Williams, Keelin R. Schaffrath, John G. Elliott, and Rodney J. Richards

Prepared in cooperation with the Upper Colorado River Endangered Fish Recovery Program, Bureau of Reclamation, U.S. Fish and Wildlife Service, Argonne National Laboratory, Western Area Power Administration, and Wyoming State Engineer's Office

Scientific Investigations Report 2012–5195

U.S. Department of the Interior
U.S. Geological Survey

U.S. Department of the Interior
KEN SALAZAR, Secretary

U.S. Geological Survey
Marcia K. McNutt, Director

U.S. Geological Survey, Reston, Virginia: 2013

For more information on the USGS—the Federal source for science about the Earth, its natural and living resources, natural hazards, and the environment, visit http://www.usgs.gov or call 1–888–ASK–USGS.

For an overview of USGS information products, including maps, imagery, and publications, visit http://www.usgs.gov/pubprod

To order this and other USGS information products, visit http://store.usgs.gov

Any use of trade, firm, or product names is for descriptive purposes only and does not imply endorsement by the U.S. Government.

Although this information product, for the most part, is in the public domain, it also may contain copyrighted materials as noted in the text. Permission to reproduce copyrighted items must be secured from the copyright owner.

Suggested citation:
Williams, C.A., Schaffrath, K.R., Elliott, J.G., and Richards, R.J., 2013, Application of sediment characteristics and transport conditions to resource management in selected main-stem reaches of the Upper Colorado River, Colorado and Utah, 1965–2007: U.S. Geological Survey Scientific Investigations Report 2012–5195, 82 p.

Contents

Figures

Tables

Conversion Factors

Inch/Pound to SI

Multiply	By	To obtain
	Length	
inch (in.)	2.54	centimeter (cm)
inch (in.)	25.4	millimeter (mm)
foot (ft)	0.3048	meter (m)
mile (mi)	1.609	kilometer (km)
	Area	
square foot (ft^2)	929.0	square centimeter (cm^2)
square foot (ft^2)	0.09290	square meter (m^2)
square mile (mi^2)	259.0	hectare (ha)
square mile (mi^2)	2.590	square kilometer (km^2)
	Flow rate	
cubic foot per second (ft^3/s)	0.02832	cubic meter per second (m^3/s)
	Mass	
ton per day (ton/d)	0.9072	metric ton per day
ton per day (ton/d)	0.9072	megagram per day (Mg/d)
	Pressure	
pound per square foot (lb/ft^2)	0.04788	kilopascal (kPa)
	Density	
pound per cubic foot (lb/ft^3)	16.02	kilogram per cubic meter (kg/m^3)
pound per cubic foot (lb/ft^3)	0.01602	gram per cubic centimeter (g/cm^3)

SI to Inch/Pound

Multiply	By	To obtain
	Length	
millimeter (mm)	0.03937	inch (in.)
meter (m)	3.281	foot (ft)
	Flow rate	
meter per second (m/s)	3.281	foot per second (ft/s)
	Density	
kilogram per cubic meter (kg/m^3)	0.06242	pound per cubic foot (lb/ft^3)

Temperature in degrees Celsius (°C) may be converted to degrees Fahrenheit (°F) as follows:

$°F=(1.8\times°C)+32$

Vertical coordinate information is referenced to the North American Vertical Datum of 1988 (NAVD 88).

Horizontal coordinate information is referenced to the North American Datum of 1983 (NAD 83).

Concentrations of chemical constituents in water are given in milligrams per liter (mg/L).

A water year is the 12-month period from October 1 for any given year through September 30 of the following year. The water year is designated by the calendar year in which it ends and which includes 9 of the 12 months. Thus, the year ending September 30, 2011, is called the "2011" water year.

Abbreviations used in this report:

ADCP	Acoustic Doppler Current Profiler
ANCOVA	ANalysis of COVAriance
d_{50}	median sediment-particle size
ERV	estimated residual variance
GPS	global positioning system
ln	natural logarithm
MD_SWMS	Multi-Dimensional Surface-Water Modeling System
MLE	maximum likelihood estimation
MVUE	minimum variance unbiased estimate
NWIS	National Water Information System
R^2	coefficient of determination
RM	river mile(s)
RMSE	root mean square error(s)
RTK	Real-Time Kinematic
TIN	Triangular Irregular Network
USGS	U.S. Geological Survey
UTM	Universal Transverse Mercator
WY	water year

Application of Sediment Characteristics and Transport Conditions to Resource Management in Selected Main-Stem Reaches of the Upper Colorado River, Colorado and Utah, 1965–2007

By Cory A. Williams, Keelin R. Schaffrath, John G. Elliott, and Rodney J. Richards

Abstract

The Colorado River Basin provides habitat for 14 native fish, including 4 endangered species protected under the Federal Endangered Species Act of 1973. These endangered fish species once thrived in the Colorado River system, but water-resource development, including the building of numerous diversion dams and several large reservoirs, and the introduction of non-native fish, resulted in large reductions in the numbers and range of the four species through loss of habitat and stream function. Understanding how stream conditions and habitat change in response to alterations in streamflow is important for water administrators and wildlife managers and can be determined from an understanding of sediment transport. Characterization of the processes that are controlling sediment transport is an important first step in identifying flow regimes needed for restored channel morphology and the sustained recovery of endangered fishes within these river systems. The U.S. Geological Survey, in cooperation with the Upper Colorado River Endangered Fish Recovery Program, Bureau of Reclamation, U.S. Fish and Wildlife Service, Argonne National Laboratory, Western Area Power Administration, and Wyoming State Engineer's Office, began a study in 2004 to characterize sediment transport at selected locations on the Colorado, Gunnison, and Green Rivers to begin addressing gaps in existing datasets and conceptual models of the river systems.

This report identifies and characterizes the relation between streamflow (magnitude and timing) and sediment transport and presents the findings through discussions of (1) suspended-sediment transport, (2) incipient motion of streambed material, and (3) a case study of sediment-transport conditions for a reach of the Green River identified as a razorback sucker spawning habitat.

Suspended-sediment transport can be a large part of the total-sediment flux within the rivers of this study and as such is strongly related to the geomorphology and habitat conditions found in these reaches. Suspended-sediment transport affects the channel form, bank and bar development, and the availability and quality of habitat for multiple life-stages of aquatic species. Regression analysis was used in this report to estimate suspended-sediment transport as a function of streamflow, seasonality, and temporal trends. Estimates of suspended-sediment (SS) flux can be helpful in determining total flux of sediments within the river at a station or to evaluate sediment budgets between stations. Understanding the processes that explain the variability of SS concentration also can provide information needed to better manage water resources within these rivers (related to the timing and magnitude of flow releases and withdrawal from reservoirs and diversion structures) and to evaluate temporal and spatial changes at a station and within river reaches.

Suspended-sediment transport equations using regression analysis were generated for the six stations that had sufficient data within the study area: three stations on the main-stem Colorado River between Cameo, Colorado, and the confluence with the Green River; one station on the Gunnison River downstream from the Aspinall Storage Unit; and two stations on the Green River below Flaming Gorge Reservoir, and downstream from the confluence of the Yampa River. Interpretations of the variables used within the regression analysis aid in identification and quantification of the processes or mechanisms that are important controls on suspended-sediment transport within the system and to provide information on the timing of sediment inputs (supply changes) to the system.

Regression analysis of the suspended-sediment data show that streamflow explains much of the variability in SS concentration at all stations and shows that increases in streamflow increase SS concentrations. Additional significant relations are characterized for SS concentration and SS flux that result from seasonality (time of year), temporal trends (time across multiple years), and climatic effect (wet and dry years). Changes in the streamflow and SS concentration relation based on time of year (hysteresis) demonstrate that for a specific streamflow there can be multiple predicted SS concentrations.

Incipient motion of streambed material (often occurring as bed-load transport) and the sorting of bed materials are important controls on channel form and habitat and are strongly related to the channel morphology and habitat conditions within these rivers. Comparison between boundary shear stresses of multiple streamflows and the relative mobility of bed material (median sediment-particle sizes) characterizes the effects of flow magnitude on mobilization of framework grain within the streambed. Observations at multiple cross sections within two reaches of the Gunnison River near Grand Junction downstream from the Aspinall Storage Unit show that peak streamflow conditions up to 14,000 cubic feet per second (ft^3/s) (recurrence interval of 5 to 10 years) produce ineffectual mobilization of most, if not all, areas within the surveyed cross sections. Observations at multiple cross sections within a study reach of the Green River downstream from Flaming Gorge Reservoir show peak streamflows of as much as 19,000 ft^3/s (recurrence interval of 2.3 to 5 years) produce ineffectual mobilization of most, if not all, areas within the surveyed cross sections of the larger bed material. However, when the sand veneer is present at these cross sections, or where the portion of sand within the bed material exceeds 20–30 percent of the total, mobilization of the bed material will occur at most locations within the surveyed cross sections for peak streamflows of 9,000–19,000 ft^3/s (recurrence intervals ranging from 1 to 5 years) with mobilization of gravels possible in some areas.

Application of the two-dimensional stream hydraulics and sediment-transport models provides enhanced capabilities for evaluations of dynamic reach-scale processes that affect habitat suitability. Understanding the processes that affect the sediment-transport characteristics, which are important to the maintenance of endangered fish spawning habitat, can be used to inform the flow-recommendations process that currently (2012) guides water management of Flaming Gorge Reservoir.

Evaluations of the processes controlling sediment deposition on the spawning habitat near a mid-channel bar are not limited to stream-transport conditions within the spawning-habitat reach. Considerations of sediment availability and net changes in sediment transport between upstream reaches and the spawning habitat are important. Sands are mobile throughout the main channel for all modeled streamflows (9,000–19,000 ft^3/s), but in areas upstream from the mid-channel bar (and spawning habitat) increases in streamflow tend to increase transport rates. Within the spawning habitat, increases in streamflow result in decreases in water-surface slope and varied responses to boundary shear stress. At larger streamflows (14,100–17,700 ft^3/s), sediment upstream from the mid-channel bar is transported in greater amounts and likely at greater rates than can be transported by the conditions at the spawning-habitat reach. This may exceed a threshold between the two areas resulting in a disequilibrium and net deposition of sands on the spawning habitat at higher streamflows (14,100–17,700 ft^3/s). Spawning habitat may be less suitable at these higher streamflows owing to deposition of sands on the spawning habitat under these conditions.

Introduction

The Colorado River Basin provides habitat for 14 native fish, including 4 endangered species protected under the Federal Endangered Species Act of 1973—Colorado pikeminnow (*Ptychocheilus lucius*), razorback sucker (*Xyrauchen texanus*), bonytail (*Gila elegans*), and humpback chub (*Gila cypha*) (U.S. Fish and Wildlife Service, 2011a). In 1988, the Upper Colorado River Endangered Fish Recovery Program (hereafter Recovery Program) began conducting research and taking action to improve river habitat for these species (U.S. Fish and Wildlife Service, 2011a). The Recovery Program is a joint effort of the U.S. Fish and Wildlife Service; Bureau of Reclamation; Western Area Power Administration; States of Colorado, Utah, and Wyoming; Upper Basin water users; environmental organizations; the Colorado River Energy Distributors Association; and the National Park Service. These endangered fish species once thrived in the Colorado River system, but water-resource development, including the building of numerous diversion dams and several large reservoirs, and the introduction of non-native fish, resulted in large reductions in the numbers and range of the four species through loss of habitat and stream function (Valdez and Muth, 2005; U.S. Fish and Wildlife Service, 2011a).

Understanding how stream conditions and habitat change in response to alterations in streamflow is important for water administrators and wildlife managers and can be determined from an understanding of sediment transport. Coordinated releases from reservoirs within the Upper Colorado River Basin have been implemented to recreate more natural streamflow patterns to restore channel functions in the system and assist recovery efforts (U.S. Fish and Wildlife Service, 2011b). These more natural streamflows provide larger peaks during the snowmelt-runoff period and provide additional base flow during late summer in dry years. These streamflows are more similar to pre-water-development conditions, but a thorough understanding of the effects of these streamflows on geomorphic processes (such as sediment supply and transport) and habitat response has yet to be gained.

Evaluation of endangered fishes habitats requires an understanding of the physical connection between streamflow and sediment-transport conditions. Characterization of the processes that are controlling sediment transport is an important first step in identifying flow regimes needed for restored channel morphology and the sustained recovery of endangered fishes within these river systems. Determination of the sediment-transport characteristics within selected reaches of the Upper Colorado River Basin has been underway since the 1990's (Elliott and Anders, 2005; Williams and others, 2009). The effects of peak- and base-flow variability (magnitude and duration) on sediment deposition, erosion, and antecedent conditions (such as quantity and availability of habitat) need further study. The U.S. Geological Survey (USGS), in cooperation with the Upper Colorado River Endangered Fish Recovery Program, Bureau of Reclamation, U.S. Fish and Wildlife Service, Argonne National Laboratory, Western Area

Power Administation, and Wyoming State Engineer's Office, began a study in 2004 to characterize sediment transport at selected locations on the Colorado, Gunnison, and Green Rivers to begin addressing gaps in existing datasets and conceptual models of the river systems.

The purpose of this report is to characterize the magnitude, timing, and size distribution of sediment transport at selected locations on the Colorado, Gunnison, and Green Rivers in order to aid the Recovery Program in the evaluation of the effects of streamflow and sediment transport on critical habitat for the endangered fishes. Evaluation of the dynamics of sediment movement in representative locations was done to aid understanding of the relation between streamflow and sediment transport throughout the critical habitat reaches. This report identifies and characterizes the relation between streamflow (magnitude and timing) and sediment transport and presents the findings through discussions of (1) suspended-sediment transport, (2) incipient motion of streambed material, and (3) a case study of sediment-transport conditions for a reach of the Green River identified as a razorback sucker spawning habitat.

Description of Study Areas

Streamflow and sediment transport were characterized at selected streamflow-gaging stations from three main-stem reaches: (1) the Colorado River downstream from Cameo, Colorado, to the confluence with the Green River; (2) the lower Gunnison River downstream from the confluence with the North Fork of the Gunnison River to the confluence with the Colorado River near Grand Junction, Colorado; and (3) the Green River downstream from the confluence with the Yampa River to the confluence with the Colorado River, 60 mi south of Green River, Utah (fig. 1). The climate in the study area varies spatially and with elevation (Apodaca and others, 1996). Common to the mountainous Western United States, the annual hydrographs of the main-stem rivers are dominated by snowmelt runoff, which usually begins in late April and peaks in late May or early June. Late-summer rain events cause localized flooding in tributaries and may increase main-stem streamflow by 10–20 percent (Pitlick and others, 1999).

Upper Colorado River Basin

The Upper Colorado River Basin includes 25,910 mi^2 of drainage upstream from the confluence with the Green River (Seaber and others, 1987). In general, streams and rivers in the headwaters of the Colorado River are characterized by lower sediment and cooler temperatures than areas in reaches associated with outcrops of sedimentary rock located in the downstream parts of the basin (Apodaca and others, 1996). Precipitation ranges from 40 in. or more at higher elevations in the basin to less than 10 in. per year at lower elevations (PRISM Climate Group, 2008).

The Gunnison and Dolores Rivers are the largest tributaries to the Upper Colorado River within the study area (fig. 2). The Gunnison River contributes more than 40 percent of the annual streamflow leaving Colorado [based on a comparison of annual streamflow record totals for 09152500, Gunnison River near Grand Junction, Colorado, period of record 1897–2007; and 09163500, Colorado River near Colorado–Utah State line, period of record 1951–2007 (U.S. Geological Survey, 2007)]. The Dolores River contributes 6 percent of the total streamflow of the Colorado River near Cisco, Utah [based on a comparison of annual streamflow record totals for 09180500, Colorado River near Cisco, Utah, period of record 1914–2007; and 09180000, Dolores River near Cisco, Utah, period of record 1950–2007 (U.S. Geological Survey, 2007)].

Various geologic formations are drained by the Upper Colorado River Basin. The Gunnison River and its tributaries drain alpine areas composed of crystalline metamorphic and igneous rocks of Tertiary and Precambrian age (Schruben and others, 1974). Commonly, the small tributaries in the Gunnison River below the Aspinall Storage Unit are seasonal streams driven by snowmelt and intense rain events. The nature of the geology in these areas and the intensity of the rain events allows for sediments to be transported into the Gunnison River (Apodaca and others, 1996; Williams and others, 2009).

The Dolores River drains much of southwestern Colorado, originating in the San Juan Mountains and flowing west-northwest. Various geological formations are found in the Dolores River Basin, most are Cretaceous sandstones and shale (Schruben and others, 1974), which are prone to erosion. Salt domes also are common along the Dolores River affecting water quality downstream. The Dolores River Basin also has many ephemeral streams that primarily are active during intense rain events. Intense rain events mobilize sand, silt, and gravel, which accumulates in the dry streambeds and empties into the Dolores River.

The underlying geology in the region can influence the water quality. The bedrock in the region is made up of crystalline and sedimentary rock. Alluvium consisting of stream, landslide, terrace, and glacial deposits is present in valleys throughout the basin (Apodaca and others, 1996). Mining was a historically significant land use in the upper reaches of the Upper Colorado River Basin. Receiving water bodies have been affected by point-source mine discharge and nonpoint-source runoff from mined areas. High concentrations of some materials, particularly salts derived from sedimentary rocks, are more common in the western part of the basin.

The water in the Upper Colorado River Basin is used for irrigation (Osmundson and others, 1995), but transmountain diversions (located near the headwaters) also provide water to municipalities along the eastern part of Colorado (Apodaca and others, 1996). Streamflows in the reach of the Colorado River from Cameo, Colorado, to the confluence with the Gunnison River are greatly reduced during the irrigation season (April–October) owing to local irrigation systems that have been in place since the early 1900s. Withdrawals by these

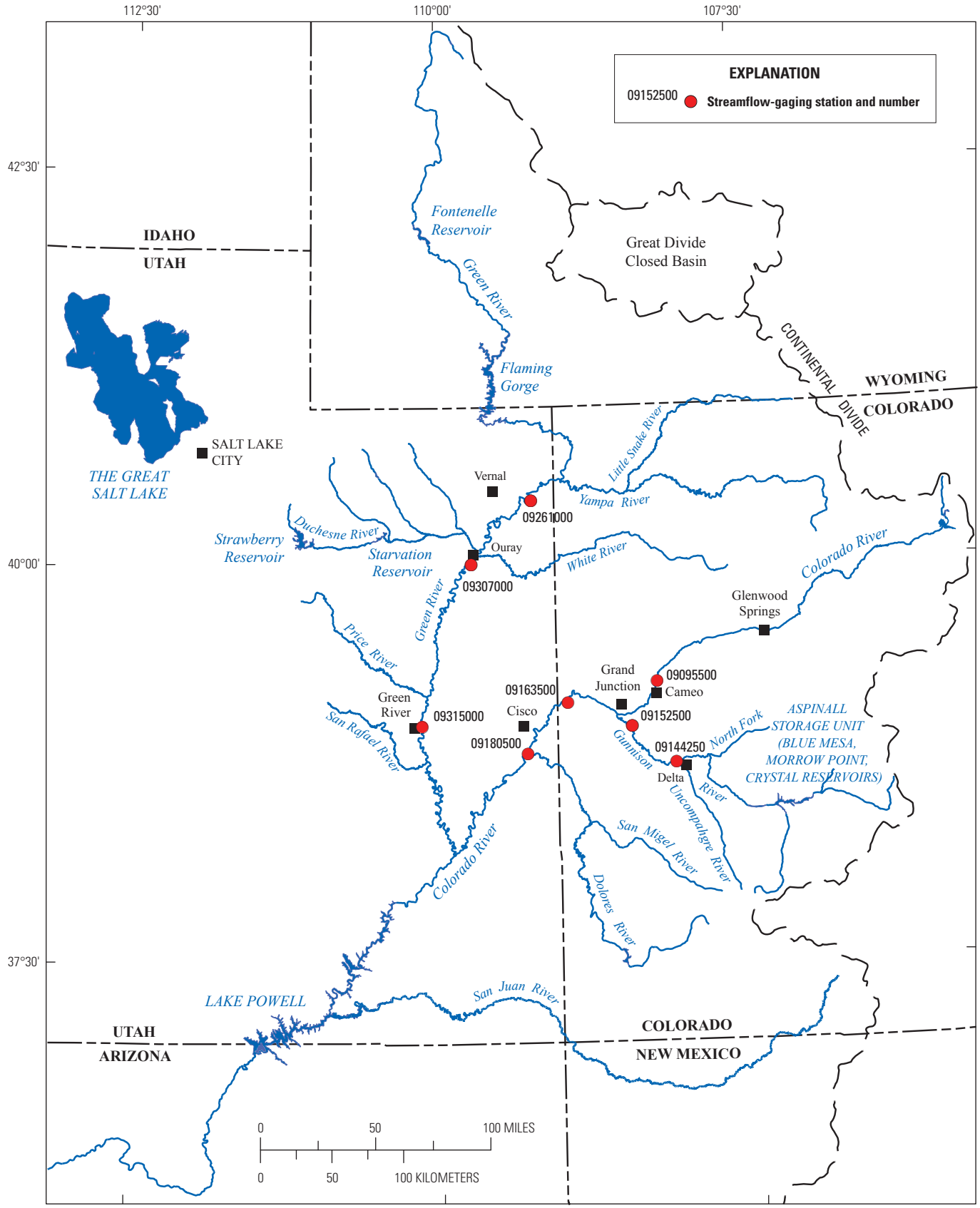

Base from U.S. Geological Survey National Atlas
Universal Transverse Mercator North American Datum 1983, Zone 12 North

Figure 1. Map showing selected U.S. Geological Survey streamflow-gaging station locations in the Upper Colorado River Basin.

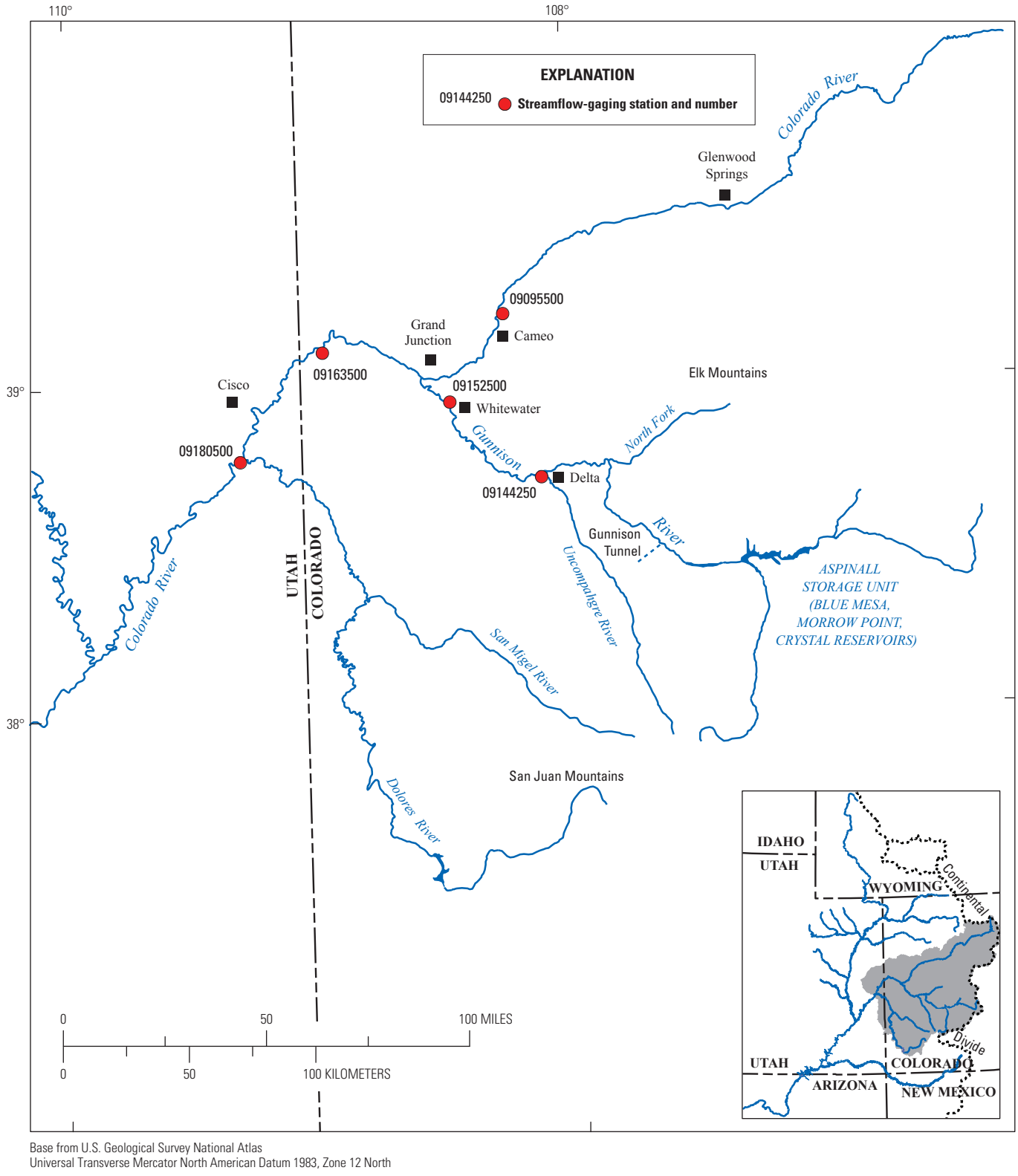

Base from U.S. Geological Survey National Atlas
Universal Transverse Mercator North American Datum 1983, Zone 12 North

Figure 2. Map showing selected U.S. Geological Survey streamflow-gaging station locations in the Upper Colorado and Gunnison River Basins.

systems are approximately 1,200–1,600 ft^3/s depending on the month (Osmundson and others, 1995). Streamflows in this part of the reach are further diminished, especially during the spring runoff period, by large dams and transmountain diversions that were built in the headwaters (upstream from Cameo) beginning in the mid-1930s (Osmundson and others, 1995).

The USGS operates three streamflow-gaging stations on the main stem of the Colorado River (U.S. Geological Survey, 2007) within the study area where suspended-sediment data are collected (fig. 2). Streamflow is recorded at streamflow-gaging station 09095500, Colorado River near Cameo, Colorado. The gage is located on the left bank 7 mi northeast of Cameo. The drainage area at the gaging station is approximately 8,050 mi^2, and the period of streamflow record and sediment data used for this study were from 1982 to 1998 (table 1).

Streamflow is recorded at streamflow-gaging station 09163500, Colorado River near the Colorado–Utah State line. The gage is located on the right bank 1.7 mi upstream from the Colorado–Utah State line. The drainage area at the gaging station is approximately 17,843 mi^2, and the period of streamflow record and sediment data used for this study were from 1976 to 2007 (table 1).

Streamflow is recorded at streamflow-gaging station 09180500, Colorado River near Cisco, Utah. The gage is located on the left bank 1 mi downstream from the Dolores River, and 11 mi south of Cisco. The drainage area at the gaging station is approximately 24,100 mi^2, and the period of streamflow record and sediment data used for this study were from 1985 to 2000 (table 1).

Gunnison River Basin

The Gunnison River originates in south-central Colorado and drains approximately 8,000 mi^2 at its confluence with the Colorado River at Grand Junction, Colorado (Elliott and Hammack, 1999). The upper Gunnison River drains areas west of the Continental Divide and flows into the Wayne Aspinall Unit of the Colorado River Storage Project (Aspinall Unit), which consists of three large reservoirs (Blue Mesa, Morrow Point, and Crystal Reservoirs) (figs. 1 and 2). The Aspinall Unit has a storage capacity of about 52 percent of the average annual streamflow of the Gunnison River (Elliott and Hammack, 1999). The lower Gunnison River begins downstream from Crystal Reservoir and continues flowing west through the town of Delta to the confluence with the Colorado River near Grand Junction, Colorado. Annual precipitation rates are a mixture of alpine and arid climates with annual totals ranging from 9 to 50 in. annually (PRISM Climate Group, 2008). Forest and herbaceous grasslands are the most abundant land cover in the alpine areas, with forest and shrublands most abundant in the high-desert landscapes; lesser areas of barren land lie along mountain peaks, and agricultural and urban areas are primarily located along the valley bottoms (National Atlas, 2010).

Tributaries in the Gunnison River Basin drain alpine areas predominately composed of igneous rocks of Tertiary age and metamorphic rocks of Precambrian age (Schruben and others, 1974). Tributaries in the Gunnison River Basin below the confluence with the North Fork drain arid areas

Table 1. Summary of streamflow and sediment data used in this study (calendar years) for selected U.S. Geological Survey streamflow-gaging stations in the Upper Colorado River Basin.

[--, no data]

Station identification number	Abbreviation used in this report	Streamflow and sediment data used in regression analysis
	Colorado River	
09095500	CAMEO	1982–98
09163500	STATELINE	1976–2007
09180500	CISCO	1967–2000
	Gunnison River	
09144250	DELTA	--
09152500	GUNNISON	1976–2007
	Green River	
09261000	JENSEN	1965–2007
09307000	OURAY[1]	--
09315000	GREEN	1965–2000

[1]Sediment and streamflow data do not adequately characterize the conditions of the stream in the time period following completion and operation of Flaming Gorge Reservoir.

predominantly composed of sedimentary rocks of Cretaceous and Jurassic age. Differences in lithology contribute to the width and slope of the river valleys; erosion-resistant crystalline rocks produce steeper, narrower canyons, and more erosive sedimentary rocks produce wider, lower-gradient reaches (for example, the Uncompahgre River valley). These differences also can affect sediment transport and storage and the relative thickness of alluvium in and around the river channel.

Large tributaries to the Gunnison River Basin below the Aspinall Storage Unit are the Uncompahgre River and the North Fork of the Gunnison River. The Uncompahgre River originates in the San Juan Mountains to the south of Delta, Colorado, and flows northwest until converging with the Gunnison River in Delta, Colorado. The Uncompahgre River flows through large agricultural-use areas and is the water source for irrigated land along the Uncompahgre River (Butler and others, 1996). Additional water is diverted from the Gunnison River into the Uncompahgre through the Gunnison Tunnel (Butler and others, 1996) (fig. 2). The North Fork of the Gunnison River originates in the Elk Mountains and flows west until converging with the main stem of the Gunnison River near Delta, Colorado. The North Fork is used for municipal and agricultural use for numerous small communities before converging with the Gunnison River. The Mancos Shale is the dominant geologic formation located in the agricultural valleys (Butler and Leib, 2002). Mancos Shale weathers into various clays, which are easily transported in fluvial systems. Depending on the season, irrigation-return waters passing over unvegetated areas within agricultural fields can increase suspended-sediment (SS) concentration and turbidity of the river owing to the high erosivity of these landscapes (Apodaca and others, 1996; Butler and Leib, 2002).

With the exception of occasional monsoonal-rain events, infrequent fall-snowmelt events, and irrigation-return flows, base flow from the surrounding highlands in the lower Gunnison River contributes little streamflow to the main stem of the Gunnison River (Butler and Leib, 2002). Since completion of the Aspinall Storage Unit (1967), changes in the timing and volume of streamflow have been observed in the Gunnison River. Peak streamflows during April–July are attenuated, and low flows during August–March have increased; however, mean annual streamflow has decreased only slightly (Kuhn and Williams, 2004).

The USGS operates two streamflow-gaging stations on the main stem of the Gunnison River (U.S. Geological Survey, 2007) downstream from the Aspinall Storage Unit in the study area (fig. 2). Streamflow is recorded at streamflow-gaging station 09144250, Gunnison River at Delta, Colorado. The gage is located on the left bank 0.7 mi downstream from the north edge of Delta, Colorado. The drainage area at the gaging station is approximately 5,628 mi^2, and the period of streamflow record used for this study were from 1976 to 2007. Suspended-sediment samples were not collected at this station (table 1).

Streamflow is recorded at streamflow-gaging station 09152500, Gunnison River near Grand Junction, Colorado. The gage is located on the right bank 0.5 mi south of Whitewater. The drainage area at the gaging station is approximately 7,928 mi^2, and the period of streamflow record and sediment data used in this study were from 1976 to 2007 (table 1).

Green River Basin

The Green River transports runoff from more than 44,200 mi^2 of contributing areas in Wyoming, Colorado, and Utah (not including the Great Divide Closed Basin) (fig. 1). It is the largest tributary in the Upper Colorado River Basin (Seaber and others, 1987). The Green River drains areas west of the Continental Divide in Wyoming, flowing first into Fontenelle Reservoir and then Flaming Gorge Reservoir near the Wyoming–Utah State line (fig. 1). The Green River flows east into Colorado before it continues back into Utah toward the town of Vernal. The Green River then flows south to Green River, Utah, and the confluence with the Colorado River (fig. 3).

The major tributaries are the Yampa River, Duchesne River, White River, Price River, and San Rafael River (fig. 3). The upper basin tributaries of the watershed generally drain snowmelt from the igneous and metamorphic lithologies of several mountain ranges, whereas the lower basin tributaries generally drain more arid regions of sedimentary lithologies (Schruben and others, 1974). Sediment sources tend to correlate with lithology and precipitation patterns, and a large amount of the annual sediment load is supplied to the Green River from the Little Snake River, by way of the Yampa River (Andrews, 1978, 1986). The Little Snake River, Yampa River, and parts of the Green River near Vernal, Utah, flow through a succession of wide, parklike reaches and narrow, steep canyons. Steep, confined canyon reaches may function as sediment-conveying zones during floods, whereas broad, park-like reaches with low gradients may be associated with depositional environments during the same floods (Elliott and Anders, 2005).

Streamflow in the Green River has been regulated by Flaming Gorge Reservoir since 1962 (Andrews, 1986). Flaming Gorge Reservoir, completed in 1964, has had a significant effect on streamflow, sediment transport, and the geomorphology of the Green River downstream from the dam (Andrews, 1986). The Green River near Jensen gage has operated since 1947, and streamflow characteristics from that gage reflect alterations in streamflow as a result of reservoir operation. Andrews (1986) used streamflow data recorded at this station from 1963 through 1981 in his analyses of downstream reservoir effects on the Green River. Annual peak streamflows and flow-duration curves for the Green River near Jensen gage, updated through water year (WY, a water year is the 12-month period from October 1 for any given year through September 30 of the following year. The water year is designated by the calendar year in which it ends and which includes 9 of the 12 months. Thus, the year ending September 30, 2011, is called the "2011" water year) 2002, reveal the changes in streamflow caused by Flaming Gorge Reservoir (Elliott and Anders, 2005). Regulation by the reservoir has altered the magnitude and

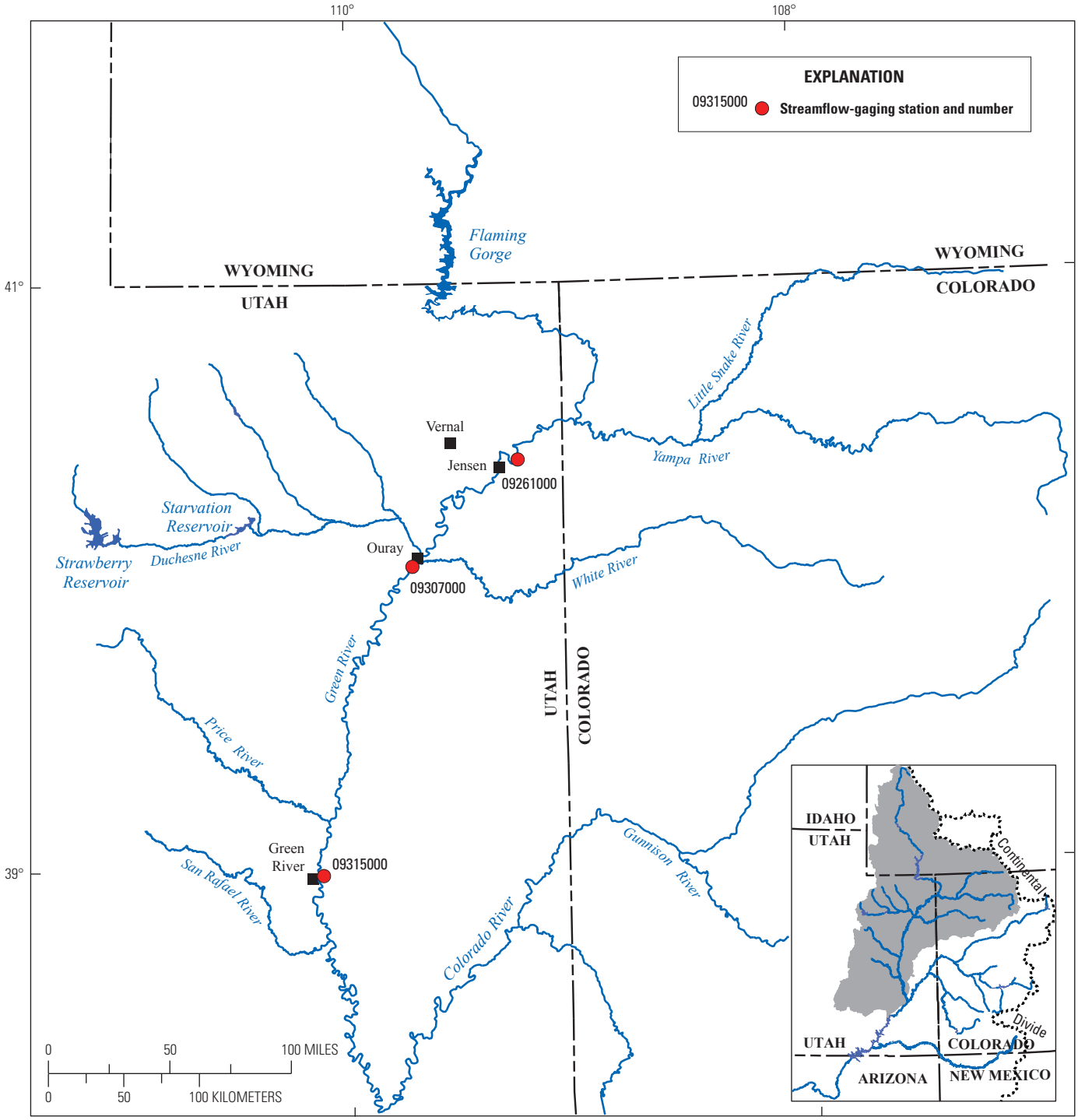

Base from U.S. Geological Survey National Atlas
Universal Transverse Mercator North American Datum 1983, Zone 12 North

Figure 3. Map showing selected U.S. Geological Survey streamflow-gaging station locations in the Green River Basin.

timing of the instantaneous peak streamflow in the Green River downstream from the reservoir, but not the annual volume of runoff (Andrews, 1986; Elliott and Anders, 2005). Streamflow regulation also has had a significant effect on sediment transport and the geomorphology of the Green River downstream from Flaming Gorge (Andrews, 1986; Elliot and Anders, 2005). Mean annual sediment load at the gage near Jensen, Utah, is estimated to have decreased by 54 percent relative to sediment load prior to the construction of the dam (Andrews, 1986). Similarly, the mean annual sediment load at the gage near Green River, Utah, decreased by 48 percent following the completion of the dam (Andrews, 1986).

Streamflow and sediment transport in the Little Snake and Yampa Rivers have been affected only slightly by water storage and transmountain diversions within the respective watersheds (Elliott and Anders, 2005), and no major dams have been constructed on the main stems of these rivers.

The USGS operates three streamflow-gaging stations on the main stem of the Green River within the study area (U.S. Geological Survey, 2007) where suspended-sediment data are collected (fig. 3). Streamflow is recorded at streamflow-gaging station 09261000, Green River near Jensen, Utah. The gage is located 6.5 mi northeast of Jensen, Utah. The drainage area at the gaging station is approximately 29,660 mi^2, and the period of streamflow record and sediment data used in this study were from 1965 to 2007 (table 1).

Streamflow was recorded at streamflow-gaging station 09307000, Green River near Ouray, Utah. The gage is located near Ouray, Utah. The drainage area at the gaging station is approximately 26,780 mi^2, and the period of streamflow record is 1947–55, 1956–66, and 2009–2012. Suspended-sediment samples were collected during the periods 1950–52 and 1958–66 but the streamflow and sediment data were not used in this study because the flow alterations related to Flaming Gorge Reservoir completion and operation in 1963 were not adequately characterized by the available data (table 1).

Streamflow was recorded at streamflow-gaging station 09315000, Green River at Green River, Utah. The gage is located on the right bank 0.9 mi southeast of Green River, Utah. The drainage area at the gaging station is approximately 44,850 mi^2, and the period of streamflow record and sediment data used in this study were from 1965 to 2000 (table 1).

Methods of Data Collection and Analysis

Topographical Surveying

Water-surface and streambed-elevation mapping was done to calculate hydrologic parameters at selected locations near three USGS streamflow-gaging stations: (1) Gunnison River at Delta, Colorado; (2) Gunnison River near Grand Junction, Colorado; and (3) Green River near Jensen, Utah (figs. 1–3). Water profiles were flagged at the three stations for various streamflow conditions covering the range of high-flow conditions and streamflow conditions typical of the rising- or falling-limb of the snowmelt-runoff hydrograph for WY 2005–8. Flagging of the water surface occurred under stable streamflow conditions when fluctuations of water-surface elevations were minimal. Multiple flagging expeditions were completed between topographical surveys to characterize streamflow conditions at each location during the near peak and falling-limb of the snowmelt-runoff hydrograph. Different colors of flagging were used to distinguish between the different water surfaces. Each water surface was flagged over an appropriate interval of 2 to 4 channel widths to ensure accurate characterization of the slope of the water surface within the reach. Where stream conditions and (or) vegetation density allowed for continuous surveys along one or both banks, flags were placed at regularly spaced intervals (5–10 ft). Under some streamflow conditions, greater spacing of flags (15– 20 ft) or the omission of some flagging locations was required to minimize the effects of changing water-surface elevations and because of bank accessibility and flagger safety.

Topographical surveying of the flagged water surfaces was done using survey-grade global positioning system (GPS) equipment, operated in a Real-Time Kinematic mode (RTK–GPS) (Trimble Navigation Limited, 1998), or total-station laser theodolite, to determine the elevation and coordinate locations of each flagged point. The RTK–GPS utilized a stationary GPS receiver (base station), positioned over a reference benchmark, and roving GPS receivers (rovers) operated by separate hand-held computers (data collectors). The RTK–GPS system calculates the locations of the rovers in real time, using the positions of orbiting NAVSTAR–GPS satellites and the known location of the base station. The total station was positioned over a reference benchmark, and the coordinate location of each of the surveyed points was determined on the basis of the relative positions from the benchmark.

Total-station methods involved surveying from a known instrument-base location and elevation to roving rod-mounted prisms placed on the ground and reference points of interest. The azimuth and distance from the instrument base to the prism was converted to local northing and easting coordinates. The ground-surface elevation was carried from the instrument base to the base of the prism rod by conventional surveying trigonometry. The completed northing, easting, and elevation data were subsequently rectified and converted to the Universal Transverse Mercator (UTM) coordinates of the RTK–GPS survey, such that data from both survey methods were compatible.

All surveyed elevations (RTK–GPS) then were exported to a personal computer for post-processing of the orthometric heights. The survey data were output to a spreadsheet program in metric Northing, Easting, and Elevation format using a UTM coordinate system (UTM, Zone 12 North). Horizontal coordinate information was referenced to the North American Datum of 1983 (NAD 83), and vertical coordinate information was referenced to the North American Vertical Datum of

1988 (NAVD 88). Elevation values were visually examined for relative accuracy by graphing and inspecting the cross section and by comparison of the elevation dataset between data-collection methods.

To determine streambed elevations, depth information at selected locations within the stream reaches was measured from a boat outfitted with a sounding reel, following standard USGS methods (Rantz and others, 1982). Cross-section locations were established within the surveyed reach perpendicular to the direction of flow. Each cross-section location was surveyed using RTK–GPS (and levels techniques) to register coordinate location and elevation. Depths along the cross section were referenced to the distance from one bank, and the elevations were determined by subtracting the depths at each location in the cross section from the established elevation at the junction of channel margin and the cross section.

Streambed-Sediment Characterization

Sediment characteristics were determined for the streambed and fluvial bars in the study reaches to characterize the range of sediment-particle sizes available for transport within the channel and typical of different geomorphic surfaces. Multiple sampling locations were selected within each reach to characterize specific features. Bars and channel margins (outside of areas strongly affected by eddies) were chosen to characterize the bed material of the channel. These areas are inundated most of the year and represent the coarser material within the river channel. Characterization of the bed material was done to determine the sediment-particle-size distribution and spatial extent of the bed materials within each reach.

Bed-material sediment-particle-size analysis was performed by volumetric- and areal-sampling methods at Gunnison River near Grand Junction, Colorado, and Green River near Jensen, Utah, during 2006–7 (Williams and others, 2009), and at Gunnison River near Delta, Colorado, during 2008 (figs. 4 and 5). Where the bed material was relatively fine (particle diameter less than 2 mm) or the streamflow was too deep to sample by wading, a boat-deployed, 7-in.-diameter pipe dredge was used to sample bed material (Benson and Dalrymple, 1967; Edwards and Glysson, 1999). Sediment-particle-size characteristics for these samples were determined through volumetric techniques (dry sieving) of each sample following procedures described by Guy (1977) at the USGS Geomorphology and Sediment Transport Laboratory in Golden, Colorado. Where the bed material was gravel- or coarser-size material (particle diameter greater than 2 mm) and it was possible to wade, sediment-particle-size characteristics were determined in the field by using areal techniques (pebble count) described by Wolman (1954). A minimum of 100 clasts were measured during each pebble count. Most measurements were made linearly and parallel to the direction of streamflow at regularly spaced intervals along the streambed or alluvial bars at each sampling location. Typically, a tape measure or graduated tag line was set up along the geomorphic surface to be sampled, for example a streambank or an elongated alluvial bar. Predetermined intervals along the tape measure or tag line then were used to determine unbiased sampling points for the particle measurement. Measurements on submerged riffles and alluvial bars were made by a nonlinear, random-path method. With this method, the sampler wanders over the desired geomorphic surface, selecting a particle for measurement without looking at the particle. Sample spacing with the random-path method usually was one or two paces.

The intermediate or "b-axis" of the sediment particle was measured to the nearest millimeter for gravel and small cobbles, and to the nearest 5 mm for large cobbles and small boulders. The b-axis length was recorded in the field notes, and sediment-particle-size statistics (d_{10}, size at the 10th percentile; d_{16}, size at the 16th percentile; d_{50} size at the 50th percentile; d_{65}, size at the 65th percentile; d_{84} size at the 84th percentile; and d_{90}, size at the 90th percentile) were computed in a spreadsheet from the cumulative-frequency distribution function of sampled-sediment particles. The d_{10} is used to conceptualize the threshold between components of sediment transport, described in the report section "Effects of Streamflow on Sediment Transport;" the d_{65} and d_{50} were used to determine the critical shear stress for sediment entrainment, described in the report section "Incipient Motion of Streambed Materials;" and the d_{16} and d_{84} are used to describe sediment transport of sands in a case study of the Green River spawning habitat near Jensen, Utah.

Suspended-Sediment Transport

Standard techniques used to measure SS concentration and SS flux require the continuous measurement of streamflow and systematic measurement of SS concentration (Porterfield, 1972). The range of SS-concentration measurements needed to compute daily SS flux within these large river systems can range from multiple samples per hour to samples every third day depending on the time of year and hydrologic conditions within the stream (Williams and others, 2009). Daily mean streamflow data obtained from the USGS National Water Information System (NWIS) database (*http://waterdata.usgs.gov/nwis*) and instantaneous SS concentration calculated from manually collected isokinetic depth- and width-integrated samples were used in equation 1 to calculate SS flux:

$$L = KC(t)Q(t)P(t) \quad (1)$$

where

- L is the calculated SS flux, in tons per day;
- K is a conversion factor, 0.0027;
- $C(t)$ is the average cross-sectional SS concentration at time t, in milligrams per liter;
- $Q(t)$ is the daily mean streamflow at time t, in cubic feet per second; and
- $P(t)$ is the proportion of the sediment-particle-size fraction of interest (sands or silt/clays) at time t, in percent of total concentration.

Suspended-Sediment Flux Transport Equations

Estimation of SS flux can be accomplished by using sediment-transport curves, which define the relation between SS flux and relevant explanatory variables such as streamflow, seasonality, and time (Porterfield, 1972; Horowitz, 2003; Cohn, 2005; Elliott and Anders, 2005). The relations can be approximated by using simple hand-drawn curves or regression techniques.

A common approach for developing sediment-transport curves using regression techniques is to relate SS flux (or concentration) as a power function of streamflow (Andrews, 1986; Elliott and Anders, 2005; Julien, 2010). Improvements to the accuracy of the relation can be made through the separation of the year into groupings based on seasonal periods or hydrological processes (Walling, 1977; Hansen and Bray, 1993; Sichingabula, 1998; Asselman, 2000). These power functions are useful for predictions of SS flux or concentration and provide an indication of seasonal influences of how the relation between streamflow and sediment transport changes relative to separate portions of the year. However, interpretation of the meaning of the streamflow variables is limited because a single explanatory variable is related to average responses of differing processes within the system and the relative significance of each variable cannot be compared directly between regression equations. The regression techniques used in this report avoid this limitation through inclusion of multiple explanatory variables (including streamflow, seasonality, and time) within a single equation.

Mathematical manipulation of the dataset (transformation) often is needed to better meet the assumptions of the linear regression in order to linearize the relation and to maintain constant variance. Compensation for differences in seasonal SS flux also can be accomplished using Fourier series and "dummy" variables to apply vertical shifts in the natural logarithm of SS flux and natural logarithm of streamflow relation (Runkel and others, 2004; Cohn, 2005; Dalby, 2006). Fourier series uses sine and cosine terms to account for continual changes over the seasonal period; dummy variables are used to account for more abrupt seasonal changes. The general equation form used in this report relates the natural logarithm of SS flux to daily mean streamflow and other explanatory variables using maximum likelihood estimation (MLE) methods within the USGS-developed LOADEST program (the FORTRAN program LOAD ESTimator, Runkel and others, 2004). The resulting general equation form used in this analysis is similar to Runkel and others (2004), Cohn (2005), and Dalby (2006) and is represented in equation 2.

$$\ln \hat{L} = \beta_0 + \beta_1(\ln Q - \ln Q^*) + \beta_2(\ln Q - \ln Q^*)^2 + \beta_3(t - t^*) + \beta_4(t - t^*)^2 + \beta_5 \sin(K2\pi T) + \beta_6(\cos(K2\pi T) + \beta_7 D + \varepsilon \quad (2)$$

where

$\ln$ is the natural logarithm function;
$\hat{L}$ is the estimated SS flux, in tons per day;
β_0 is the regression equation intercept;
β_n is the coefficient on the nth regression variable;
Q is daily mean streamflow, in cubic feet per second;
Q^* is the streamflow centering value from the calibration dataset, in cubic feet per second;
t is time, in decimal years;
t^* is the time centering value from the calibration dataset, in decimal years;
K is an integer, 1 or 2, that defines the wavelength of the sine and cosine functions;
T is a seasonality term representing the decimal portion of the year starting January 1;
D is a seasonality dummy variable, for rain events or the rising-limb of the hydrograph; and
ε is the error associated with the regression equation.

Orthogonalizing of the explanatory variables (time and streamflow) was done following methods in Cohn and others (1992) to "center" the dataset and remove multicolinearity between the explanatory variables (equations 3–6). This removes the effects of using a function and additional mathematical relation of the function (for example in the quadratic terms related to flow and time) and also reduces the leverage within the regression analysis that results from differences in the magnitude of the measure of each explanatory variable (for example, time in decimal years is of the scale 10^3 years; daily mean streamflow is on the scale of 10^3 to 10^4 ft^3/s; and seasonality is on the scale of 10^{-1} to 10^0 years), thus providing better relative comparisons between each.

$$\ln Q^* = \ln \overline{Q} + \frac{\sum_{i=1}^{N}\left(\ln Q_i - \ln \overline{Q}\right)^3}{2\sum_{i=1}^{N}\left(\ln Q_i - \ln \overline{Q}\right)^2} \quad \text{and}$$

$$\ln \overline{Q} = \frac{\sum_{i=1}^{N} \ln Q_i}{N} \quad (3 \text{ and } 4)$$

where

$\ln$ is the natural logarithm function;
Q^* is the streamflow centering value for the dataset, in cubic feet per second;
$\overline{Q}$ is the mean of the streamflow in the dataset, in cubic feet per second;
Q_i is the i^{th} daily mean streamflow, in cubic feet per second; and
N is the number of observations in the dataset.

$$t^* = \overline{t} + \frac{\sum_{i=1}^{N}\left(t_i - \overline{t}\right)^3}{2\sum_{i=1}^{N}\left(t_i - \overline{t}\right)^2} \quad \text{and} \quad \overline{t} = \frac{\sum_{i=1}^{N} t_i}{N} \qquad (5 \text{ and } 6)$$

where

t^* is the time centering value for the dataset, in decimal years;
$\overline{t}$ is the mean of the time values in the dataset, in decimal years;
t_i is the i^{th} time value, in decimal years; and
N is the number of observations in the dataset.

Retransformation of regression predictions back from logarithmic scale produces median SS flux estimates in tons per day. A bias-correction factor is applied to the retransformed estimates to correct for the transformation bias and to produce mean estimates. Using median estimates can result in underestimations of SS flux by as much as 50 percent (Ferguson, 1986; Cohn and others, 1989; Cohn, 1995). According to Bradu and Mundlak (1970), the majority of the transformation bias can be eliminated by multiplying the estimated response by a bias-correction factor. Bias-correction factors for the MLE estimates were applied following modified methods from Bradu and Mundlak (1970) described in Runkel and others (2004) and Likes (1980) and resulted in a minimum variance unbiased estimate (MVUE) of the SS flux. The bias-correction factor used for MLE estimates of SS flux within LOADEST $\left(g_m\left(m,s^2,V\right)\right)$ is replaced with a similar function, phi, that is described in Likes (1980):

$$\hat{L}_{MVUE} = e^{\left(\beta_0 + \sum_{i=1}^{M}\beta_i X_i\right)} g_m\left(m, s^2, V\right) \qquad (7)$$

where

$\hat{L}_{MVUE}$ is the minimum variance unbiased estimate of SS flux, in tons per day;
e is the base of the natural logarithm,
β_0 is the regression-equation intercept estimated by the MLE method;
β_i is the coefficient on the ith regression variable estimated by the MLE method;
X_i is the ith regression variable;
$g_m\left(m, s^2, V\right)$ is the bias-correction factor,
m is the number of degrees of freedom,
s^2 is the residual variance, and
V is a function of the explanatory variables (Cohn and others, 1989).

Error assessment was done at stations with available daily mean SS flux estimates. Root mean square errors (RMSE; Helsel and Hirsch, 2002) (as percent of the mean value) were calculated from comparison of daily mean SS flux and transport equation estimates. Although error is inherent in both of these methods, for this analysis, available daily mean SS flux data were assumed to be most accurate and were treated as the actual SS fluxes at the station for that day.

Comparisons were made for multiple time steps (daily, weekly, monthly, and seasonal totals) corresponding to one of three hydrologic "seasons" (base flow, rising limb of the snowmelt hydrograph, and falling limb of the snowmelt hydrograph). To provide a worst-case estimation of error, consecutive days were used to preserve serial correlation of the predictions. Use of consecutive days may result in consistent biases (non-random errors) that would increase the error of the prediction. Consecutive 7-day periods were used for weekly totals, 30 or 31 day periods were used for monthly totals, and each day of each season was combined by year for seasonal totals.

If data were insufficient to be totaled into each of these time steps, days were reused from other totals to complete the number of days in the time step. For example, if there were 33 consecutive days that were used for weekly total calculation, the days would be totaled as follows: 1–7, 8–14, 15–21, 22–28, and 27–33. This method results in the reuse of days 27 and 28 in two weekly totals but is appropriate in this analysis (Brent Troutman, U.S. Geological Survey, Lakewood, Colorado, oral commun., 2009). Similarly, separation of monthly totals into 30 and 31 day periods was done to best fit the available data and minimize reuse of data.

Suspended-Sediment Concentration and Streamflow Relations

Understanding the relation between streamflow and suspended-sediment transport can aid in the evaluation of physical and temporal processes that affect sediment transport. Regression analysis can be used to detect processes that explain variability in sediment transport within the river systems. The general equations used in this report is similar to Runkel and others (2004), Cohn (2005), and Dalby (2006) and is represented in equation 8:

$$\ln \hat{C} = \beta_0 + \beta_1(\ln Q - \ln Q^*) + \beta_2(\ln Q - \ln Q^*)^2 + \beta_3(t - t^*) + \beta_4(t - t^*)^2 + \varepsilon \qquad (8)$$

where

ln is the natural logarithm function;
$\hat{C}$ is the estimated SS concentration or sand portion of the SS concentration (sand SS), in milligrams per liter;
β_0 is the regression equation intercept;
β_n is the coefficient on the nth regression variable;
Q is daily mean streamflow, in cubic feet per second;
Q^* is the streamflow centering value from the calibration dataset, in cubic feet per second;
t is time, in decimal years;
t^* is the time centering value from the calibration dataset, in decimal years;
ε is the error associated with the regression equation.

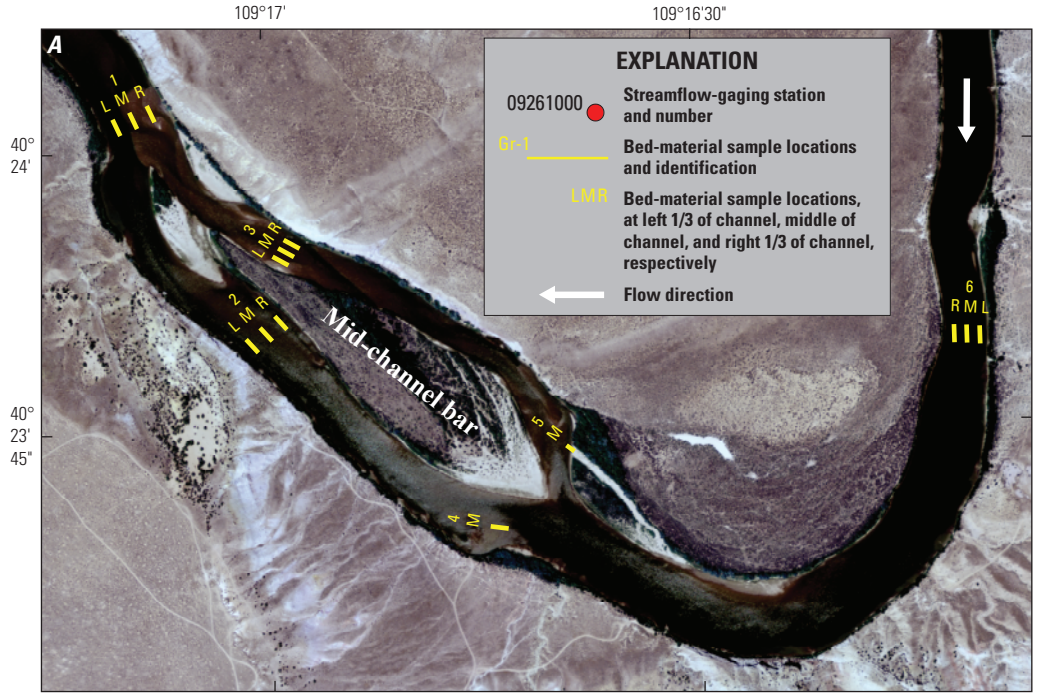

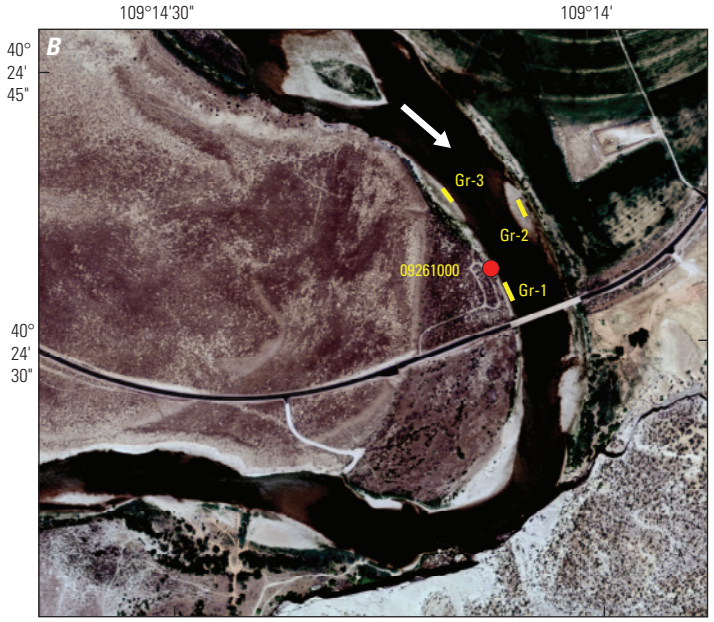

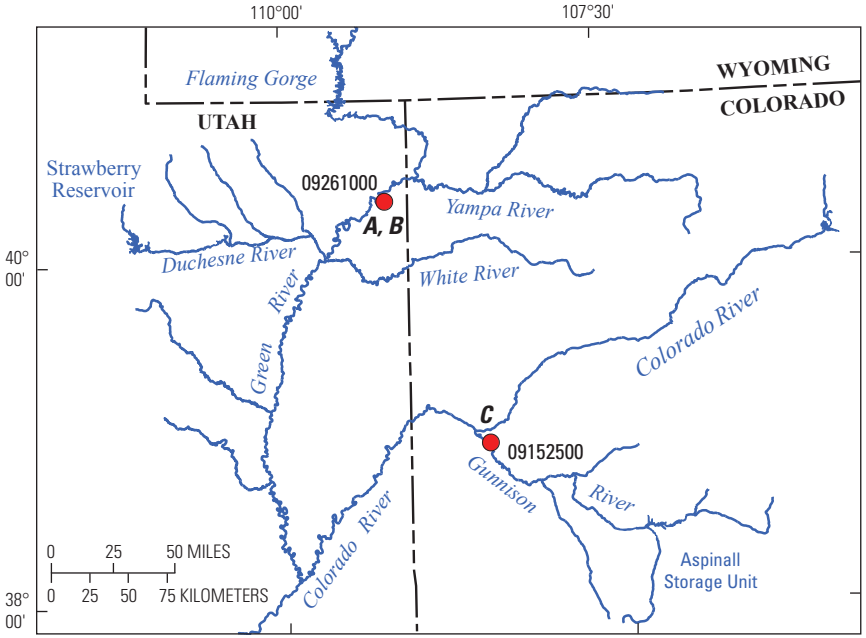

Base from U.S. Geological Survey National Atlas
Universal Transverse Mercator North American Datum 1983, Zone 12 North

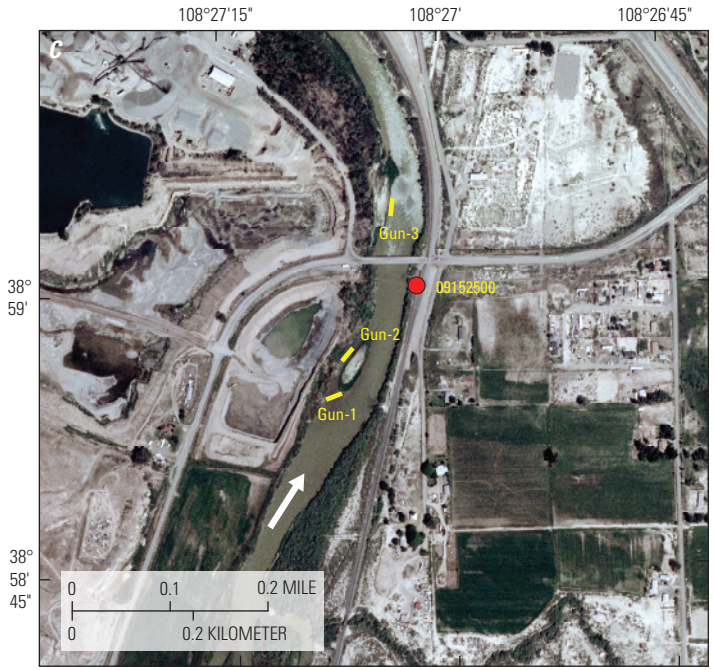

Orthoimages from U.S. Department of Agriculture National Agriculture Imagery Program (2007)
Universal Transverse Mercator North American Datum 1983, Zone 12 North

Figure 4 (previous page). Map showing bed-material sampling locations. *A*, the Jensen mid-channel bar (spawning habitat), 5 miles downstream from the Green River near Jensen, Utah, streamflow-gaging station. *B*, 09261000, Green River near Jensen, Utah, streamflow-gaging station. *C*, 09152500, Gunnison River near Grand Junction, Colorado, streamflow-gaging station.

Comparisons of the relations between the natural logarithm of streamflow and the natural logarithm of SS concentration were done to determine the effects of antecedent conditions on sediment transport within the river systems. Inter-annual conditions can be important in sediment supply and storage. The sediment-streamflow relation may change following a hydrological "wet" or "dry" year or period. An evaluation of peak streamflow magnitude (relative to post-reservoir streamflow percentiles) was used to classify each year as (1) wet, peak streamflow greater than 75th percentile; (2) average, peak streamflow between 50–75th percentile; or (3) dry, peak streamflow less than 25th percentile. Comparisons were made between differing annual cycles (1-year periods) and between multi-year cycles (1-year periods following specific multi-year periods). Comparison of the relation between natural logarithm of streamflow and the natural logarithm of SS concentration was done between (1) wet and dry years, (2) wet years and wet years following two or more dry years, and (3) dry years and dry years following two or more wet years. This analysis was designed to identify antecedent conditions that produced discernable changes in the slope and intercept of the streamflow sediment-transport relation. Separation of the data into the rising and falling limbs of the snowmelt hydrograph was done to account for seasonal differences. ANalysis of COVAriance (ANCOVA) was used to test for significant differences in the slope and intercept of the relation between natural logarithm of streamflow and the natural logarthim of SS concentration for each station by using R statistical software (R Development Core Team, 2008).

Two-Dimensional Streamflow and Sediment-Transport Model

The Multi-Dimensional Surface-Water Modeling System (MD_SWMS) was used to model various streamflows for a study reach on the Green River near Jensen, Utah. MD_SWMS is a graphical user interface that was developed by the USGS (McDonald and others, 2001). The FaST-MECH computational model within MD_SWMS was used to simulate water-surface elevation, boundary shear stress, velocity, and sediment transport (Nelson and McDonald, 1997; Thompson and others, 1998; Lisle and others, 2000; Nelson and others, 2003). The sediment-transport model followed methods described by Yalin (1977) as defined in equations 9 and 10:

$$a\left(\frac{\tau_\circ}{\tau_{cr}}-1\right)-\frac{1.575aq_t}{\gamma_s u_* d_{50}}=\ln\left[1+a\left(\frac{\tau_\circ}{\tau_{cr}}-1\right)\right] \quad (9)$$

and

$$a=2.45\left(\frac{\gamma_s}{\gamma}\right)\sqrt{\frac{\rho u_*^2}{\left(\gamma_s-\gamma\right)d_{50}}} \quad (10)$$

where

ln is the natural logarithm function;
$\tau_\circ$ is the boundary shear stress, in pascal,
τ_{cr} is the critical shear stress of the d_{50}, in pascal,
a is an intermediate variable,
q_t is the bed-material load transport rate per unit width, in newtons per meter-second,
γ_s is the specific weight of sediment, in newtons per cubic meter,
γ is the specific weight of water, in newtons per cubic meter,
u^* is the shear velocity, in meter per second,
d_{50} is the median sediment particle diameter of the bed material, in meters, and
ρ is the mass density of water, in kilograms per cubic meter.

Equation 9 can be converted from metric units (newtons per meter-second or pascals) to English units (pounds per foot-second) by multiplying q_t by 0.06853.

The dataset requirements of the model include channel geometry, streamflow at the upstream end of the study reach, and water-surface elevation at the downstream end of the study reach. Velocity information also was used to verify model results following calibration of the model. The FaST-MECH model uses a curvilinear orthogonal grid with a user-defined centerline, which approximates the path of streamflow for the modeled reach. User-defined parameters are calculated for each node of the grid. Additional information on the interface and the model can be found in McDonald and others (2001) and Nelson and others (2003).

The majority of the data collected to calibrate the two-dimensional model were collected when the Green River streamflow was 9,000 ft^3/s. For that streamflow, there are 110 measured water-surface elevations and 101 measurements of average velocity. For each of the other streamflows (10,600; 14,100; 17,700; and 19,000 ft^3/s), there are two measurements of water-surface elevation and no velocity measurements. Therefore, model calibration was performed most rigorously for the 9,000 ft^3/s model (discussed in the "Two-Dimensional Streamflow and Sediment-Transport Model Calibration and Sensitivity Analysis" section).

In and near the channel, topographic and bathymetric data were collected using RTK-GPS in conjunction with a boat-mounted Acoustic Doppler Current Profiler (ADCP) and an echo sounder. The methodology is explained in further detail in Williams and others (2009). Topographic data needed to define channel-geometry were collected on May 8–12,

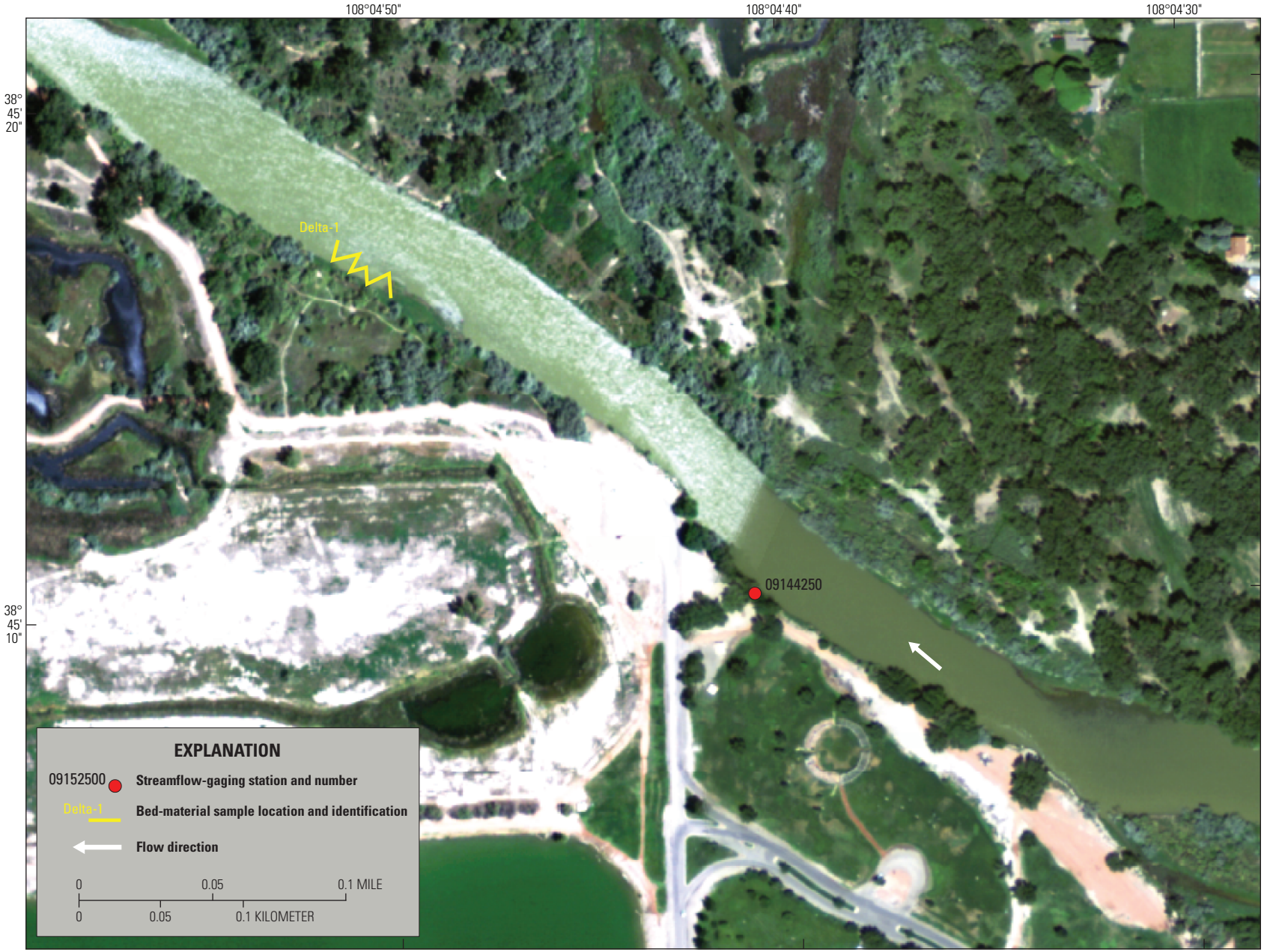

Orthoimages from U.S. Department of Agriculture National Agriculture Imagery Program (2007)
Universal Transverse Mercator North American Datum 1983, Zone 12 North

Figure 5. Map showing bed-material sampling location in the study reach on the Gunnison River near Delta, Colorado.

2006, for a 1.5-mi reach of the Green River. These data were combined with existing LiDAR data (Bowen and others, 2001) to characterize the reach geometry.

Interpolation between measured data points was done using two separate processes, in conjunction, to obtain the most accurate representation of the channel geometry for the study reach (see also, Barton and others, 2005). The template algorithm was used first, and then the Triangular Irregular Network (TIN) method was used to develop the final topographic surface. The template algorithm follows a method similar to a nearest neighbor search in which elevation values are interpolated based on comparisons to a selection of data points within a rectangular bin, which is oriented so that it is longest in the stream-wise direction (parallel to the stream channels). This approach leverages an observation that topographic data within a stream reach tend to be more strongly correlated over longer distances in the stream-wise direction (parallel to the general flow direction) than in the cross-stream direction. To optimize this observed relation between elevation data within a stream reach, the measured data for the study reach were initially divided into five subreaches. For each subreach the measured elevations were mapped to a 16 ft nominal grid. The resulting topography from the five subreaches were combined with the original measured data to form a densely spaced set of topographic data from which a final dataset for channel geometry was created using the TIN method. The final computational grid was approximately 9,842-ft (3,000-m) long and 1,148-ft (350-m) wide with 601 stream-wise points, or nodes, and 71 cross-stream points, approximating a 16.4- by 16.4-ft grid area (5.0- by 5.0-m) (fig. 6).

The other data requirements for the model are streamflow at the upstream boundary of the reach and the corresponding water-surface elevation at the downstream boundary of the reach. Instantaneous streamflows were obtained from USGS NWIS (*http://waterdata.usgs.gov/ut/nwis/*). The Green River near Jensen, Utah, 09261000, streamflow-gaging station was used for streamflow data within the study reach.

Water-surface elevations were measured by using pressure transducers and RTK-GPS surveys for a range of streamflows. Water-surface elevations are used as the downstream-boundary condition for the model and for calibrating the model results in the remainder of the channel. During the survey and bathymetry mapping data collection, water-surface elevations were surveyed using the RTK-GPS (mentioned previously in the "Topographical Surveying" section) and described in further detail in Williams and others (2009). Those water-surface elevations were used to calibrate the model parameters for a streamflow of 9,000 ft^3/s at the gage upstream on the day that corresponded with the measurement of the elevations. Water-surface elevations also were measured for a range of streamflows (1,200–19,000 ft^3/s) through the deployment of temporary water-surface elevation gages (pressure transducers) located at two strategic locations (fig. 7) within the study reach during May 16–July 27, 2006. The pressure transducers were surveyed using the RTK-GPS to facilitate the calculation of water-surface elevations.

Water-velocity data were collected at the 9,000 ft^3/s streamflow and were used for model calibration and verification. An ADCP was used to collect stream-velocity data at cross sections at important streamflow locations (fig. 7). At each location, 10 traverses were completed consecutively to represent the temporal and depth-averaged velocity along the cross section. Comparisons of the modeled velocities to the measured velocities were done to evaluate model accuracy for velocity data and are discussed in the "Two-Dimensional Streamflow and Sediment-Transport Model Calibration and Sensitivity Analysis" section.

The model uses a parameter referred to as "lateral eddy viscosity" to represent the lateral-momentum exchange owing to turbulence or other variability that is not generated by the bed (Nelson and others, 2003). The parameter was computed for each model by multiplying the average velocity and the average depth of the best-fit model by the lateral-eddy coefficient, which was assigned a value of 0.01 (Nelson and others, 2003; Barton and others, 2005). Drag coefficients ranged from 0.0078 for the modeled streamflow of 9,000 ft^3/s down to 0.004 for the highest modeled streamflow of 19,000 ft^3/s.

Incipient Motion of Streambed Materials

Incipient motion of particles in gravel-bed streams is an important component of sediment transport. This process determines the relative grain stability and is the most important component of sediment transport relative to channel form adjustment (Knighton, 1998). In general, sediment transport occurs within a stream when the boundary shear stress exceeds the critical shear stress of the particle (Julien, 2010). In order to determine the precise conditions that will result in the initiation of motion for more than one particle of interest, reasonable generalizations of the particle shape, orientation, submerged weight, and protrusion into flow must be assessed. Analysis of each particle within a stream is unfeasible so instead particle movement is characterized for groups of particles classified by size distribution. Sediment entrainment in a streambed is a function of the boundary shear stress acting on sediment particles resting on or in the streambed or other inundated alluvial surfaces where boundary refers to the boundary between the channel bed and the water. Mean boundary shear stress in a channel cross section is approximated by the DuBoys' equation (Chow, 1959):

$$\tau_o = \gamma h S \tag{11}$$

where

τ_o is the mean boundary shear stress, in pounds per square foot;
γ is the specific weight of water (62.4 pounds per cubic foot);
h is the mean flow depth, in feet; and
S is the energy gradient for a specific streamflow, in feet per foot.

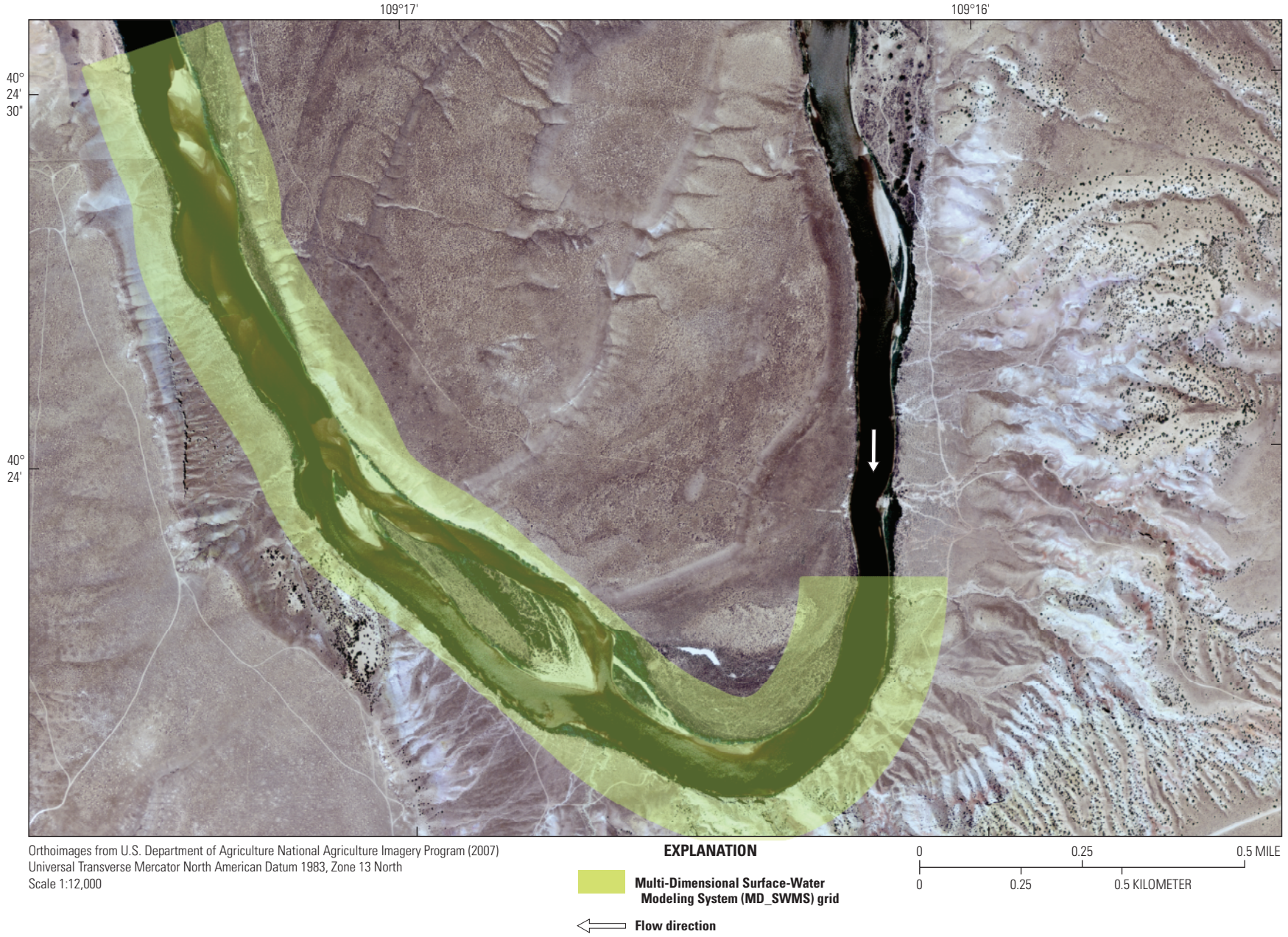

Figure 6. Map showing a Multi-Dimensional Surface-Water Modeling System (MD_SWMS) grid, 5 miles downstream from the Green River near Jensen, Utah, streamflow-gaging station (see figure 4).

Orthoimages from U.S. Department of Agriculture National Agriculture Imagery Program (2007)
Universal Transverse Mercator North American Datum 1983, Zone 13 North
Scale 1:10,000

Figure 7 (previous page). Map showing temporary water-surface elevation gages and Acoustic Doppler Current Profiler (ADCP) cross-sections locations, 5 miles downstream from the Green River near Jensen, Utah, streamflow-gaging station.

The assumptions behind this equation include (1) the channel cross section has a regular, trapezoidal shape and that the width of the channel is at least 10 times the depth; (2) streamflow is steady or that there is a continuity of streamflow from one cross section to the next; and (3) streamflow is uniform or that velocity is constant in both magnitude and direction for the reach. In this study, the cross-section shapes were not trapezoidal though the widths of the cross sections were at least 10 times the mean flow depths at the smallest streamflow. Streamflow was assumed to be steady as there were no inflows into the study reaches, and exchange between surface water and groundwater were assumed to be negligible.

Most natural streams do not satisfy all of the assumptions for equation 11, and the resulting boundary shear stress for a cross section is nonuniformly distributed across the channel. Additionally, in natural systems, lateral and downstream variations in cross-section morphology, flow depth, bedform and particle drag, and variations in energy gradient with streamflow result in a wide range of boundary shear stresses that are nonuniformly distributed across the channel (Graf, 1971). To rectify the violations of the assumptions made in equation 11, point depths along the cross sections were substituted for the cross-section mean flow depth to examine the relative effects on the boundary shear-stress distribution of different streamflows along multiple cross sections within a study reach.

For areas where the calibrated two-dimensional streamflow and sediment-transport model was available, FaSTMECH was used to calculate boundary shear stress using the following equation (Barton and others, 2005):

$$\tau_b = \frac{\rho C d(u^2 + v^2)}{k} \quad (12)$$

where

τ_b is the boundary shear stress, in pounds per square foot;
ρ is the fluid density, in kilograms per cubic meter;
Cd is the non-dimensional drag coefficient;
u is the vertically averaged stream-wise velocity, in meters per second;
v is the vertically averaged cross-stream velocity, in meters per second; and
k is a conversion factor, 47.88.

The critical shear stress (τ_c) for a particle is the minimum shear stress needed for general movement of the particle to begin. Sediment-particle size, density, shape, and sorting affect transport and have been related to sediment-particle-size characteristics (Shields, 1936; Lane, 1955; Fahnestock, 1963; Carling, 1983; Komar, 1987; Wilcock, 1992). Critical shear stress for entrainment of the sediment d_{50} particle was calculated using the Shields (1936) equation to estimate when many of the particles along the streambed within the reach would begin movement:

$$\tau_c = \tau_c^*(\gamma_s - \gamma)d_{50} \quad (13)$$

where

τ_c is the critical shear stress, in pounds per square foot;
τ_c^* is the dimensionless critical shear stress or Shields parameter;
γ_s is the specific weight of sediment (165.5 pounds per cubic foot);
γ is the specific weight of water (62.4 pounds per cubic foot); and
d_{50} is the median sediment-particle size, in feet.

Two critical shear stress values were selected for the incipient-motion analyses in this study. One critical shear stress value was computed with a dimensionless critical shear stress, or Shields (1936) parameter of 0.035, and the second critical shear stress value was computed with a Shields parameter of 0.050. The dimensionless critical shear stress and critical shear stress values have been experimentally determined for streambeds ranging in sediment-particle size from silt to boulders (Julien, 1998). The dimensionless critical shear stress values range from 0.054 for boulders to 0.033 for coarse sand and to 0.25 for medium silt (Julien, 1998). The channel beds in the rivers included in this study are composed of mixed sediment ranging from fine sands to cobbles up to 6 in. in diameter. The cobbles form a subsurface pavement layer that often is covered in a layer of sand. In channels where the channel bed is tightly structured or where the particles are strongly imbricated, the dimensionless critical shear stress was found to range from 0.055 to 0.065; in loosely structured beds the dimensionless critical shear stress is as low as 0.0096 to 0.011 (Parker and others, 1982; Andrews, 1983; Komar, 1987; Powell and Ashworth, 1995). Shields parameter values of 0.035 and 0.050 result in a range of possible hydraulic conditions at which incipient motion or sediment entrainment may begin in the study reaches. Incipient motion estimated with a Shields parameter value of 0.035 resulted in estimates of the critical shear stress, and therefore of the streamflow, necessary to entrain sediment of the d_{50} particle size on the streambed. Conversely, a Shields parameter value of 0.050 resulted in a more conservative estimate of the critical shear stress and streamflow necessary to entrain the same-size sediment.

In natural river systems, the portion of the boundary shear stress available to move sediment grains can be referred to as the "grain shear stress" (Julien, 2010). In wide, straight streams the boundary shear stress calculated using equations 11 and 12 is equal to the grain shear stress. In other instances, the boundary shear stress estimates for the system include

energy that is unavailable for sediment transport owing to additional energy losses within the stream. These losses can be the result of turbulent eddy formation and bedforms. In sand-bed streams, bedforms such as ripples, dunes, and anti-dunes are common causes for these energy losses. In gravel-bed streams, these losses can arise from channel expansions and contractions, alluvial bars, and meander bends. Study reaches presented in this report were located where these secondary losses were expected to be minimal.

Comparisons of boundary shear stress and grain shear stress were made using two methods. For gravel reaches, estimates of grain shear stress were obtained following methods described in Wilcock and others (2009) and represented by equations 14–16:

$$\frac{\tau_o^{'}}{\tau_o} = \left(\frac{n_D}{n}\right)^{3/2} \tag{14}$$

$$n_D = 0.013 D^{1/6} \tag{15}$$

$$n = \frac{\phi}{Q} w h^{5/3} S_f^{1/2} \tag{16}$$

where

$\tau_o^{'}$ is the grain shear stress, in pounds per square foot;
τ_o is the boundary shear stress, in pounds per square foot;
n_D is the Manning coefficient of roughness attributed to grain roughness;
n is the Manning coefficient of roughness of the cross section;
D is two times the d_{65} sediment-particle size, in millimeters;
ϕ is a conversion factor, 1.486;
Q is streamflow, in cubic feet per second;
w is the channel width, in feet;
h is the mean flow depth, in feet; and
S_f is the energy gradient for a specific streamflow, in feet per foot.

For sand-bed reaches, estimates of grain shear stress were obtained following methods described in Julien (2010) and represented by equations 17 and 18:

$$\tau_*^{'} \approx 0.04 \left(\frac{d_{50}}{h}\right)^{1/3} \left(\frac{V^2}{g(G-1)d_{50}}\right) \tag{17}$$

$$\tau^{'} = \frac{\tau_*^{'}(\gamma_s - \gamma) d_{50}}{k} \tag{18}$$

where

$\tau_*^{'}$ is the grain shear stress, dimensionless;
d_{50} is median sediment-particle size, in meters;
h is the average flow depth, in meters;
G is the specific gravity of sediment, 2.65 (dimensionless);
V is the average flow velocity, in meters per second;
g is the gravitation constant, 9.81 meters per square second;
$\tau^{'}$ is the grain shear stress, in pounds per square foot;
γ_s is the specific weight of sediment, 165.5 pounds per cubic foot ;
γ is the specific weight of water, 62.4 pounds per cubic foot; and
k is a conversion factor, 0.3048.

For reaches where differences between boundary and grain shear stress exceeded 2 percent, grain shear stress calculated from equations 14 or 18 was used to assess incipient-motion potentials for a range of streamflows at each cross section. Grain shear stress along intervals within the cross section were scaled by the proportion of grain shear stress to the bed shear stress of each cross section.

The boundary shear stresses were compared to the critical shear stresses for sediment in the channel to evaluate sediment-entrainment potential of each streamflow. Sediment-entrainment potential at each cross section associated with the reference streamflows was expressed as the ratio of the shear stress (τ) to the critical shear stress for the median sediment-particle size at the cross section (τ_c). The τ/τ_c ratio (sediment-entrainment ratio) integrates several geomorphic and sediment variables (flow depth, energy gradient or water-surface slope, median sediment-particle size, and critical shear stress) and is applicable over a wide range of values (Elliott and Hammack, 1999, 2000). The sediment entrainment ratio also was calculated for each point along a cross section to evaluate incipient motion of sediment on different geomorphic surfaces traversed by the cross section.

The critical shear stress should be considered the minimum value for incipient motion of the d_{50} particle because at that critical shear stress only a small fraction of the sediment of the d_{50} size class will be entrained (Milhous, 1982). Complete mobilization of the d_{50} size class has been shown to occur at roughly twice the value for incipient motion of the individual sediment particles of that size class (Wilcock and McArdell, 1993). Critical streamflow, or the minimum streamflow required to entrain the sediment d_{50}, can be estimated by equating τ with τ_c and using the relation between boundary or grain shear stress and streamflow at a specific cross section.

Rouse Number and Sediment-Transport Mode

The ratio of settling forces to suspension forces, Rouse number, can be used to determine the mode of sediment transport (bed load, suspended load, or wash load) within a stream reach (Julien, 2010). Values greater than one represent

stream conditions where sediment particles are exposed to greater settling forces than suspension forces and will tend to bounce along the streambed as bed load. Rouse numbers less than one relate to stream conditions where sediment particles are exposed to greater suspension forces than settling forces and will tend to travel within the water column as suspended load. Wash load occurs when the sediment is transported in suspension without interaction with the streambed. Comparisons of the Rouse numbers to these definitions will be used to determine the primary mode of sediment transport within this report and are summarized in table 2.

Table 2. Mode of sediment transport based on Rouse number (modified after Julien, 2010).

[>, greater than; %, percent; <, less than]

Rouse number	Sediment-transport mode
>5.0	Bed load
2–5.0	<50% suspended, >50% bed load
0.5–1.99	>50% suspended, <50% bed load
<0.5	Suspended load

Rouse number:

$$R = \frac{W_s}{k u_*} \quad \text{and} \quad u_* = \sqrt{\frac{\tau}{\rho}} \qquad (19 \text{ and } 20)$$

where

R is the Rouse number, dimensionless;
W_s is the settling velocity of the sediment particle, in meters per second;
k is the Von Karman's constant, 0.4;
u_* is the shear velocity of the stream, in meters per second;
τ is the boundary shear stress, in pascals;
ρ is the density of the water in the stream, 999.58 kilograms per square meter at 12 degrees Celsius.

Two-Dimensional Streamflow and Sediment-Transport Model Calibration and Sensitivity Analysis

The two-dimensional model was first calibrated based on continuity of mass. Calibration was achieved when the root-mean squared value for streamflow was less than 6 percent from the nominal streamflow achieved in each model scenario. In each scenario, adjustments were made to the roughness value, as described by the drag-coefficient parameter, until model-predicted water-surface elevations and velocities (when available) acceptably matched those measured in the field (fig. 8). Water-surface elevations from the best-fit models were within 0.12 ft of measured water-surface elevations for all models except the model for the 9,000 ft^3/s streamflow. For the 9,000 ft^3/s model, there were more data to compare, and the maximum difference was 0.39 ft. Generally, the larger differences between predicted and measured water-surface elevations for this model occurred in the middle of the study reach whereas the upstream and downstream boundaries had smaller differences, closer to 0.10 ft or less (fig. 8). For the other modeled streamflows, there were only data at the upstream and downstream boundaries. The velocity data from the ADCP measurements along the five transects were plotted against the modeled velocity at each of the five cross sections to ensure that the modeled velocities were within the range of observed values. Additional comparisons of measured velocities at selected cross sections to model output show general agreement in magnitude and distribution; however, high velocities at some locations were under predicted (fig. 8).

Sensitivity of the lateral eddy viscosity and drag coefficient were evaluated by individually adjusting each parameter by plus or minus 25 percent relative to the calibrated value (tables 3 and 4). Differences relative to the mean were less than 1 percent for all models except the 10,600 ft^3/s model. In that model, decreasing the lateral eddy viscosity by 25 percent resulted in a difference of 11.25 percent in mean velocity and 16.91 percent in mean boundary shear stress. The model was more sensitive to adjustments of the drag coefficient parameter. Varying the drag coefficient by plus or minus 25 percent resulted in differences in the mean water-surface elevation of 5 percent or less of mean depth. Differences in mean velocities were 1.8 percent of mean velocity or less, and differences in boundary shear-stress values were up to 23 percent of the calibrated model boundary shear stress. The large percentages are a reflection of the small values of mean boundary shear stress.

Effects of Streamflow on Sediment Transport

Sediment transport can be conceptualized as the interaction of transport capacity and sediment supply for a given streamflow condition (depicted in fig. 9). Transport capacity refers to the ability of the stream to move sediment particles and is a function of hydraulic variables and the shape of the stream cross section; whereas, sediment supply is determined by the availability of the materials in the stream and can be a function of both in-stream processes and overland processes within the basin (Julien, 2010).

In figure 9, the areas located below both of the curves represent the sediment transported within the stream at a fixed streamflow condition. The brown-shaded area to the left of the d_{10} represents conditions where sediment transport occurs in suspension and is limited by the availability of sediment delivered to the stream or found within the streambed (wash

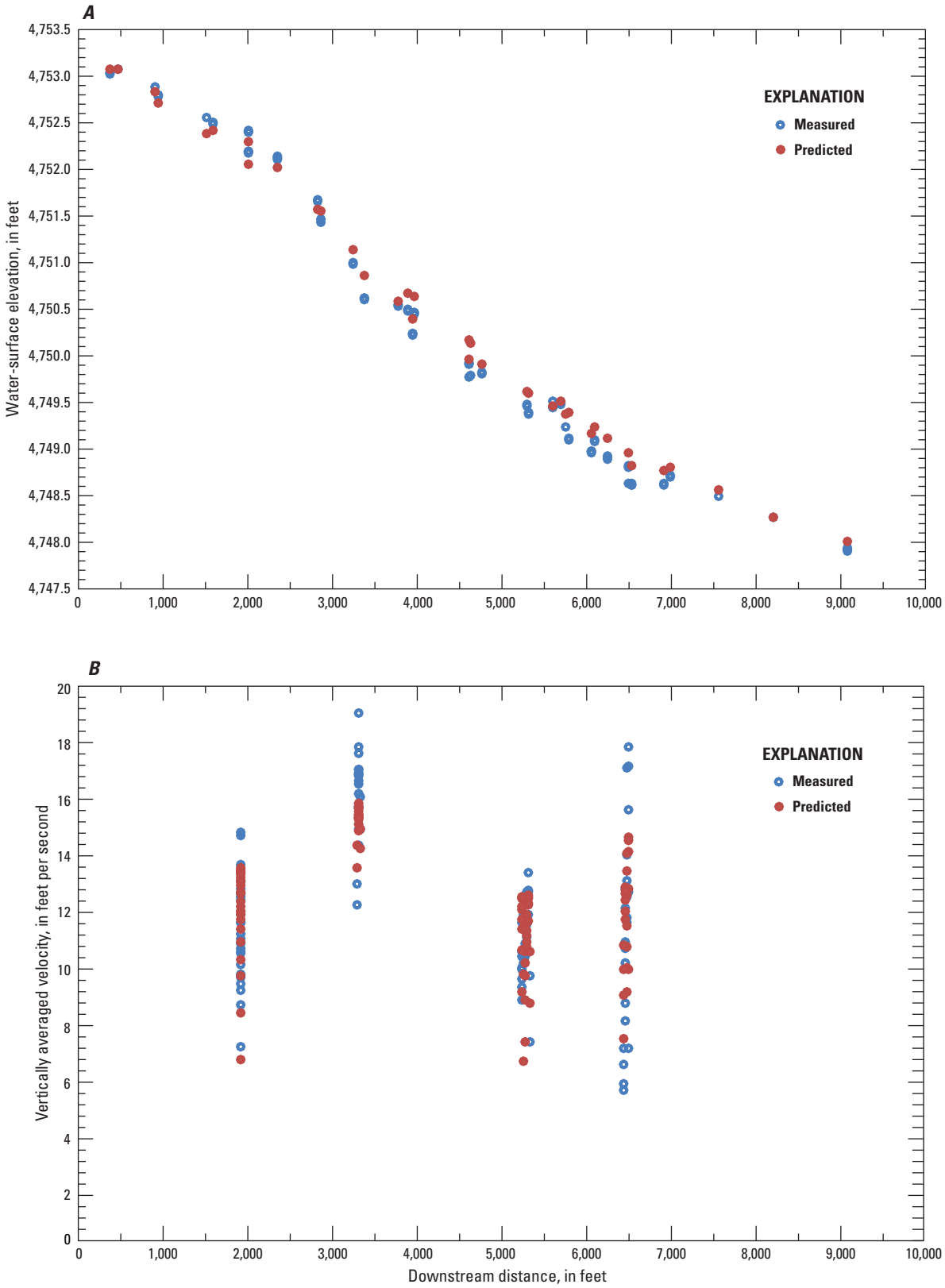

Figure 8. Graph showing *A*, water-surface elevations and *B*, mean velocities for the best-fit model for the 9,000 cubic feet per second streamflow.

Table 3. Lateral eddy viscosity sensitivity analysis and results for the five streamflows simulated in the two-dimensional streamflow and sediment-transport model for the Green River near Jensen, Utah, study reach.

[Sensitivity analyses of calibrated lateral eddy viscosity were made at **75** (indicated in bold) and *125* (indicated in italics) percent of the lateral eddy viscosity value. The mean values are based on non-zero values in the model. Percent differences are relative to the mean of the calibrated model and percent difference in water-surface elevation is relative to the mean depth; ft^3/s, cubic foot per second; ft, foot; ft/s, foot per second; lb/ft^2, pound per square foot; --, not applicable]

Streamflow (ft^3/s)	Lateral eddy viscosity value (ft^3/s)	Model output				Percent difference from the mean		
		Mean depth (ft)	Mean water-surface elevation (ft)	Mean velocity (ft/s)	Mean shear stress (lb/ft^2)	Water-surface elevation	Velocity	Shear stress
9,000	0.00780	5.69	4,750.00	3.17	0.17	--	--	--
9,000	**.00585**	**5.69**	**4,750.00**	**3.15**	**.17**	**–0.18**	**–0.35**	**–0.64**
9,000	*.00975*	*5.68*	*4,749.99*	*3.16*	*.17*	*.07*	*–.63*	*–1.10*
10,600	.00550	6.11	4,750.35	3.42	.14	--	--	--
10,600	**.00413**	**6.12**	**4,750.36**	**3.41**	**.14**	**–.87**	**–11.25**	**–16.91**
10,600	*.00688*	*6.08*	*4,750.30*	*3.03*	*.12*	*.20*	*–.32*	*–.49*
14,100	.00450	7.08	4,751.53	3.92	.15	--	--	--
14,100	**.00338**	**7.10**	**4,751.55**	**3.89**	**.15**	**–.14**	**.27**	**.53**
14,100	*.00563*	*7.07*	*4,751.52*	*3.93*	*.15*	*.37*	*–.58*	*–.94*
17,700	.00470	8.04	4,752.75	4.11	.18	--	--	--
17,700	**.00353**	**8.06**	**4,752.78**	**4.09**	**.17**	**–.20**	**.09**	**.28**
17,700	*.00570*	*8.02*	*4,752.74*	*4.11*	*.18*	*.30*	*–.34*	*–.62*
19,000	.00400	8.27	4,753.01	4.28	.16	--	--	--
19,000	**.00300**	**8.30**	**4,753.04**	**4.26**	**.16**	**–.15**	**–.31**	**–.32**
19,000	*.00480*	*8.26*	*4,753.00*	*4.27*	*.16*	*.35*	*–.45*	*–.83*

Figure 4. Drag coefficient sensitivity analysis and results for the five streamflows simulated in the two-dimensional streamflow and sediment transport model for the Green River near Jensen, Utah, study reach.

[Sensitivity analyses of calibrated drag coefficient were made at **75** (indicated in bold) and ***125*** (indicated in italics) percent of the drag-coefficient value. Percent differences are relative to the mean of the calibrated model, and percent difference in water surface elevation is relative to the mean depth. The mean values are based on non-zero values in the model; ft^3/s, cubic foot per second; ft, foot; ft/s, foot per second; lb/ft^2, pound per square foot; --, not applicable]

Streamflow (ft3/s)	Drag-coefficient value	Model output				Percent difference from the mean		
		Mean depth (ft)	Mean water-surface elevation (ft)	Mean velocity (ft/s)	Mean shear stress (lb/ft^2)	Water-surface elevation	Velocity	Shear stress
9.000	0.0078	5.69	4,750.00	3.17	0.17	--	--	--
9.000	**.0059**	**5.95**	**4,750.26**	**3.04**	**.19**	**–5.01**	**1.49**	**–16.70**
9.000	*.0098*	*5.41*	*4,749.71*	*3.22*	*.14*	*4.62*	*–4.31*	*13.18*
10.600	.0055	6.11	4,750.35	3.42	.14	--	--	--
10.600	**.0041**	**6.35**	**4,750.59**	**3.30**	**.16**	**–4.94**	**1.81**	**–20.18**
10.600	*.0069*	*5.82*	*4,750.05*	*3.48*	*.11*	*3.93*	*–3.52*	*15.02*
14.100	.0045	7.08	4,751.53	3.92	.15	--	--	--
14.100	**.0034**	**7.31**	**4,751.76**	**3.80**	**.17**	**–4.05**	**.91**	**–21.06**
14.100	*.0056*	*6.80*	*4,751.24*	*3.95*	*.12*	*3.35*	*–3.02*	*15.97*
17.700	.0047	8.04	4,752.75	4.11	.18	--	--	--
17.700	**.0035**	**8.29**	**4,753.00**	**4.00**	**.20**	**–4.38**	**–.06**	**–19.77**
17.700	*.0057*	*7.68*	*4,752.39*	*4.09*	*.14*	*3.08*	*–2.34*	*13.63*
19.000	.0040	8.27	4,753.01	4.28	.16	--	--	--
19.000	**.0030**	**8.48**	**4,753.23**	**4.19**	**.18**	**–3.92**	**–.39**	**–-22.52**
19.000	*.0048*	*7.95*	*4,752.69*	*4.26*	*.13*	*2.57*	*–2.22*	*13.20*

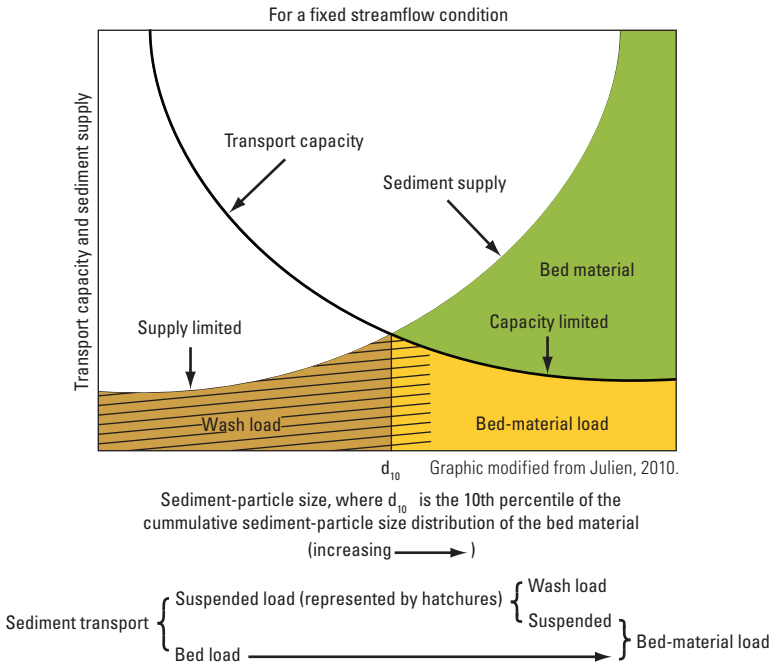

Figure 9. Graph showing conceptual diagram of sediment transport with suspended-sediment load indicated by diagonal hachuring.

load); the yellow-shaded area to the right of the d_{10} and below the transport-capacity curve represents conditions where capacity limitations dominate (bed-material load). The green-shaded area to the left of the d_{10} and above the transport-capacity curve represents the sediment-particle sizes and relative abundances within the streambed (bed material). Bed-material load can be further separated by mode of sediment motion as (1) bed load, a thin layer along the streambed; and (2) suspended load, within the water column. For sand-sized particles, both bed- and suspended-load transport can occur simultaniously.

Sediment transport can be separated into bed-material load and wash load based on the sediment-particle-size distribution of the streambed (fig. 9). Bed-material load represents transport of sediment-particle sizes found in appreciable quantities within the size distribution of the bed material and relates to interaction between the bed and the transported material. The sediment-particle sizes of the wash load are not found in appreciable quantities within the streambed and represent transient deposition that has negligible effects on the streambed morphology over longer time periods (months to a year). The 10th percentile of the bed-material sediment-particle-size distribution (d_{10}) often is designated as the threshold between bed-material load and wash load (wash-load sediment-particle sizes < d_{10} < bed-material load sediment-particle sizes) (Julien, 2010). Separation of the components of sediment transport (bed-material load and wash load) can be useful when evaluating what factors relate to channel morphology and aquatic habitat within the stream.

Within this report, incipient-motion analysis is used to characterize transport initiation of the bed-material load. Bed-material load is capacity limited and as such, transport conditions can be evaluated as a function of the forces acting on particles within the stream, providing a direct link between streamflow management and sediment-transport conditions.

Within this report, regression analysis is used to characterize the suspended-sediment load within the system (Cohn, 2005; Dalby, 2006; Runkel and others, 2004). Complications arise from concurrent transport of both wash load and the suspended fraction of the bed-material load within the suspended-sediment load. Wash load is limited by sediment supply and is controlled by a range of in-channel and out-of-channel processes that may not be directly related to streamflow conditions. As such, characterization of the suspended-sediment load within these systems must be empirically derived (SS flux and SS concentration transport equations) from observed conditions within the system. Separation of wash load from the suspended fraction of the bed-material load is done based on available sediment-particle-size information. In the following discussion, a distinction will be made between sediments that range from 0.0625 to 2.0 mm (sand SS flux) in diameter from SS flux, as warranted. Interpretations of the variables used within the regression analysis will aid in identification and quantification of the processes or mechanisms that are important controls on suspended-sediment transport within the system and to provide information on the timing of sediment inputs (supply changes).

Suspended-Sediment Transport Equations

Suspended-sediment transport equations were generated for the six stations that had sufficient data within the study area: (1) USGS streamflow-gaging station, 09095500, Colorado River near Cameo, Colorado, 1982–98, (hereafter, CAMEO); (2) USGS streamflow-gaging station, 09163500, Colorado River near the Colorado–Utah State line, 1976–2007 (hereafter, STATELINE); (3) USGS streamflow-gaging station, 09180500, Colorado River near Cisco, Utah, 1967–2000 (hereafter, CISCO); (4) USGS streamflow-gaging station, 09152500, the Gunnison River near Grand Junction, Colorado, 1976–2007 (hereafter, GUNNISON); (5) USGS streamflow-gaging station, 09261000, Green River near Jensen, Utah, 1965–2007 (hereafter, JENSEN); and (6) USGS streamflow-gaging station, 09315000, Green River at Green River, Utah, 1965–2000 (hereafter, GREEN) (table 5). Regression analysis using multiple explanatory variables can provide a means to assess the relative importance of differing variables and allows a single regression equation to be used to evaluate the entire dataset. Sediment-transport equations can be used to assess the persistence of temporal trends (between-year variations) and to quantify the seasonal variation (within-year variations) in sediment transport that may be important to future water management.

Comparisons of the calibration dataset to suspended-sediment-transport equation predictions (equation fit) are shown in figures 10–13 as scatterplots depicting the relations between streamflow and SS concentration or sand SS concentration (sand SS). This representation simplifies the depiction of the transport equation by excluding explicit representation of seasonality and temporal trends that would necessitate additional axes or the use of an axis that is the mathematical combination of all explanatory variables. Figures 10–13 simplify the regression equations to a two-dimensional space, which aids understanding and interpretation; however, this representation requires incorporation of multiple data series within the graphs to accurately depict the equation fit. To account for seasonality, figures 10 and 12 present regression predictions for each day of the year derived from artificial hydrographs (produced from daily mean streamflow record) representing three hydrologic conditions: (1) a dry year, 5th percentile of the daily mean streamflow; (2) an average year, mean of the daily mean streamflow; and (3) a wet year, 95th-percentile of the daily mean streamflow. Similarly, to account for limitations in depictions of temporal trends, figures 11 and 13 are used to present regression predictions for each day of the year given the average-year artificial hydrograph at three intervals within the transport-equation time period (where time trends were characterized as statistically significant): (1) early year, beginning of time period; (2) middle year, middle of time period or year of minimum trend value; and (3) late year, end of time period.

The variables that were found to have a significant statistical relation to natural logarithm SS flux (and natural logarithm SS concentration) were typically consistent along river reaches and are shown in table 5. Based on the coefficient of determination (adjusted R^2 values) from manipulated forms of these equations, approximately 75 percent of the variability of the sampled natural logarithm SS flux at these stations can be explained by a combination of streamflow, seasonality, and temporal trends (approximately 80 percent for natural logarithm sand SS flux). Use of an adjusted R^2 value prevents over estimation of the variance explained within the regression equation so that the addition of explanatory variables does not artificially inflate the perceived explanatory power of the regression (Helsel and Hirsch, 2002).

Comparisons of the adjusted R^2 for manipulated forms of the natural logarithm SS concentration equations show that approximately 49–60 percent of the variability of the sampled natural logarithm SS concentration is explained by a combination of streamflow, seasonality, and temporal trends (approximately 57–87 percent for natural logarithm sand SS concentration) (fig. 14). For each station, the linear or quadratic relation with natural logarithm streamflow (Q, Q^2, and β_0, in table 5) explained 26–40 percent of the observed variability in natural logarithm SS concentration (39–72 percent for natural logarithm sand SS concentration); seasonality (time within the year) explained 13–16 percent of the observed variability in natural logarithm SS concentration (2.1–14 percent for natural logarithm sand SS concentration); and temporal trends (time over multiple years) explained 1.5–8.9 percent of the observed variability in natural logarithm SS concentration (0–6.2 percent for natural logarithm sand SS concentration).

Streamflow Effects on Suspended-Sediment Transport

Variation in seasonal streamflow source water and sediment supply can have a significant effect on the shape, slope, and intercept of the streamflow and sediment-transport relation (Glysson, 1987; Horowitz, 2003). This relation is dependent on the mobility and abundance of in-stream sediment supplies. When streambed sediments are immobile or sediment quantity is limited by out-of-channel sources, such as tributary input or streambank failure, the relation between streamflow and sediment transport may have greater variability or difference in shape. For a nonlinear fit of the data, quadratic natural logarithm streamflow (when statistically significant) helped define the natural logarithm SS concentration-streamflow relation as a portion of a parabola. To further explore the processes important to sediment transport, it is useful to relate each explanatory variable to the occurrences within the stream that result in suspension and transport of the sediment (forces) and the availability of the sediment to be transported (sediment supply).

Streamflow quantity can be thought of as a surrogate for the forces within these streams. Within alluvial streams, increases in streamflow typically results in increased sediment transport. In general, this relation held true at each station. Natural logarithm streamflow explained 26–40 percent of the observed variability in natural logarithm SS concentration

Table 5. Regression coefficients and equation properties for suspended-sediment transport at selected U.S. Geological Survey streamflow-gaging stations in the Upper Colorado River Basin.

[β_0, regression equation intercept; Ln, natural logarithm; K, positive integer used in seasonality variables; T, seasonal time; Q, centered streamflow; Q^2, centered streamflow squared; Q*, centering value for streamflow; Sin, sine function; Cos, cosine function; t, centered decimal time in decimal years; t^2, centered decimal time in decimal years, squared; t*, centering value for decimal time; ERV, estimated residual variance; SCR, serial correlation of residual; R^2, coefficient of determination (adjusted R^2); N, number of data points; C, number of censored data points; SS, suspended-sediment; *, statistical significance (p-value <0.01); --, variables not used in the regression; #, not statistically significant (p-value >0.05); and Sand, sediments with diameters between 2.0–0.0625 millimeters]

Abbreviation	β_0	Ln streamflow			Seasonality variables						Decimal time			Statistical diagnostics			
					Fourier series				Dummy variables								
					$K\ 2\pi T,\ K=1$		$K\ 2\pi T,\ K=2$										
		Q	Q^2	Q*	Sin	Cos	Sin	Cos	Rain event	Rising limb	t	t^2	t*	ERV	SCR	R^2	N/C
Ln SS flux																	
Cameo	7.459*	2.087*	--	5,305	0.518*	0.215	0.297*	–0.363*	1.077*	0.876*	–0.047*	--	1,989.87	0.934	0.264	74.4	529
Gunnison	6.165*	1.725*	0.245*	2,750	–.064#	–.673*	.031#	–.275*	.473*	.670*	--	0.00465*	1,991.20	.748	.098	77.9	242
Stateline	7.857*	1.603*	.168	7,710	.019#	–.667*	–.001#	–.352*	.730*	.837*	–.026*	--	1,991.02	.864	.129	76.7	261
Cisco	8.738*	1.892*	–.252	8,306	–.179#	–.582*	.263	–.476*	1.148*	.883*	–.043*	--	1,984.42	1.182	.332	74.2	308
Jensen	7.761*	1.856*	--	5,178	.150#	–.447*	.224#	–.701*	.833*	.549*	–.023*	.00187*	1,986.40	.983	.152	72.8	235
Green	9.500*	2.043*	–.208	6,871	–.071#	–.609*	.182	–.515*	--	--	–.040*	--	1,983.1	.941	.235	73.5	329
Ln Sand SS flux																	
Cameo	5.963*	2.313*	--	5,226	0.434*	0.0560#	–0.094#	–0.268*	0.408*	0.506*	–0.029	--	1,990.12	0.712	0.245	83.2	449
Gunnison	4.875*	2.367*	--	2,797	.146#	–.403*	–.014#	–.413*	--	--	--	0.00396*	1,994.33	.900	.129	80.11	143/3
Stateline	6.328*	2.016*	--	8,298	–.446*	–.397*	--	--	--	1.302*	–.038*	.00453*	1,990.34	.936	.315	78.9	166/1
Cisco	6.729*	2.694*	–0.392	7,869	.573*	–.096#	--	--	--	--	--	--	1,988.05	1.852	.234	74.31	154/8
Jensen	5.822*	2.703*	--	4,407	1.030*	.803*	.585	.146#	--	--	.054*	--	1,988.5	.710	.410	93.07	57/12
Green	7.261*	3.366*	–.754*	6,575	--	--	--	--	–.968*	--	--	--	1,987.8	2.511	.228	72.99	159/12
Ln SS concentration																	
Cameo	4.797*	1.087*	--	5,305	0.518*	0.215	0.297*	–0.363*	1.077*	0.876*	–0.047*	--	1,989.87	0.934	0.264	53.65	529
Gunnison	4.161*	.725*	0.245*	2,750	–.064#	–.673*	.031#	–.275*	.473*	.670*	--	0.00465*	1,991.20	.748	.098	59.88	242
Stateline	4.821*	.603*	.168	7,710	.019#	–.667*	–.001#	–.352*	.730*	.837*	–.026*	--	1,991.02	.864	.129	57.19	261
Cisco	5.627*	.892*	–.252	8,306	–.179#	–.582*	.263	–.476*	1.148*	.883*	–.043*	--	1,984.42	1.182	.332	55.37	308
Jensen	5.124*	.856*	--	5,178	.150#	–.447*	.224#	–.701*	.833*	.549*	–.023*	.00187*	1,986.40	.983	.152	48.85	235
Green	6.579*	1.040*	–.208	6,871	–.071#	–.609*	.182	–.515*	--	--	–.040*	--	1,983.1	.941	.235	51.45	329
Ln Sand SS concentration																	
Cameo	3.316*	1.313*	--	5,226	0.434*	0.0560#	–0.094#	–0.268*	0.408*	0.506*	–0.029	--	1,990.12	0.712	0.245	66.41	449
Gunnison	2.854*	1.367*	--	2,797	.146#	–.403*	–.015#	–.412*	--	--	--	0.00395*	1,994.33	.900	.129	59.76	143/3
Stateline	3.218*	1.016*	--	8,298	–.446*	–.397*	--	--	--	1.302*	–.038*	.00453*	1,990.34	.936	.315	59.3	166/1
Cisco	3.673*	1.694*	–0.393	7,869	.572*	–.096#	--	--	--	--	--	--	1,988.05	1.852	.234	56.69	154/8
Jensen	3.342*	1.704*	--	4,407	1.039*	.799*	.588	.148#	--	--	.054*	--	1,988.5	.706	.410	87.19	57/12
Green	4.384*	2.366*	–.754*	6,575	--	--	--	--	–.968*	--	--	--	1,987.8	2.510	.228	58.48	159/12

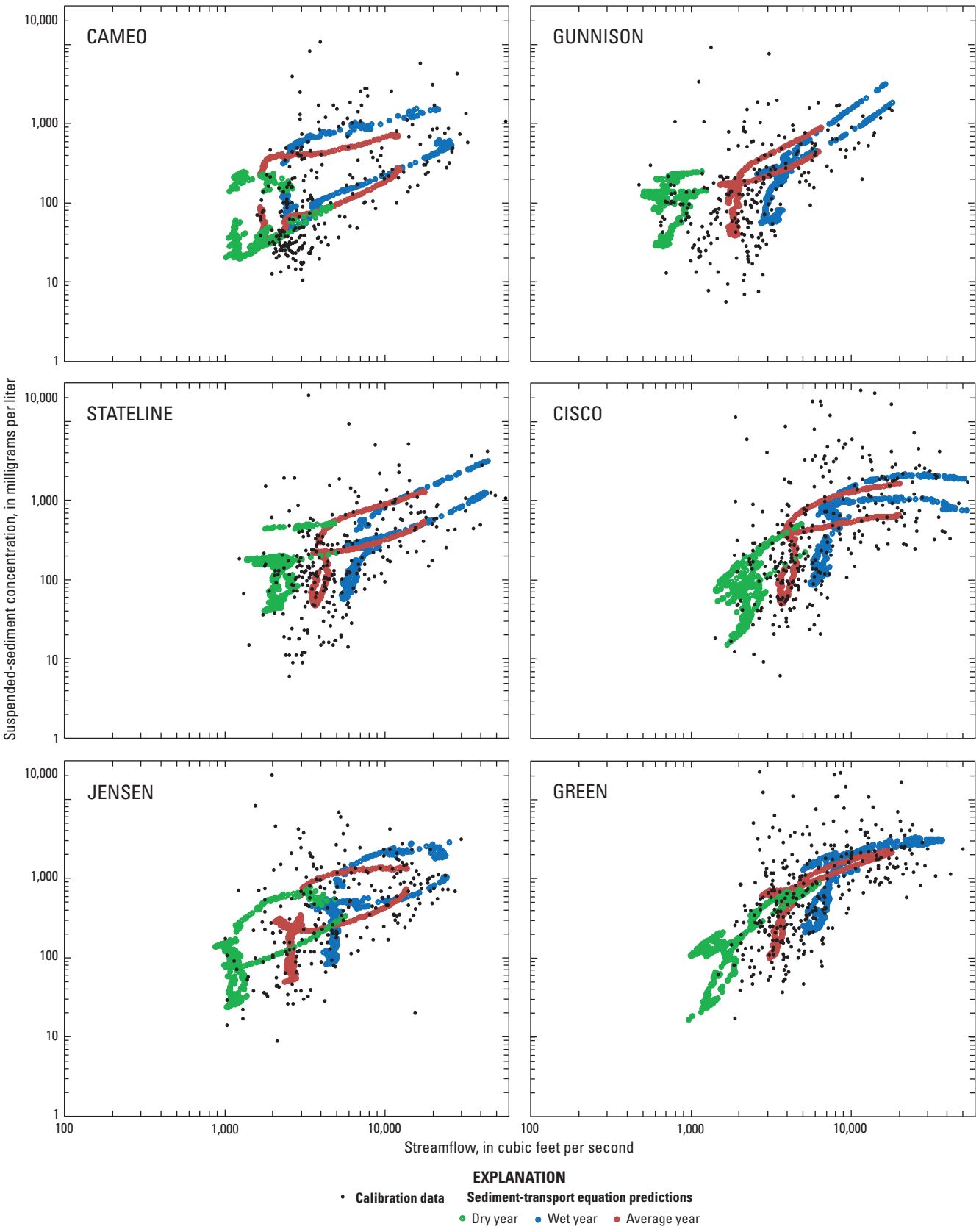

Figure 10. Graphs showing calibration data with sediment-transport equation predictions for suspended-sediment concentration at three hydrologic conditions calculated as (1) dry year, 5th-percentile; (2) average year, mean; and (3) wet year, 95th-percentile of the daily mean streamflow record for each day.

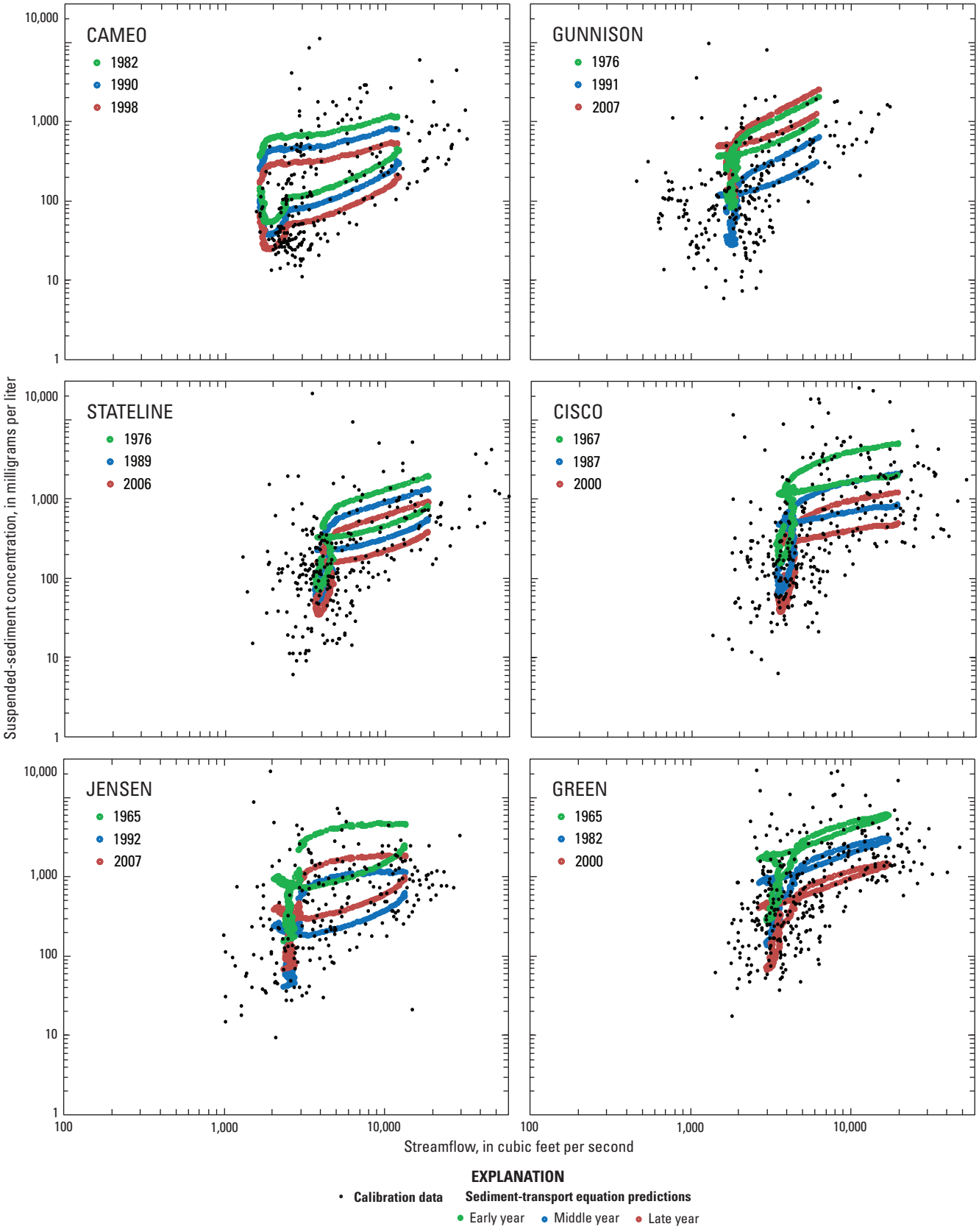

Figure 11. Graphs showing calibration data with sediment-transport equation predictions for suspended-sediment concentration at three time periods: (1) early year, beginning of sediment-transport equation period; (2) middle of sediment-transport equation period or year of minimum trend value; and (3) late year, end of sediment-transport equation period.

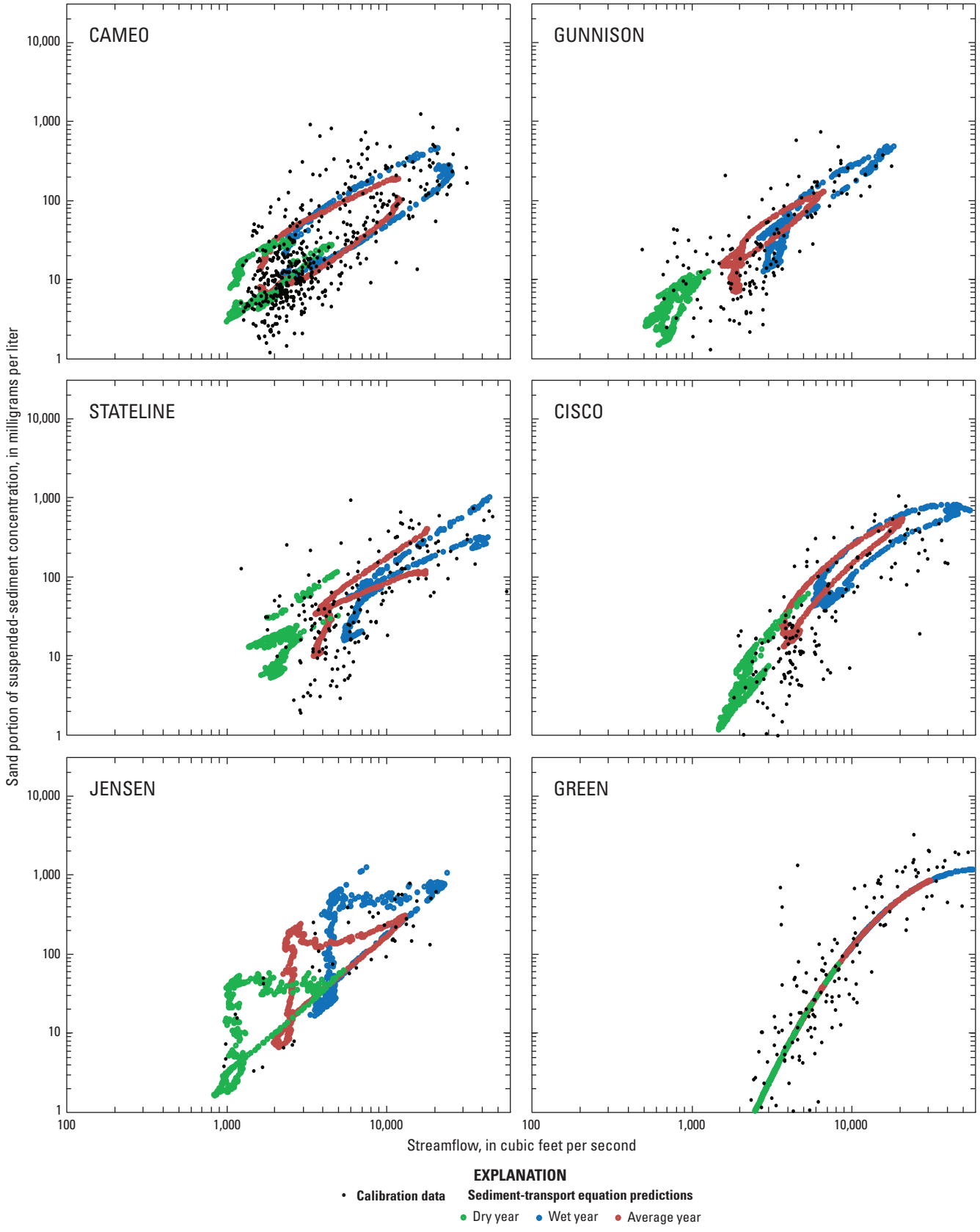

Figure 12. Graphs showing calibration data with sediment-transport equation predictions for the sand portion of the suspended-sediment concentration at three hydrologic conditions calculated as (1) dry year, 5th-percentile; (2) average year, mean; and (3) wet year, 95th-percentile of the daily mean streamflow record for each day.

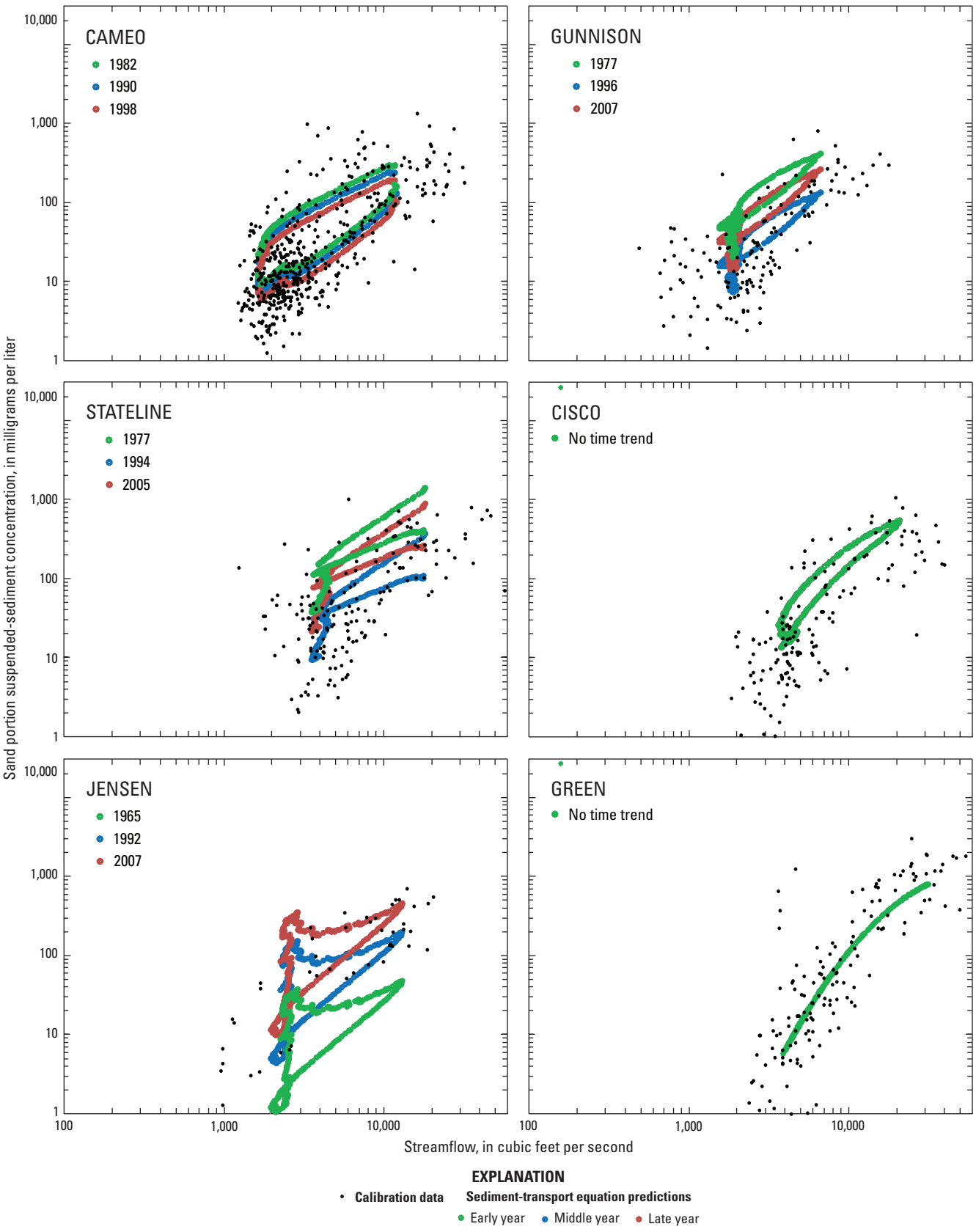

Figure 13. Graphs showing calibration data with sediment-transport equation predictions for the sand portion of the suspended-sediment concentration at three time periods: (1) early year, beginning of sediment-transport equation period; (2) middle of sediment-transport equation period or year of minimum trend value; and (3) late year, end of sediment-transport equation period.

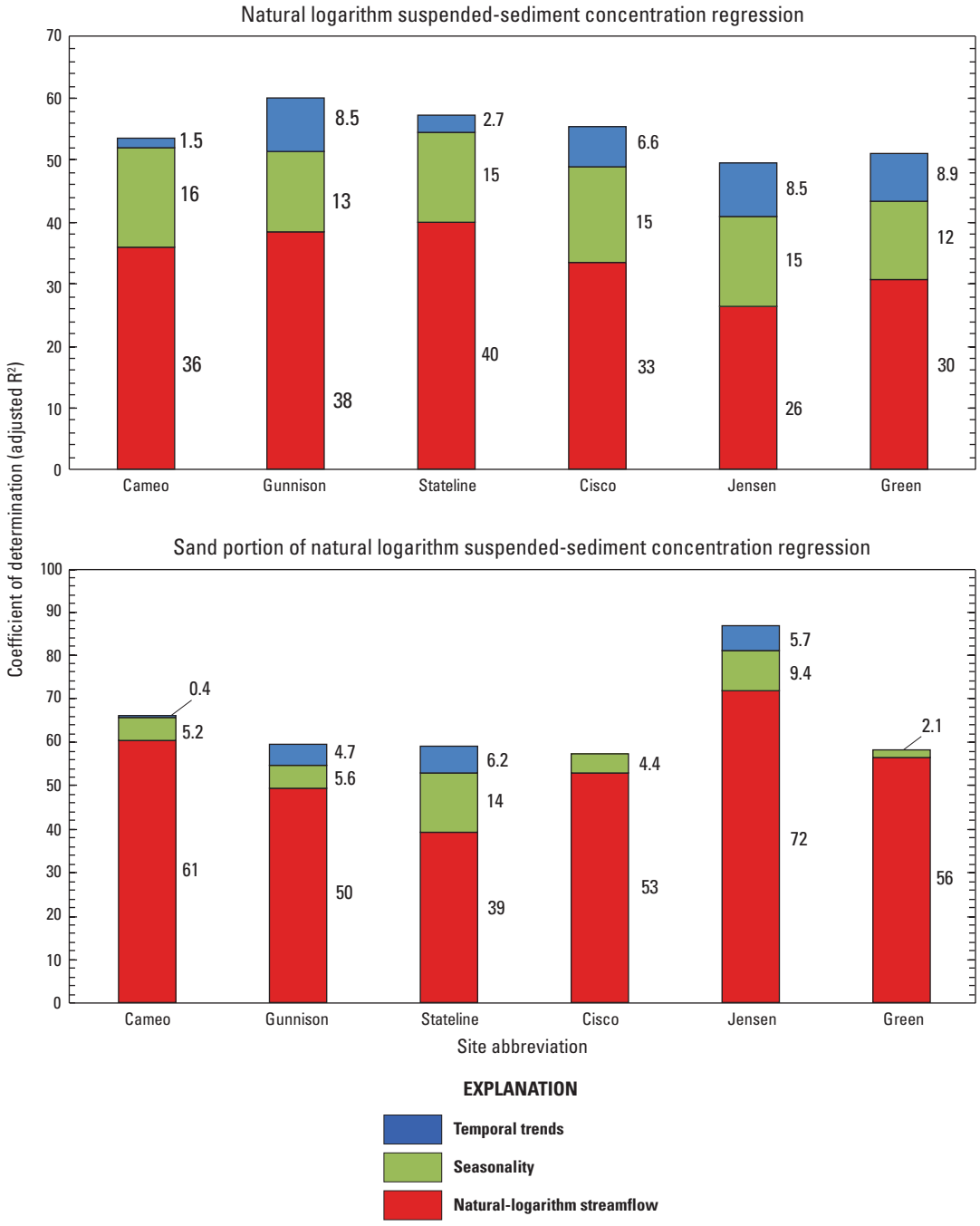

Figure 14. Graphs showing comparison of the coefficient of determination (adjusted R^2) for explanatory variables within the suspended-sediment-transport regression analysis at selected U.S. Geological Survey streamflow-gaging stations.

(39–72 percent for natural logarithm sand SS concentration); however, 60 percent or more of the variability in natural logarithm SS concentration is explained by variables other than streamflow or remains unexplained (28 percent or more for natural logarithm sand SS concentration).

The streamflow relation to SS concentration inherently includes factors related to sediment supply when increases in streamflow include additions of sediment. Examples include intense snowmelt-runoff conditions or rain events that result in new sediment supplies to main-stem areas from tributaries, or initial inundation and transport of sediments from bars or overbank areas. Understanding the shape of the streamflow relation can provide information on how the rivers respond to changes in streamflow and if sediment supply is inherent in the relation (Asselman, 2000). The typical (median) relations between streamflow and SS concentration (and sand SS concentration) are shown in figure 15 for each station.

The concavity (upward or downward) of the transport curve at a station relates how changes in streamflow relate to changes in SS concentration. Concave-downward SS concentration-transport equations may indicate that sediment supplies can become limited at larger streamflows (Horowitz, 2003) or relate to the effects of changes in the channel geometry as streamflow increases (for example, reductions in the rate-of-change of boundary shear stress as flow begins to transition into larger cross sections or out-of-bank areas may cause reduced slopes within the transport curve at larger streamflows). The streamflow and sediment-transport relation at CISCO and GREEN are the only stations with a concave-downward transport equation (fig. 15). The transport-curve shape for these stations, for both SS concentration and sand SS concentration, may indicate that sediment supplies are limited during larger streamflow events (because the reduction in transport occurs for both SS concentration and sand SS concentration, which is less likely to occur if the change is owing to out-of-bank flow).

Concave-upward transport equations may show that sediment transport is less restricted by streamflow forces at the lower end of the transport curve and are more strongly controlled by sediment supplies (Horowitz, 2003). The STATELINE and GUNNISON stations have concave-upward relations for SS concentration with linear relations at the remaining stations. The transport-curve shape at STATELINE and GUNNISON may result from sediment inputs derived from rain events, agriculture, or other processes that produce increases in SS concentration without substantial increases in main-channel streamflows during base-flow conditions.

Seasonal and Temporal Effects on Suspended-Sediment Transport

Depictions of the typical annual cycle for each station were done to evaluate changes within the sediment-transport relation with streamflow. Figure 16 shows the annual cycle of SS concentration derived from each transport equation for an average year (artificial hydrograph produced from mean of daily mean streamflow record, shown as inset on each graph). Examination of the chronological sequences within the plots shows that the SS concentration for a given flow is seasonally dependent; that is, for a specific streamflow there can be multiple predicted SS concentrations depending on time of year. Seasonal differences in the relation between streamflow and SS concentration (hysteresis) are evident in the differences in the slopes and shapes of each plot when compared between stations or between SS concentration and sand SS concentration. Hysteresis can result from differences in source waters (tributary contributions) or sediment sources within the basin and may be owing to differing processes or sediment availability within the watershed (Cohn and others, 1992; Asselman, 2000; Horowitz, 2003). To increase sediment transport, sediments of the correct size class must be available. Sediment supply is not limited to a single-source area or process, and these processes can vary within the system and through time (seasonally and over multiple years). First-flush events from early snowmelt, rainstorm runoff, and intermittent streamflows from ephemeral streams typically are characterized with high SS concentration relative to streamflow (Curtis and others, 2005; Williams and others, 2009). Conversely, late-season runoff from snowmelt and base-flow conditions typically are characterized by reduced SS concentration. Both observations are related to sediment-supply conditions within the system instead of the forces within the stream and can be observed through comparison in SS concentration and sand SS concentration in figure 16.

Seasonality will account for consistent changes in the availability of sediments that are not as well represented by changes in streamflow alone. Seasonality coefficients, including the Fourier series and dummy variables (rain events and rising-limb of the hydrograph), explain approximately 15 percent of the variability in natural logarithm SS concentration at each station (fig. 14). Within the seasonality grouping, the variables that represent the rain events and the rising-limb of the hydrograph were significant at all stations except the GREEN station for natural logarithm SS concentration. These variables augment the Fourier series and better represent more abrupt seasonal changes, as well as variations that occur in less consistent patterns. Augmentation of the Fourier series during rain events was most significant at CAMEO, CISCO, JENSEN, and STATELINE (4.8, 4.3, 2.6, and 2.5 percent of the variability in natural logarithm SS concentration, respectively); with less of the variability in natural logarithm SS concentration being explained at GUNNISON and GREEN (1.4 and 0 percent of the variability in natural logarithm SS concentration, respectively) (fig. 14). Augmentation of the Fourier series during the rising-limb of the hydrograph was most significant at STATELINE, CAMEO, CISCO, and GUNNISON (2.9, 2.4, 2.1, and 1.9 percent of the variability in natural logarithm SS concentration, respectively); with less of the

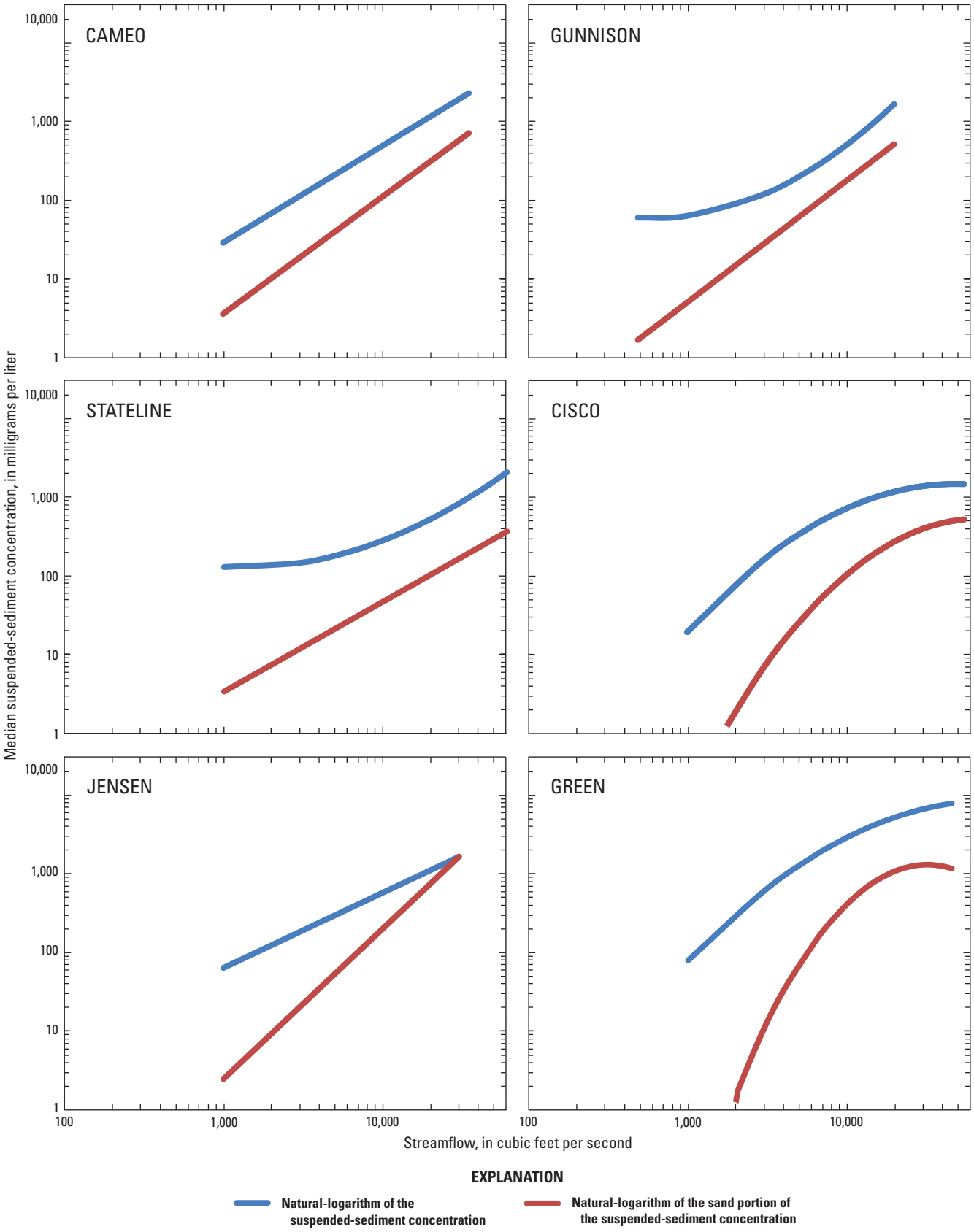

Figure 15. Graphs showing statistical relation between median suspended-sediment concentration and streamflow at selected U.S. Geological Survey streamflow-gaging stations.

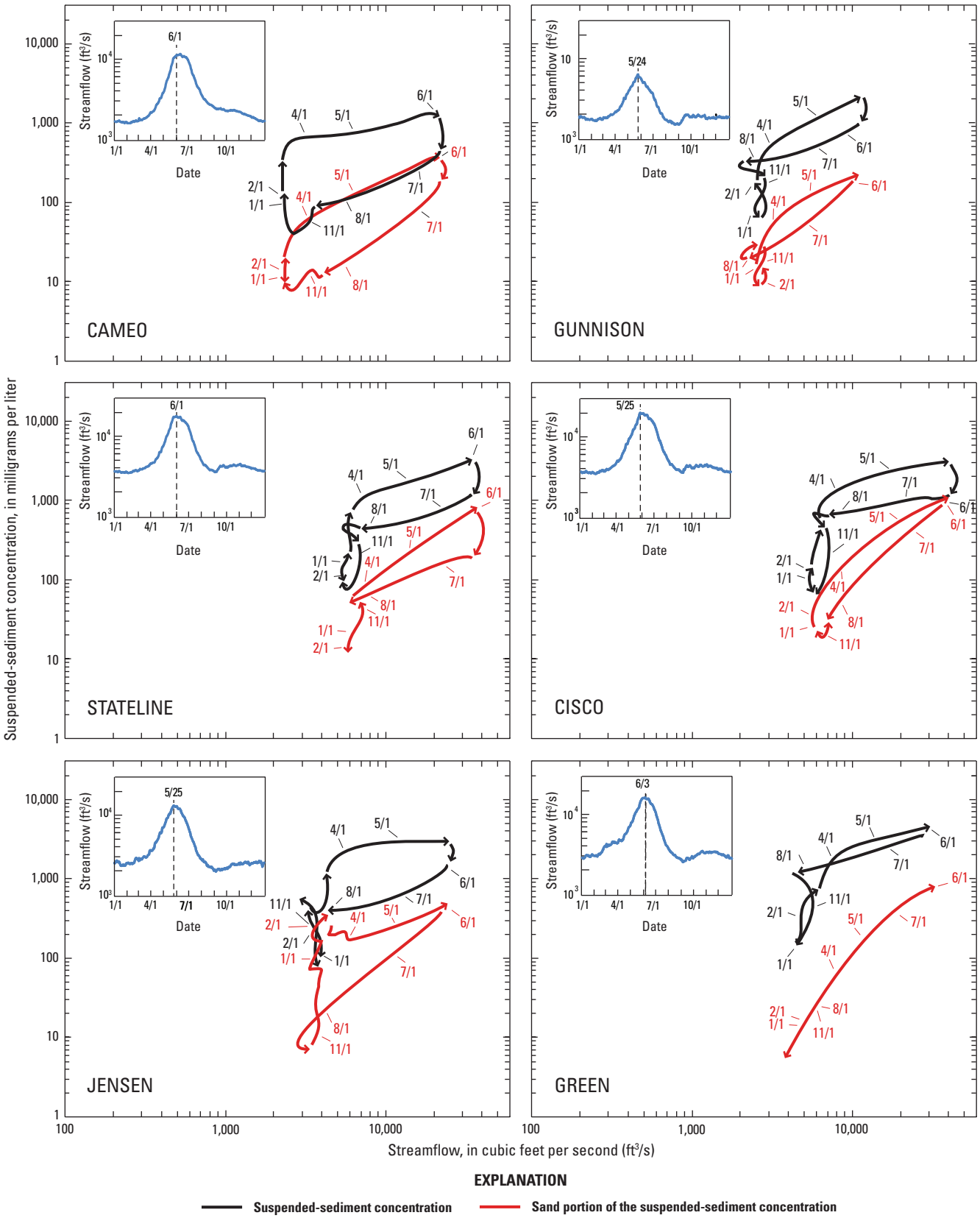

Figure 16. Graphs showing hysteresis loops (seasonal changes in suspended-sediment concentration) at selected U.S. Geological Survey streamflow-gaging stations.

variability in natural logarithm SS concentration explained at JENSEN and GREEN (1.5 and 0 percent of the variability in natural logarithm SS concentration, respectively). Seasonal differences in SS concentration arising from the seasonality variables are shown in figure 16 for an average year (artificial hydrograph produced from mean of daily mean streamflow record).

The seasonality coefficients, including the Fourier series and dummy variables (rain events and rising-limb of the hydrograph), explain 2.1–14 percent of the variability in natural logarithm sand SS concentration at each station (STATELINE, 14; JENSEN, 9.4; GUNNISON, 5.6; CAMEO, 5.2; CISCO, 4.4; and GREEN, 2.1 percent of the variability in natural logarithm sand SS concentration) (fig. 14). Within the seasonality grouping, the variables that represent the rain events and the rising-limb of the hydrograph were not significant at most stations for natural logarithm sand SS concentration. At CAMEO, both rain events and rising-limb of the hydrograph were significant (0.7 and 0.8 percent of the variability in natural logarithm sand SS concentration, respectively); at STATELINE the rising-limb of the hydrograph was significant (8.5 percent of the variability in natural logarithm sand SS concentration); at GREEN the rain event was significant and negatively correlated (2.1 percent of the variability in natural logarithm sand SS concentration). At stations where the rain-events dummy variable is significant for SS concentration and not for sand SS concentration (or negatively correlated to sand SS concentration), rain events increase fine-sediment supplies (particle diameters less than 0.0625 mm) without appreciable increases in sand. This explanation is supported by observed sediment-particle sizes of suspended sediments from rain events at GUNNISON and JENSEN where nearly 100 percent of the suspended material transported from large rain events was less than 0.0625 mm in diameter (Williams and others, 2009). Seasonal differences in sand SS concentration arising from the seasonality variables are shown in figure 16 for an average year (artificial hydrograph produced from mean of daily mean streamflow record).

Temporal-trend analysis can identify consistent patterns in the dataset as changes over multiple years. Temporal trends within this analysis described changes in sediment transport and changes in suspended-sediment-particle sizes. Statistically significant temporal trends were found for all stations analyzed in this report for natural logarithm SS concentration and had adjusted R^2 ranging from 1.5 to 8.9 percent (0 to 6.2 percent for natural logarithm sand SS concentration) (fig. 14). Temporal trends may be most substantial at stations located in reaches downstream from large main-stem reservoirs (GREEN, 8.9; GUNNISON, 8.5; JENSEN, 8.5; and CISCO, 6.6 percent of the variability in natural logarithm SS concentration) with less of the variability in natural logarithm SS concentration explained at STATELINE and CAMEO (2.7 and 1.5 percent of the variability in natural logarithm SS concentration, respectively). CAMEO, STATELINE, CISCO, and GREEN showed linear downward trends in natural logarithm SS concentration (fig. 17). GUNNISON and JENSEN were best fit by concave-upward natural logarithm SS concentration trends that describe downward trends followed by upward trends (trend reversals 1991 and 1992, respectively) (fig. 17).

The temporal trends in natural logarithm sand SS concentration were similar in shape for GUNNISON and CAMEO (4.7, 0.4 percent of the variability in natural logarithm sand SS concentration, respectively); and with changes in the shape of the trends at STATELINE and JENSEN (6.2 and 5.7 percent of the variability in natural logarithm sand SS concentration, respectively) (fig. 18). No trends were detected in natural logarithm sand SS concentration at CISCO and GREEN. For GUNNISON and STATELINE, the natural logarithm sand SS concentration trends were best fit by concave-upward parabolas that describe downward trends followed by upward trends (trend reversals 1996 and 1994, respectively). At JENSEN, trends in natural logarithm sand SS concentration are upward over the entire period. The trend at JENSEN shows reductions in overall natural logarithm SS concentration up to the early 1990s, followed by increases in natural logarithm SS concentration. The proportion of sand transported at this station increased over the entire period.

The temporal trends determined by this analysis show changes in the relation between streamflow and SS concentration within the post-reservoir period (post 1965 for JENSEN and GREEN; post 1967 for GUNNISON, STATE, and CISCO). When these patterns are present at a station, interpretation of the time variable is a relative increase or decrease in sediment response under equivalent stream conditions (figs. 17 and 18). Time trends indicate that mean annual SS concentration for CAMEO, STATELINE, CISCO, and GREEN decreased by 12.9, 11.3, 37.6, and 62.6 milligrams per liter (mg/L) per year, respectively (total change in concentrations over period was 220; 350; 1,278; and 2,255 mg/L, respectively). Linear approximations of the parabolic trends in mean annual SS concentration for GUNNISON and JENSEN decreased by 19.2 and 47.4 mg/L per year, respectively (total change in concentrations over period was 307 and 1,328 mg/L, respectively); followed by increases of 27.1 and 14.1 mg/L, respectively (total change in concentrations over period was 460 and 226 mg/L, respectively).

Mean annual sand SS concentration for CAMEO decreased by 2.0 mg/L per year (total change in concentration over period was 34 mg/L). At JENSEN, concentration increased by 4.1 mg/L per year with a total change in concentration over the period of 174 mg/L. Linear approximations of the parabolic trends in mean annual sand SS concentration for GUNNISON and STATELINE decreased by 5.6 and 12.4 mg/L per year, respectively (total change in concentrations over period was 112 and 224 mg/L, respectively); followed by increases of 2.2 and 4.6 mg/L, respectively (total change in concentrations over period was 26 and 55 mg/L, respectively).

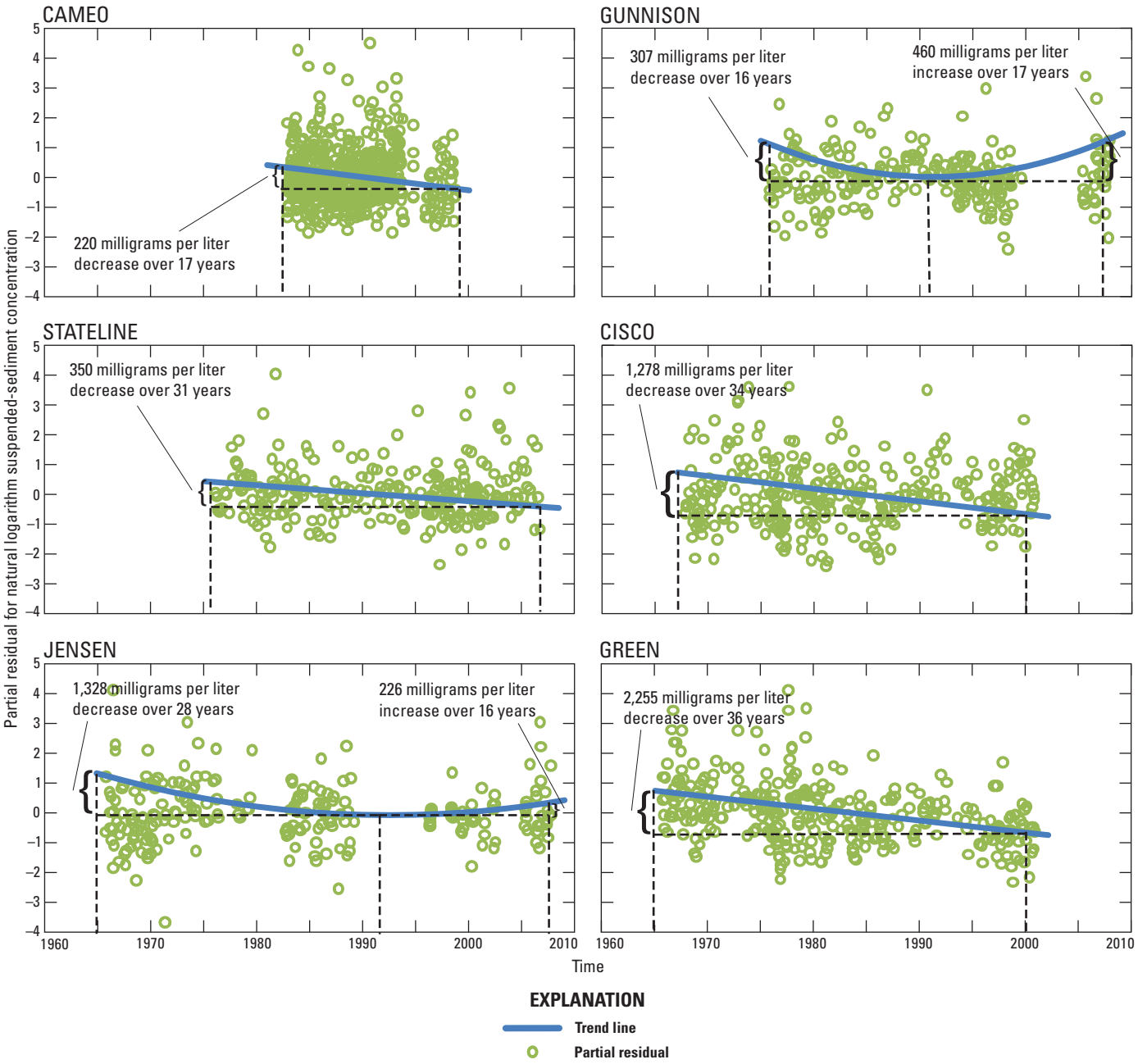

Figure 17. Graphs showing temporal trends in total suspended-sediment concentration at selected U.S. Geological Survey streamflow-gaging station locations.

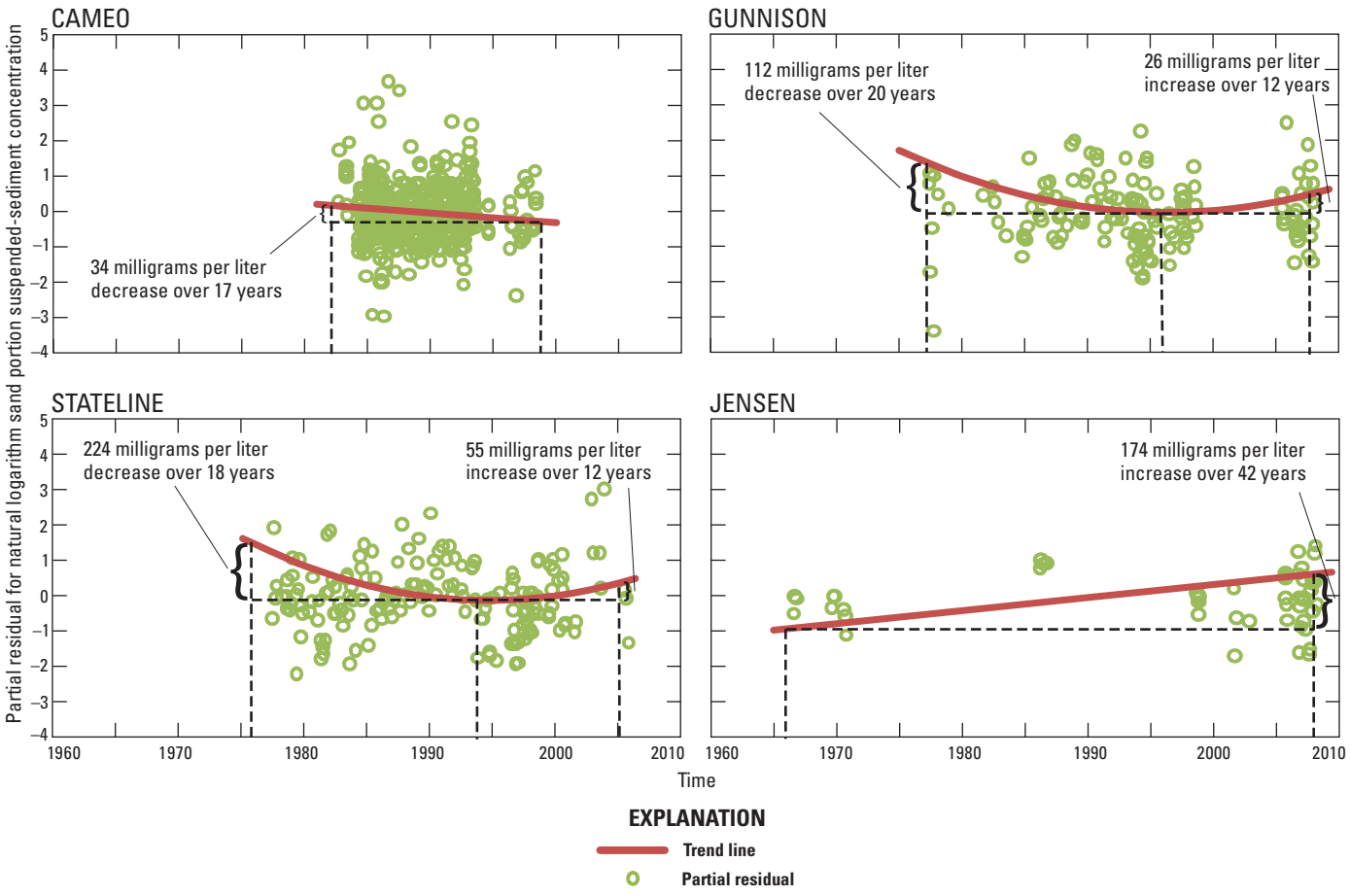

Figure 18. Graphs showing temporal trends in sand portion of the suspended-sediment concentration at selected U.S. Geological Survey streamflow-gaging station locations.

Climatic Effects on Suspended-Sediment Transport Equations

As previously discussed, suspended-sediment transport is governed not only by sediment-transport capacity of a stream but also by sediment supply (fig. 9). During wet years, channel-bed scour and erosion can remove substantial amounts of stored bed sediment. The reduction in sediment abundance may result in an adjustment in the shape of the relation between streamflow and sediment concentration (Horowitz, 2003). In the same manner, dry years also can affect sediment storage. Periods of drought may result in temporary increases in sediment supply and storage when sediment is derived from in-stream sources (streambed and channel margins) or reduction of sediment storage when sediment is stored in overbank areas that are only inundated during high-flow periods. Comparisons between relations of natural logarithm streamflow and natural logarithm SS concentration were made between annual comparisons (wet and dry years) and multi-year cycles (wet years compared to wet years following dry periods, and dry years compared to dry years following wet periods).

Significant differences (p-value less than 0.05) in the slope and intercepts of the relation of natural logarithm streamflow and natural logarithm SS concentration were determined between wet and dry years. For the rising-limb of the snowmelt-runoff hydrograph, four of the six stations showed significant differences (CAMEO, CISCO, JENSEN, and GREEN); on the falling-limb of the snowmelt-runoff hydrograph, one of six stations showed significant differences (GUNNISON) (fig. 19). For each of the four stations during the rising-limb of the snowmelt-runoff hydrograph, the natural logarithm SS concentration during wet years generally is higher than natural logarithm SS concentration during dry years for the same streamflow. This indicates that natural logarithm SS concentration is less strongly controlled (flatter slopes) by streamflow magnitude in wet years. At CAMEO for wet years, the slope of the relation between natural logarithm

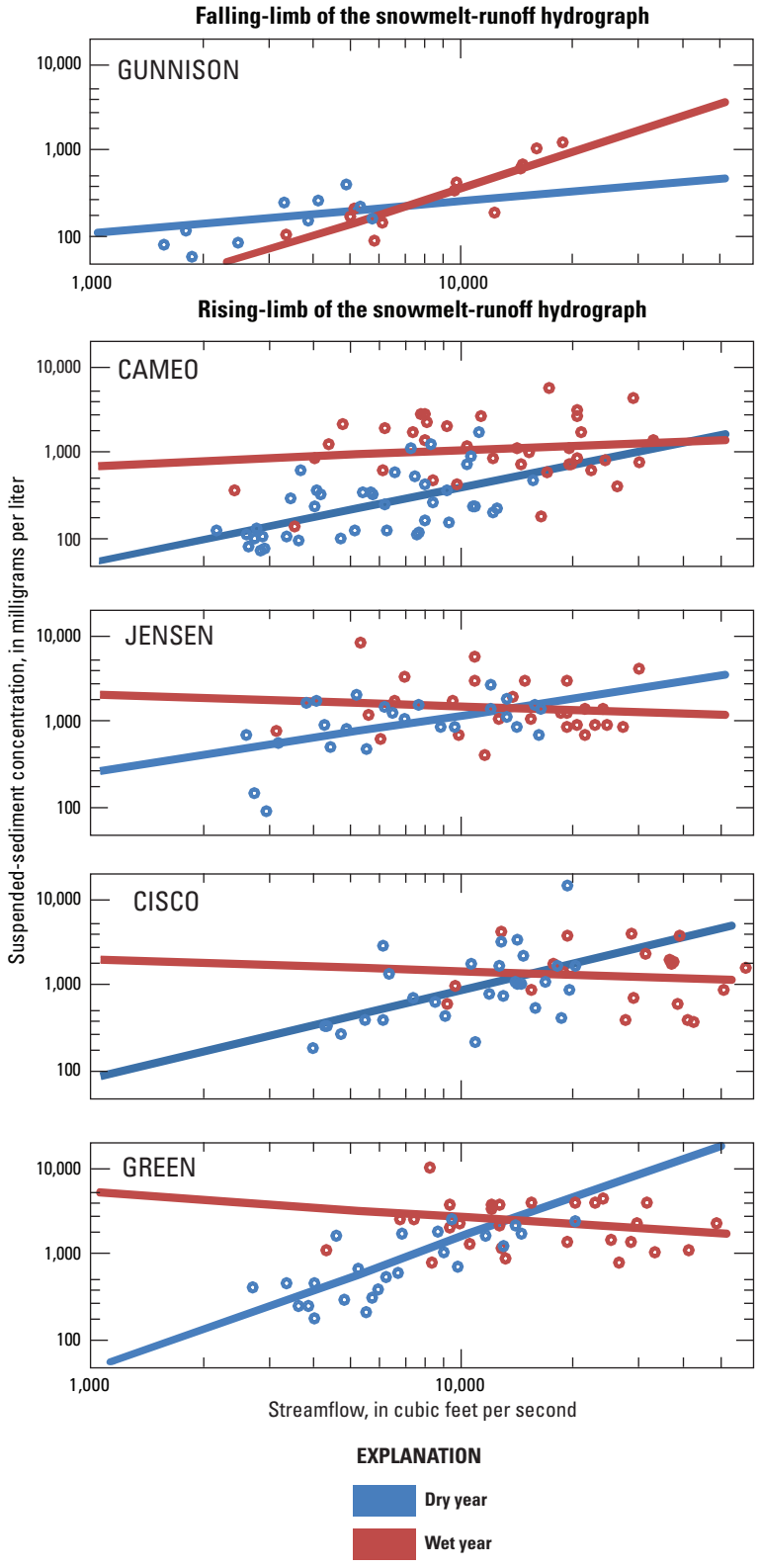

Figure 19. Graphs showing differences in the statistical relation between suspended-sediment concentration and streamflow between wet and dry years at selected U.S. Geological Survey streamflow-gaging stations.

streamflow and natural logarithm SS concentration is positive (upward) and small in magnitude; this means that large increases in streamflow correspond to small increases in natural logarithm SS concentration. At CISCO, JENSEN, and GREEN for wet years, the slope of the relation between natural logarithm streamflow and natural logarithm SS concentration is negative (downward) and small in magnitude; this means that large increases in streamflow correspond to small decreases in natural logarithm SS concentration.

Significant differences between wet and dry years on the falling-limb of the hydrograph at GUNNISON differ depending on flow conditions. At smaller streamflow values (less than 7,000 ft^3/s), dry years have higher SS concentrations than wet years, and at larger streamflows the concentrations are lower than wet years. Differences in sediment-transport processes or water management on the Gunnison River (Aspinall Storage Unit and (or) Ridgeway Reservoir) may be causing the inconsistency along the study reaches of the Gunnison and Colorado Rivers between GUNNISON and between CAMEO and CISCO. Comparisons between wet and dry years for the rising-limb of the hydrograph at stations other than GUNNISON did not show significant (p-value less than 0.05) differences in the slope or intercept.

No statistically significant differences were determined between any multi-year cycle comparison and may be indicative of the smaller dataset available for such comparisons.

Suspended-Sediment Transport Equation-Error Analysis

Sediment-transport equations are based on periodic sediment data and represent average sediment-transport conditions in a river. The average condition defined by the equations may not adequately represent the true condition in the stream. Further, shorter duration sediment-transport characteristics may not be well defined by the average condition represented by the sediment-transport equations.

It is useful to characterize the consistency of the relation between the explanatory and response variables over the period of data collection. The magnitude of the variability within the measured dataset can be identified within the regression analysis as the estimated residual variance (ERV) for regression equations. This is characterized by the error term in equation 2 and is summarized for each regression equation in table 5.

Two of the transport-equation datasets had daily SS flux data that were suitable for additional evaluation of transport-equation error (GUNNISON and JENSEN). The analysis was performed to characterize the "error" of the estimated SS flux at varying time steps. RMSE were calculated (as percent of the mean) from a comparison of daily observations to predicted values. Comparisons of RMSE for the SS flux transport-equation estimates show that the error associated with the transport equation varied (1) between the two stations; (2) at each station depending on the time step of the estimate (daily, weekly, monthly, or seasonal estimates); and (3) between the different seasons (rising limb, falling limb, or base flow) (fig. 20).

Both GUNNISON and JENSEN show decreasing errors as the time step increases for all seasons. Base-flow errors were highest at a daily time step and lowest at a seasonal time step at both stations. The variability of the base-flow analysis could be attributed to rain events, which affect the daily predictions. The variability observed during estimates of the rising-limb appears consistent regardless of the specified time step. This could be attributed to the high streamflows and concentrations associated with snowmelt. This analysis shows that applications of transport equations for suspended-sediment-transport estimates need to be used in accordance with the level of accuracy the specific application warrants. To limit the amount of error in any application, the largest applicable time step needs to be used.

Incipient Motion of Streambed Material

Determination of the incipient motion for streambeds composed of mixtures of sediment-size classes including sand, and gravel- or cobble-sized particles (hereafter referred to as "sands" or "gravels," respectively) requires an understanding of how these sediments are arranged within the streambed (bed structure). The bed structure can occur over a continuum from two end-member conditions: pure sands and pure gravels. For each of these two conditions, the prediction of motion can be defined by sediment-particle size (Julien, 2010). When sands and gravels are intermixed, substantial increases or decreases in the sediment mobility (or incipient motion) can occur for both size classes. In a gravel-framework bed (less than 20–30 percent sand), the gravel dominates the sediment mixture, and the bed structure is supported by gravel-on-gravel contact with sand filling the interstitial spaces between and beneath the gravel clasts. Under these conditions, the larger clasts shelter the sand and both grains remain immobile until the critical-shear stress for the gravels is exceeded. This produces conditions where as the portion of sand decreases to zero, the critical shear stress of both particles approaches that of pure gravels (Wilcock, 1998). In a sand-matrix bed (greater than 20–30 percent sand), the gravel clasts are supported by contact with sand deposits between each gravel clast. Under these conditions, sheltering of the sands is minimal and incipient motion of the gravels occurs at boundary shear stresses lower than the critical shear stress of gravels alone. This produces conditions where as the portion of sand approaches 100 percent, the critical shear stress for both size classes approaches that of pure sand (Wilcock, 1998).

Characterization of the sediment-particle size for each location is presented in table 6. For locations that are relatively free of sand, characterization of the d_{50} sediment-particle size is used to determine the boundary shear stress needed to entrain the streambed material within a given reach. At locations that demonstrate bimodal sediment-particle size distributions, the analysis is separated into the end-member conditions of sands and gravel and can be used to infer the range of mobility of these sediments along the continuum of possible combinations found within the study reaches. Comparisons of

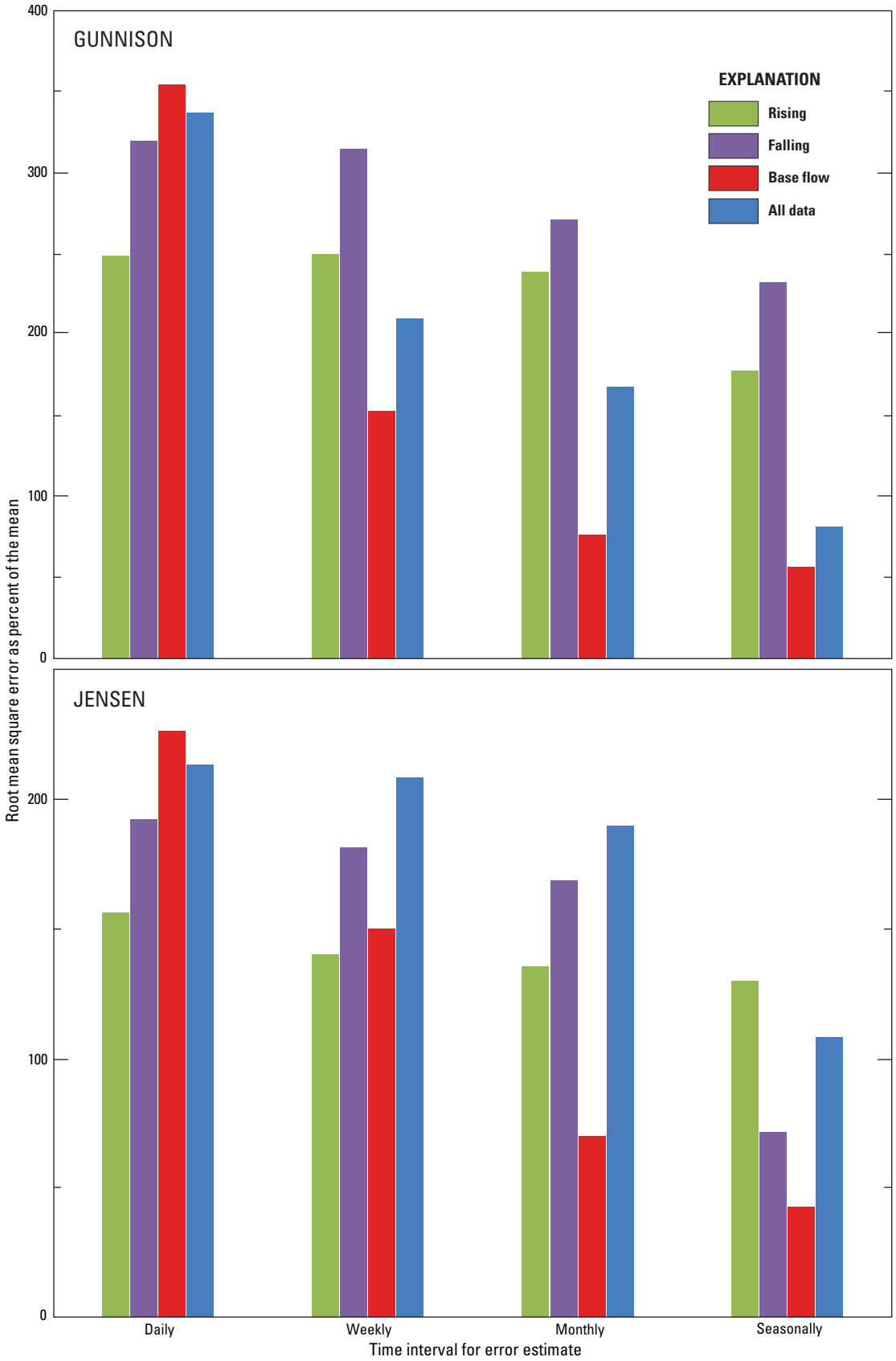

Figure 20. Graphs showing error between the regression predictions and available daily suspended-sediment records at U.S. Geological Survey streamflow-gaging stations GUNNISON, 09152500, Gunnison River near Grand Junction, Colorado; and JENSEN, 09261000, Green River near Jensen, Utah; water years 2005–8.

Table 6. Sediment-particle size distribution summary statistics of bed-material samples collected at selected locations in the Gunnison and Green Rivers in 2008 and 2006–7, respectively.

[mm, millimeters; <, less than; Gun, Gunnison River; Gr, Green River; L, bed material sampled at the center of the left 1/3 of the channel; M, bed material sampled at the center of the channel; R, bed material sampled at the center of the right 1/3 of the channel]

Site number (figs. 4 and 5)	Size distribution, in mm, shown for the following percentiles					Percent sand
	10	16	50	65	84	
Gunnison River at Delta, Colorado[1] (09144250)						
Delta-1	11.9	23	79	104	137	< 2
Gunnison River near Grand Junction, Colorado[1] (09152500)						
Gun-1	30.9	37	77	104	124	< 1
Gun-2	37.6	50	74	81	106	< 1
Gun-3	30.9	35	71	92	112	< 1
Green River near Jensen, Utah[1] (09261000)						
Gr-1	20	25	56	69	124	< 1
Gr-2	.1	.4	64	80	106	11
Gr-3	.3	13	56	82	112	< 2
Spawning-bar habitat, 5 miles downstream of Green River near Jensen, Utah[2] (09261000)						
1-L	0.500–0.710	0.710–1.0	1.0–1.4	1.0–1.4	1.4–2.0	91
1-M	0.250–0.355	0.355–0.500	0.710–1.0	1.0–1.4	16.0–22.4	67
1-R	0.355–0.500	0.355–0.500	0.500–0.710	0.710–1.0	0.710–1.0	99
2-L	0.500–0.710	0.710–1.0	1.0–1.4	1.0–1.4	1.4–2.0	92
2-M	0.355–0.500	0.500–0.710	0.710–1.0	1.0–1.4	1.4–2.0	86
2-R	0.180–0.250	0.250–0.355	0.500–0.710	0.710–1.0	0.710–1.0	92
3-L	0.250–0.355	0.355–0.500	0.500–0.710	0.710–1.0	0.710–1.0	91
3-M	0.355–0.500	0.500–0.710	0.710–1.0	0.710–1.0	0.710–1.0	100
3-R	0.500–0.710	0.500–0.710	1.0–1.4	16.0–22.4	16.0–22.4	54
4-M	0.250–0.355	0.355–0.500	0.710–1.0	0.710–1.0	1.0–1.4	97
5-M	0.180–0.250	0.180–0.250	0.355–0.500	0.355–0.500	0.500–0.710	100
6-L	0.180–0.250	0.180–0.250	0.250–0.355	0.355–0.500	0.500–0.710	99
6-M	0.250–0.355	0.355–0.500	0.710–1.0	0.710–1.0	1.4–2.0	91
6-R	0.500–0.710	0.710–1.0	1.4–2.0	2.0–2.8	4.0–5.6	62

[1]Areal-sampling method (Wolman, 1954).

[2]Volumetric-sampling method (Guy, 1977).

Table 7. Summary of boundary shear stress and grain shear stress for selected locations in the Gunnison and Green Rivers.

[Q, streamflow; ft^3/s, cubic foot per second; w, width of channel; ft, foot; h, mean flow depth; S_f, friction slope; ft/ft, feet per foot; n, Mannings coefficient of roughness of the cross section; V, mean velocity; ft/s, feet per second; d_{65}, size distribution of bed sediment for the 65-percentile; mm, millimeter; n_D, the Mannings coefficient of roughness attributed to grain roughness; lb/ft^2, pound per square foot]

Q (ft^3/s)	w (ft)	h (ft)	S_f (ft/ft)	n	V (ft/s)	d_{65} (mm)	n_D	Grain shear stress (lb/ft^2)	Grain shear stress as percent of boundary shear stress
Cross section 450 feet upstream from cableway – Gunnison River near Grand Junction, Colorado (09152500)									
1,950	248	2.41	0.00036	0.016	3.257	81	0.030	0.05	100
3,750	249	3.22	0.00063	0.017	4.670	81	0.030	0.13	100
7,700	250	5.81	0.00083	0.026	5.303	81	0.030	0.30	100
11,000	253	7.31	0.00082	0.027	5.948	81	0.030	0.37	100
14,000	260	8.85	0.00094	0.032	6.087	81	0.030	0.48	92
Cross section 300 feet upstream from cableway – Gunnison River near Grand Junction, Colorado (09152500)									
1,950	171	3.56	0.00036	0.020	3.207	81	0.030	0.08	100
3,750	172	4.89	0.00063	0.024	4.454	81	0.030	0.19	100
7,700	178	7.36	0.00083	0.028	5.876	81	0.030	0.38	100
11,000	181	8.92	0.00082	0.027	6.810	81	0.030	0.46	100
14,000	185	10.64	0.00094	0.031	7.111	81	0.030	0.61	97
Cross section 150 feet upstream from cableway – Gunnison River near Grand Junction, Colorado (09152500)									
1,950	173	4.63	0.00036	0.032	2.437	81	0.030	0.10	91
3,750	178	5.80	0.00063	0.033	3.630	81	0.030	0.20	87
7,700	181	8.16	0.00083	0.033	5.212	81	0.030	0.37	87
11,000	185	9.46	0.00082	0.030	6.283	81	0.030	0.49	100
14,000	189	11.07	0.00094	0.034	6.694	81	0.030	0.55	85
Cross section at Cableway – Gunnison River near Grand Junction, Colorado (09152500)									
1,950	165	4.91	0.00036	0.034	2.407	81	0.030	0.09	85
3,750	170	5.96	0.00063	0.033	3.704	81	0.030	0.21	88
7,700	178	8.37	0.00083	0.034	5.170	81	0.030	0.36	84
11,000	181	10.02	0.00082	0.033	6.068	81	0.030	0.46	90
14,000	187	11.17	0.00094	0.034	6.700	81	0.030	0.55	84
Cross-section 2 – Gunnison River at Delta, Colorado (09144250)									
1,400	154	2.66	0.00080	0.024	3.417	104	0.032	0.13	100
2,870	163	3.93	0.00130	0.030	4.476	104	0.032	0.32	100
11,250	241	6.30	0.00160	0.027	7.408	104	0.032	0.63	100
13,300	241	6.71	0.00160	0.026	8.225	104	0.032	0.67	100
Cross-section 3 – Gunnison River at Delta, Colorado (09144250)									
1,400	147	4.36	0.00080	0.051	2.184	104	0.032	0.11	48
2,870	150	5.66	0.00130	0.050	3.382	104	0.032	0.23	50
11,250	190	8.46	0.00160	0.035	7.000	104	0.032	0.72	85
13,300	209	8.85	0.00160	0.035	7.177	104	0.032	0.75	84
Cross-section 4 – Gunnison River at Delta, Colorado (09144250)									
1,400	198	2.90	0.00080	0.035	2.439	104	0.032	0.12	86
2,870	208	4.14	0.00130	0.041	3.336	104	0.032	0.22	67
11,250	227	7.55	0.00160	0.035	6.560	104	0.032	0.65	86
13,300	244	8.10	0.00160	0.036	6.729	104	0.032	0.68	84

Table 7. Summary of boundary shear stress and grain shear stress for selected locations in the Gunnison and Green Rivers.—Continued

[Q, streamflow; ft^3/s, cubic foot per second; w, width of channel; ft, foot; h, mean flow depth; S_f, friction slope; ft/ft, feet per foot; n, Mannings coefficient of roughness of the cross section; V, mean velocity; ft/s, feet per second; d_{65}, size distribution of bed sediment for the 65-percentile; mm, millimeter; n_D, the Mannings coefficient of roughness attributed to grain roughness; lb/ft^2, pound per square foot]

Q (ft^3/s)	w (ft)	h (ft)	S_f (ft/ft)	n	V (ft/s)	d_{65} (mm)	n_D	Grain shear stress (lb/ft^2)	Grain shear stress as percent of boundary shear stress
Cross-section 1 – Sand - Green River near Jensen, Utah (09261000)									
9,000	460	4.64	0.00063	0.025	4.217	1.4	0.015	0.14	75
10,600	459	5.63	0.00061	0.028	4.102	1.4	0.015	0.12	57
14,100	459	6.54	0.00062	0.028	4.697	1.4	0.015	0.15	60
17,700	476	7.43	0.00061	0.028	5.005	1.4	0.015	0.17	59
19,000	476	7.58	0.00058	0.026	5.266	1.4	0.015	0.18	66
Cross-section 2 – Sand - Green River near Jensen, Utah (09261000)									
9,000	820	3.07	0.00100	0.028	3.575	1.4	0.015	0.11	59
10,600	820	3.86	0.00093	0.033	3.349	1.4	0.015	0.09	41
14,100	820	4.96	0.00191	0.054	3.467	1.4	0.015	0.09	15
17,700	853	5.96	0.00145	0.053	3.482	1.4	0.015	0.09	16
19,000	1,050	6.00	0.00042	0.033	3.016	1.4	0.015	0.06	41
Cross-section 3 – Sand - Green River near Jensen, Utah (09261000)									
9,000	245	3.58	0.00076	0.009	10.261	1.4	0.015	0.17	100
10,600	246	4.51	0.00072	0.011	9.554	1.4	0.015	0.20	100
14,100	279	5.09	0.00076	0.012	9.929	1.4	0.015	0.24	100
17,700	344	5.37	0.00046	0.010	9.582	1.4	0.015	0.15	100
19,000	361	5.36	0.00088	0.014	9.819	1.4	0.015	0.29	100
Cross-section 4 – Sand - Green River near Jensen, Utah (09261000)									
9,000	279	3.53	0.00065	0.010	9.138	1.4	0.015	0.14	100
10,600	279	4.33	0.00048	0.010	8.774	1.4	0.015	0.13	100
14,100	279	5.59	0.00034	0.010	9.041	1.4	0.015	0.12	100
17,700	279	6.85	0.00031	0.010	9.261	1.4	0.015	0.13	100
19,000	279	7.12	0.00027	0.009	9.565	1.4	0.015	0.12	100
Cross-section 5 – Sand - Green River near Jensen, Utah (09261000)									
9,000	262	4.20	0.00017	0.006	8.179	1.4	0.015	0.04	100
10,600	262	4.42	0.00013	0.005	9.153	1.4	0.015	0.04	100
14,100	262	5.67	0.00009	0.005	9.491	1.4	0.015	0.03	100
17,700	262	6.93	0.00007	0.005	9.749	1.4	0.015	0.03	100
19,000	279	6.68	0.00007	0.004	10.195	1.4	0.015	0.03	100
Cross-section 6 – Sand - Green River near Jensen, Utah (09261000)									
9,000	409	5.86	0.00035	0.024	3.755	1.4	0.015	0.10	79
10,600	410	7.38	0.00091	0.049	3.503	1.4	0.015	0.08	19
14,100	410	8.67	0.00037	0.030	3.967	1.4	0.015	0.10	49
17,700	426	9.43	0.00052	0.034	4.406	1.4	0.015	0.12	39
19,000	426	9.73	0.00042	0.030	4.584	1.4	0.015	0.13	50

Table 7. Summary of boundary shear stress and grain shear stress for selected locations in the Gunnison and Green Rivers.—Continued

[Q, streamflow; ft^3/s, cubic foot per second; w, width of channel; ft, foot; h, mean flow depth; S_f, friction slope; ft/ft, feet per foot; n, Mannings coefficient of roughness of the cross section; V, mean velocity; ft/s, feet per second; d_{65}, size distribution of bed sediment for the 65-percentile; mm, millimeter; n_D, the Mannings coefficient of roughness attributed to grain roughness; lb/ft^2, pound per square foot]

Q (ft^3/s)	w (ft)	h (ft)	S_f (ft/ft)	n	V (ft/s)	d_{65} (mm)	n_D	Grain shear stress (lb/ft^2)	Grain shear stress as percent of boundary shear stress
Cross-section 1 – Gravel - Green River near Jensen, Utah (09261000)									
9,000	460	4.64	0.00063	0.025	4.217	82	0.030	0.18	100
10,600	459	5.63	0.00061	0.028	4.102	82	0.030	0.21	100
14,100	459	6.54	0.00062	0.028	4.697	82	0.030	0.25	100
17,700	476	7.43	0.00061	0.028	5.005	82	0.030	0.28	100
19,000	476	7.58	0.00058	0.026	5.266	82	0.030	0.27	100
Cross-section 2 – Gravel - Green River near Jensen, Utah (09261000)									
9,000	820	3.07	0.00100	0.028	3.575	82	0.030	0.19	100
10,600	820	3.86	0.00093	0.033	3.349	82	0.030	0.20	87
14,100	820	4.96	0.00191	0.054	3.467	82	0.030	0.25	42
17,700	853	5.96	0.00145	0.053	3.482	82	0.030	0.23	43
19,000	1,050	6.00	0.00042	0.033	3.016	82	0.030	0.14	87
Cross-section 3 – Gravel - Green River near Jensen, Utah (09261000)									
9,000	245	3.58	0.00076	0.009	10.261	82	0.030	0.17	100
10,600	246	4.51	0.00072	0.011	9.554	82	0.030	0.20	100
14,100	279	5.09	0.00076	0.012	9.929	82	0.030	0.24	100
17,700	344	5.37	0.00046	0.010	9.582	82	0.030	0.15	100
19,000	361	5.36	0.00088	0.014	9.819	82	0.030	0.29	100
Cross-section 4 – Gravel - Green River near Jensen, Utah (09261000)									
9,000	279	3.53	0.00065	0.010	9.138	82	0.030	0.14	100
10,600	279	4.33	0.00048	0.010	8.774	82	0.030	0.13	100
14,100	279	5.59	0.00034	0.010	9.041	82	0.030	0.12	100
17,700	279	6.85	0.00031	0.010	9.261	82	0.030	0.13	100
19,000	279	7.12	0.00027	0.009	9.565	82	0.030	0.12	100
Cross-section 5 – Gravel - Green River near Jensen, Utah (09261000)									
9,000	262	4.20	0.00017	0.006	8.179	82	0.030	0.04	100
10,600	262	4.42	0.00013	0.005	9.153	82	0.030	0.04	100
14,100	262	5.67	0.00009	0.005	9.491	82	0.030	0.03	100
17,700	262	6.93	0.00007	0.005	9.749	82	0.030	0.03	100
19,000	279	6.68	0.00007	0.004	10.195	82	0.030	0.03	100
Cross-section 6 – Gravel - Green River near Jensen, Utah (09261000)									
9,000	409	5.86	0.00035	0.024	3.755	82	0.030	0.13	100
10,600	410	7.38	0.00091	0.049	3.503	82	0.030	0.21	50
14,100	410	8.67	0.00037	0.030	3.967	82	0.030	0.20	100
17,700	426	9.43	0.00052	0.034	4.406	82	0.030	0.26	83
19,000	426	9.73	0.00042	0.030	4.584	82	0.030	0.26	100

boundary shear stress and calculated grain shear stress at each location is presented in table 7. At most locations, less than 2 percent difference exists between boundary shear stress and grain shear stress. Where differences exceeded 2 percent, grain shear stress was used to assess entrainment potential of the streambed material in the reach.

Gunnison River at Delta

A study reach was established near the Gunnison River at Delta, Colorado (0914450) streamflow-gaging station to re-evaluate incipient-sediment-motion estimates at a previously studied location, 57 river miles (RM) upstream from the confluence of the Gunnison River with the Colorado River (cross-section 57 in Pitlick and others, 1999). The exact location of the 1999 cross section at RM 57 could not be determined; therefore, an 1,800-ft long reach consisting of four cross sections that bracketed the original 1999 cross section was established near the USGS streamflow-gaging station Gunnison River at Delta, Colorado (fig. 21). Initially, a fourth cross section, cross-section 1, was established; however, this cross section was not monumented or surveyed because, on closer inspection, it was not representative of the study reach channel geometry (width, depth, gradient) and sediment-particle size. Cross-section 3 in this report is believed to most closely replicate the cross section at RM 57 of the 1999 report (Pitlick and others, 1999).

Incipient motion analysis was performed for stream conditions of 13,300 ft^3/s (05/22/2008); 11,250 ft^3/s (05/29/2008); 2,850 ft^3/s (07/02/2008); and 1,400 ft^3/s (09/24/2008). On-site observations indicated that the streambed sediment in the Gunnison River at Delta study reach was relatively uniform. The median sediment-particle size (d_{50}) of the streambed sediment was 79 mm within a gravel-framework bed in the Gunnison River at Delta study reach (table 6). The critical shear stress for this material was 0.93 and 1.33 lb/ft^2 using dimensionless Shields parameter values of 0.035 and 0.050, respectively (table 8).

Cross-sections 2 and 3 in the Delta study reach had relatively uniform cross-channel geometries and, consequently, relatively uniform cross-channel boundary shear-stress distributions (fig. 22). Mean boundary shear stresses at cross-sections 2 and 3 (table 7) do not approach the minimum critical shear stress for 79 mm sediment in the Delta study reach (calculated with a Shields parameter of 0.035) at any evaluated streamflow (table 8). Boundary shear stresses, calculated for a continuum of points along cross-sections 2 and 3, do not approach the minimum critical shear stress for sediment in the Delta study reach until streamflows approach or exceed the 11,250 ft^3/s reference streamflow (fig. 22). The critical shear stress calculated with the more conservative 0.050 Shields parameter cannot be attained at these cross sections, even with the 2008 peak streamflow of 13,300 ft^3/s. These plots indicate that the streambed sediment in cross-sections 2 and 3 potentially is mobile only in limited locations and at high streamflows like that of 2008.

Cross-section 4 in the Delta study reach is slightly asymmetrical in cross-channel geometry because of the presence of a low-elevation, partially submerged gravel and cobble bar, which occupies the left half of the streambed (fig. 23). As at cross-sections 2 and 3, mean boundary shear stress at cross-section 4 (table 7) does not approach the minimum critical shear stress for 79 mm sediment at any streamflow evaluated in 2008 (table 8). Boundary shear stress, calculated with a Shields parameter of 0.035, did not exceed the minimum critical shear stress for 79 mm sediment even in the deeper, right side of the streambed when the streamflow approached 11,250 and 13,300 ft^3/s (fig. 23). The critical shear stress calculated with the more conservative 0.050 Shields parameter was not attained at any location on cross-section 4. The left side of the streambed and alluvial bar at cross-section 4 likely is a place of sediment accumulation of d_{50}-size material transported from upstream owing to the lesser boundary shear stresses in this area. This gravel and cobble bar was the location of the 2008 pebble count. Field observations confirm the above transport conditions; while the pebble count was being made it was noted that the sediment in this area was loosely compacted indicating that the particles recently had been entrained or deposited.

The mean boundary shear stress was highest for all cross sections for the peak streamflow of 13,300 ft^3/s (table 7). Yet, it was still no more than 81 percent of the minimum critical shear stress for the d_{50} in the Delta study reach (table 8) and represents a peak streamflow with a 5- to 10-year recurrence interval and streamflow values of 11,000 ft^3/s and 14,900 ft^3/s, respectively (table 9).

Pitlick and others (1999) evaluated sediment-entrainment potential for a 56-mi reach of the Gunnison River from Delta, Colorado, to the confluence with the Colorado River (fig. 2) and for specific cross sections at 1-mi intervals in this reach. Pitlick and others (1999) noted that "framework gravel and cobble particles begin to move at about half-bankfull streamflow" and that "mobilization and reworking of most all particles on the bed (termed significant motion) is associated with…bankfull streamflow," which is a median flow of 13,300 ft^3/s within the reach analyzed by Pitlick within the Gunnison River. Coincidently, the 2008 Gunnison River peak streamflow at Delta was 13,300 ft^3/s, and this streamflow exceeded a streamflow that would be needed to overtop the banks (a condition used to define bankfull streamflow in stable stream reaches) within the study reach (water-surface elevations of 4,927, 4,927, and 4,928 at cross-sections 2, 3, and 4, respectively; figs. 21–23). Flood-frequency analysis was completed using U.S. Geological Survey software PeakFQ, version 4.1 (Flynn and others, 2006) following Bulletin 17-B Guidelines (U.S. Interagency Advisory Committee on Water Data, 1982). The flood-frequency analysis of the streamflow data recorded at the Gunnison River at Delta, indicated that 13,300 ft^3/s has a recurrence interval of 5 to 10 years (table 9) or less frequently than the bankfull discharge, which generally

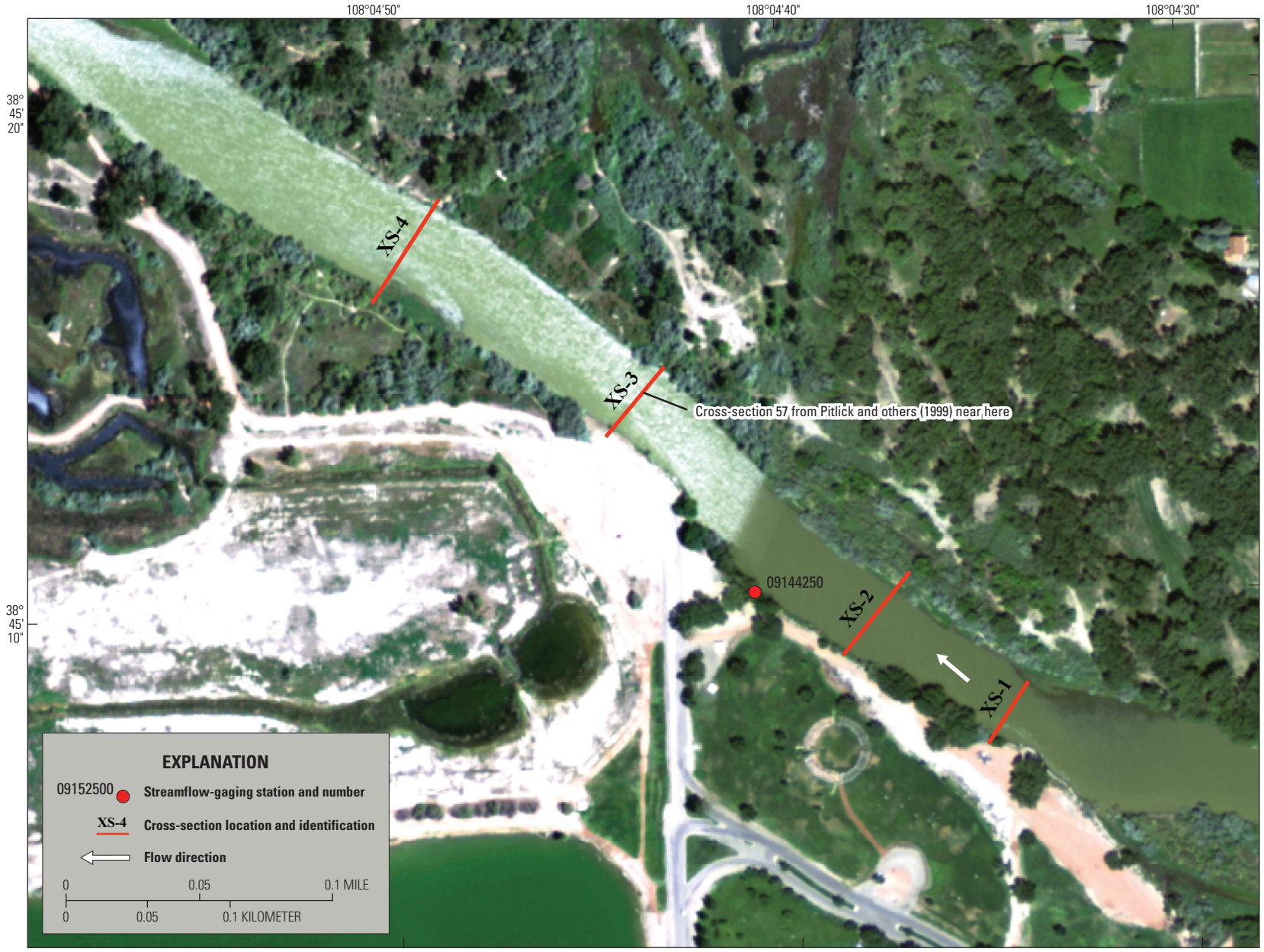

Orthoimages from U.S. Department of Agriculture National Agriculture Imagery Program (2007)
Universal Transverse Mercator North American Datum 1983, Zone 12 North

Figure 21. Map showing locations of the four cross sections of the study reach on the Gunnison River near Delta, Colorado. (Cross-section 1 (XS-1) was not surveyed in the study.)

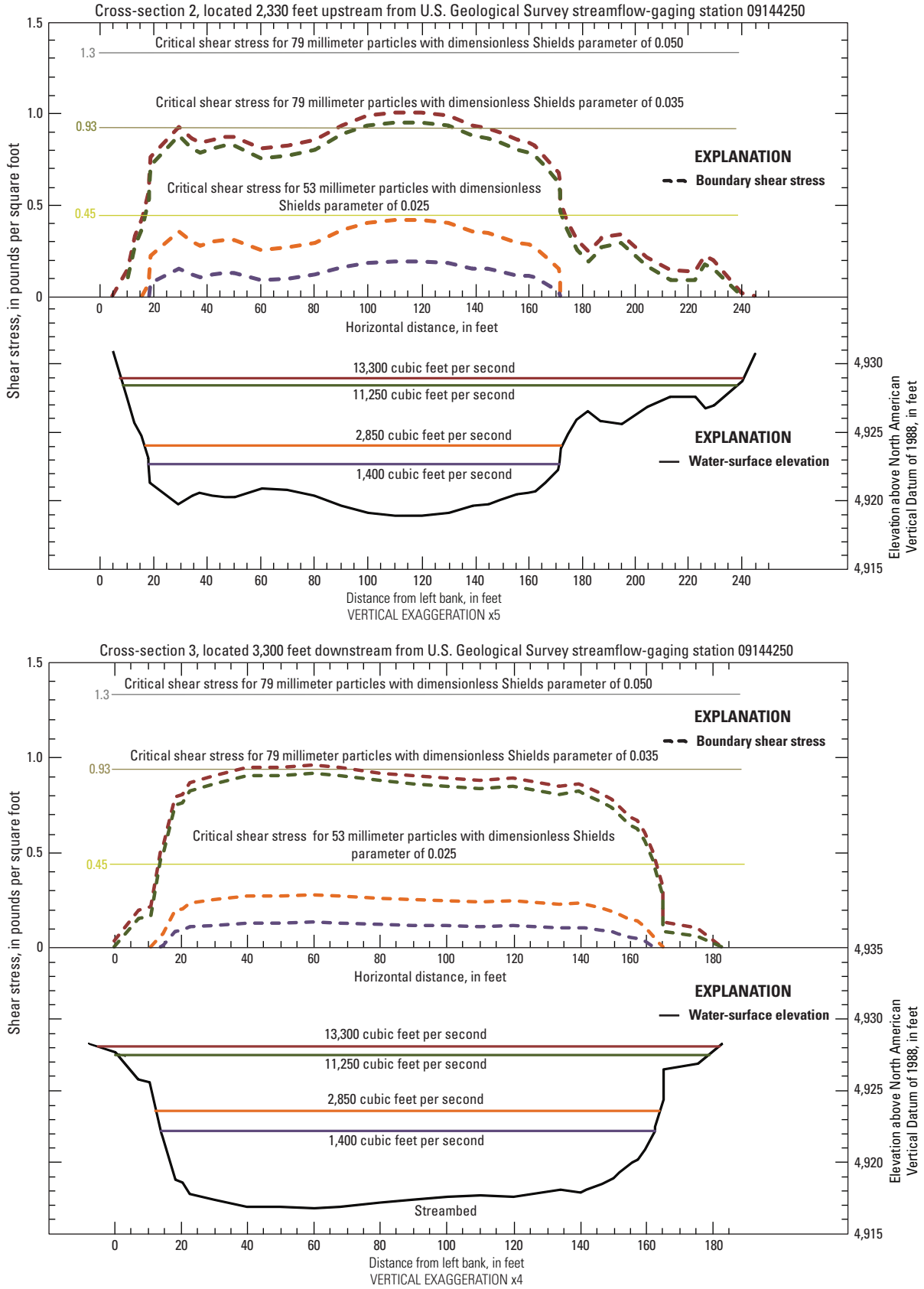

Figure 22. Graphs showing boundary shear stresses, water-surface elevations, and streambed elevations at cross-sections 2 and 3 for selected streamflows at U.S. Geological Survey streamflow-gaging station, 09144250, Gunnison River at Delta, Colorado.

Table 8. Cross-section characteristics, grain shear stress, and critical shear stress for the median sediment-particle sizes (d_{50}) at selected U.S. Geological Survey streamflow-gaging stations in the Upper Colorado River Basin.

[ft^3/s, cubic foot per second; ft/ft, feet per foot; ft, foot; lb/ft^2, pound per square foot]

Discharge (ft^3/s)	Cross-section location identification (figs. 21, 24, and 27)	Slope (ft/ft)	Mean flow depth (ft)	Grain shear stress (lb/ft^2)	Critical shear stress (Shields parameter 0.035) (lb/ft^2)	Critical shear stress (Shields parameter 0.050) (lb/ft^2)
Gunnison River near Delta, Colorado (09144250)						
1,400	Cross-section 2	0.0008	2.66	0.13	0.93	1.33
2,850	Cross-section 2	0.0013	3.93	0.32	0.93	1.33
11,250	Cross-section 2	0.0016	6.30	0.63	0.93	1.33
13,300	Cross-section 2	0.0016	6.71	0.67	0.93	1.33
1,400	Cross-section 3	0.0008	4.36	0.11	0.93	1.33
2,850	Cross-section 3	0.0013	5.66	0.23	0.93	1.33
11,250	Cross-section 3	0.0016	8.46	0.72	0.93	1.33
13,300	Cross-section 3	0.0016	8.85	0.75	0.93	1.33
1,400	Cross-section 4	0.0008	2.90	0.12	0.93	1.33
2,850	Cross-section 4	0.0013	4.14	0.22	0.93	1.33
11,250	Cross-section 4	0.0016	7.55	0.65	0.93	1.33
13,300	Cross-section 4	0.0016	8.10	0.68	0.93	1.33
Gunnison River near Grand Junction, Colorado (09152500)						
1,950	450 feet upstream from cableway	0.00036	2.41	0.05	0.88	1.25
3,750	450 feet upstream from cableway	0.00063	3.22	0.13	0.88	1.25
7,700	450 feet upstream from cableway	0.00083	5.81	0.30	0.88	1.25
11,000	450 feet upstream from cableway	0.00082	7.31	0.37	0.88	1.25
14,000	450 feet upstream from cableway	0.00094	8.85	0.48	0.88	1.25
1,950	300 feet upstream from cableway	0.00036	3.56	0.08	0.88	1.25
3,750	300 feet upstream from cableway	0.00063	4.89	0.19	0.88	1.25
7,700	300 feet upstream from cableway	0.00083	7.36	0.38	0.88	1.25
11,000	300 feet upstream from cableway	0.00082	8.92	0.46	0.88	1.25
14,000	300 feet upstream from cableway	0.00094	10.64	0.61	0.88	1.25
1,950	150 feet upstream from cableway	0.00036	4.63	0.09	0.88	1.25
3,750	150 feet upstream from cableway	0.00063	5.80	0.21	0.88	1.25
7,700	150 feet upstream from cableway	0.00083	8.16	0.37	0.88	1.25
11,000	150 feet upstream from cableway	0.00082	9.46	0.48	0.88	1.25
14,000	150 feet upstream from cableway	0.00094	11.07	0.56	0.88	1.25
1,950	Cableway	0.00118	4.91	0.09	0.88	1.25
3,750	Cableway	0.00063	5.96	0.21	0.88	1.25
7,700	Cableway	0.00083	8.37	0.36	0.88	1.25
11,000	Cableway	0.00082	10.02	0.46	0.88	1.25
14,000	Cableway	0.00094	11.17	0.55	0.88	1.25
Green River near Jensen, Utah (09261000)						
9,000	Cross-section 1	0.00059	5.26	0.18/0.14[1]	0.66/0.01[2]	0.95/0.02[2]
10,600	Cross-section 1	0.00051	5.49	0.21/0.12[1]	0.66/0.01[2]	0.95/0.02[2]
14,100	Cross-section 1	0.00045	6.28	0.25/0.15[1]	0.66/0.01[2]	0.95/0.02[2]

Table 8. Cross-section characteristics, grain shear stress, and critical shear stress for the median sediment-particle sizes (d_{50}) at selected U.S. Geological Survey streamflow-gaging stations in the Upper Colorado River Basin.—Continued

[ft^3/s, cubic foot per second; ft/ft, feet per foot; ft, foot; lb/ft^2, pound per square foot]

Discharge (ft^3/s)	Cross-section location identification (figs. 21, 24, and 27)	Slope (ft/ft)	Mean flow depth (ft)	Grain shear stress (lb/ft^2)	Critical shear stress (Shields parameter 0.035) (lb/ft^2)	Critical shear stress (Shields parameter 0.050) (lb/ft^2)
17,700	Cross-section 1	0.00045	7.45	0.28/0.17[1]	0.66/0.01[2]	0.95/0.02[2]
19,000	Cross-section 1	0.00042	7.60	0.27/0.18[1]	0.66/0.01[2]	0.95/0.02[2]
9,000	Cross-section 2	0.00059	3.35	0.19/0.11[1]	0.66/0.01[2]	0.95/0.02[2]
10,600	Cross-section 2	0.00051	3.63	0.20/0.09[1]	0.66/0.01[2]	0.95/0.02[2]
14,100	Cross-section 2	0.00045	4.60	0.25/0.09[1]	0.66/0.01[2]	0.95/0.02[2]
17,700	Cross-section 2	0.00045	5.78	0.23/0.09[1]	0.66/0.01[2]	0.95/0.02[2]
19,000	Cross-section 2	0.00042	6.00	0.14/0.06[1]	0.66/0.01[2]	0.95/0.02[2]
9,000	Cross-section 3	0.00059	3.69	0.17	0.66/0.01[2]	0.95/0.02[2]
10,600	Cross-section 3	0.00051	3.63	0.20	0.66/0.01[2]	0.95/0.02[2]
14,100	Cross-section 3	0.00045	4.80	0.24	0.66/0.01[2]	0.95/0.02[2]
17,700	Cross-section 3	0.00045	5.91	0.15	0.66/0.01[2]	0.95/0.02[2]
19,000	Cross-section 3	0.00042	6.19	0.29	0.66/0.01[2]	0.95/0.02[2]
9,000	Cross-section 4	0.00059	4.89	0.14	0.66/0.01[2]	0.95/0.02[2]
10,600	Cross-section 4	0.00051	5.21	0.13	0.66/0.01[2]	0.95/0.02[2]
14,100	Cross-section 4	0.00045	6.39	0.12	0.66/0.01[2]	0.95/0.02[2]
17,700	Cross-section 4	0.00045	7.66	0.13	0.66/0.01[2]	0.95/0.02[2]
19,000	Cross-section 4	0.00042	7.93	0.12	0.66/0.01[2]	0.95/0.02[2]
9,000	Cross-section 5	0.00059	4.17	0.04	0.66/0.01[2]	0.95/0.02[2]
10,600	Cross-section 5	0.00051	4.68	0.04	0.66/0.01[2]	0.95/0.02[2]
14,100	Cross-section 5	0.00045	5.62	0.03	0.66/0.01[2]	0.95/0.02[2]
17,700	Cross-section 5	0.00045	6.83	0.03	0.66/0.01[2]	0.95/0.02[2]
19,000	Cross-section 5	0.00042	7.10	0.03	0.66/0.01[2]	0.95/0.02[2]
9,000	Cross-section 6	0.00059	6.38	0.13/0.10[1]	0.66/0.01[2]	0.95/0.02[2]
10,600	Cross-section 6	0.00051	6.76	0.21/0.08[1]	0.66/0.01[2]	0.95/0.02[2]
14,100	Cross-section 6	0.00045	7.90	0.20/0.10[1]	0.66/0.01[2]	0.95/0.02[2]
17,700	Cross-section 6	0.00045	9.11	0.26/0.12[1]	0.66/0.01[2]	0.95/0.02[2]
19,000	Cross-section 6	0.00042	9.42	0.26/0.13[1]	0.66/0.01[2]	0.95/0.02[2]

[1]Grain shear stress for sand veneer differs from grain shear stress calculated from median particle size (d_{50}).

[2]Critical shear stress calculated from median particle size (d_{50}) of transient sand veneer.

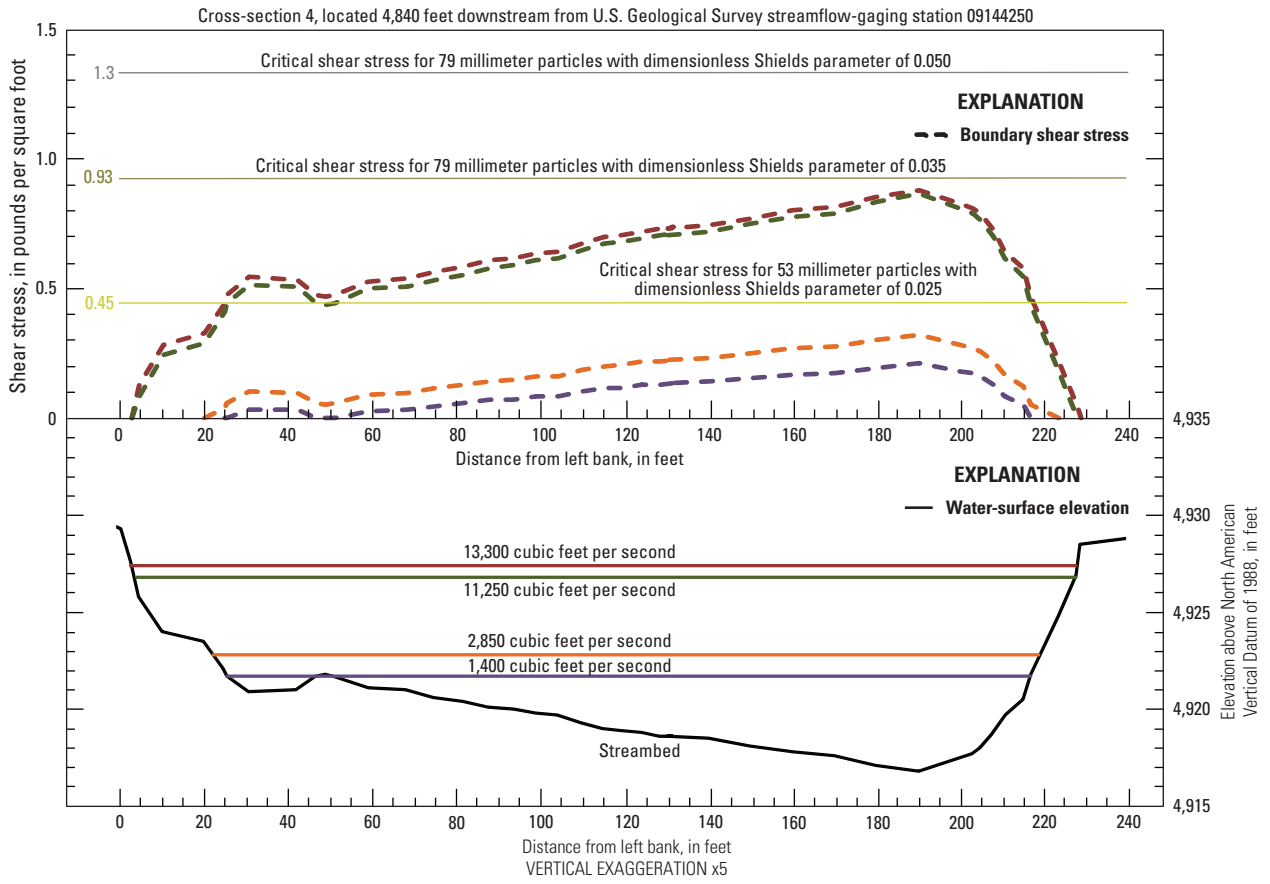

Figure 23. Graphs showing boundary shear stresses, water-surface elevations, and streambed elevations at cross-section 4 for selected streamflows at U.S. Geological Survey streamflow-gaging station, 09144250, Gunnison River at Delta, Colorado.

Table 9. Estimates of peak streamflow values for selected recurrence intervals at U.S. Geological Survey streamflow-gaging stations in the Upper Colorado River Basin.

[Data are in cubic feet per second]

		Recurrence interval, years[1]										
Station number	Abbreviation	1	1.3	2	2.3	5	10	25	50	100	200	500
09095500	CAMEO	8,300	15,100	18,300	19,700	25,400	29,300	34,200	37,400	40,300	43,000	46,300
09144250	DELTA	970	3,400	6,150	7,050	11,000	14,900	20,400	25,000	30,000	35,400	43,200
09152500	GUNNISON	2,000	5,100	8,050	8,900	12,800	16,300	21,100	24,900	28,900	33,200	39,300
09163500	STATELINE	4,150	13,900	22,900	25,100	35,700	44,300	54,800	62,400	69,700	76,900	89,200
09180500	CISCO	5,050	15,700	25,400	28,000	39,600	49,200	61,200	70,000	78,700	87,300	98,600
09261000	JENSEN	5,500	12,200	17,000	18,100	22,800	26,200	30,000	32,700	35,100	37,400	40,200
09315000	GREEN	5,650	14,400	21,200	22,900	30,000	35,400	41,700	46,100	50,300	54,300	59,200

[1]The "100-year recurrence interval" means that a flood of that magnitude has a one percent chance of occurring in any given year. In other words, the chances that a river will exceed the 100-year flood stage in any given year is 1 in 100. Each year begins with the same 1-percent chance that a 100-year event will occur. Recurrence intervals were calculated based on flood-frequency analysis using U.S. Geological Survey software PeakFQ, version 4.1 (Flynn and others, 2006) following Bulletin 17-B Guidelines (U.S. Interagency Advisory Committee on Water Data, 1982).

is less than a 5-year (and closer to a 2-year) recurrence for many Rocky Mountain regions and perennial rivers (Williams, 1978; Andrews, 1980).

Pitlick and others (1999) surveyed channel geometry and calculated cross-section average hydraulic characteristics for 13,300 ft^3/s at RM 57, which is comparable with cross-section 3 of this study (figs. 21 and 22). Pitlick and others (1999) estimated "bankfull" boundary shear stress at RM 57 to be 1.09 lb/ft^2 (52.4 N/m^2, table A-9), with isolated locations across the streambed in the three Delta reach cross sections surveyed in 2008 showing similar values for grain shear stress (approximaltey 1.0 lb/ft^2) (figs. 21–23). Observations from the 2008 surveys and the flood-frequency analysis at the Delta streamgage indicate that 13,300 ft^3/s was a greater-than bankfull flood; therefore, entrainment of the streambed in the Delta reach likely occurs less frequently than previously estimated by Pitlick and others (1999). Widespread entrainment (or "significant motion") of the streambed likely occurs only at streamflows greater than 13,300 ft^3/s. These comparisons are for the Delta reach only; no analysis was performed near the other cross sections surveyed by Pitlick and others (1999) for this river reach.

The disparity between the two studies of entrainment potential for the Delta study reach stems from differences in the bed-material sediment-particle sizes, Shields parameters selected, and energy slopes used in the calculations. Pitlick and others (1999) measured d_{50} at RM 56.6 as 53 mm assessed with a Shields paramter of 0.025; this study characterized the d_{50} at cross-section 4 (or RM 56.9) as 79 mm and selected Shields' parameters of 0.035 and 0.050 (table 6). The difference in bed-material sediment-particle size likely is because two different techniques were used for the sediment-particle-size analysis. Pitlick and others (1999) classified sediment-particle sizes using a gravelometer to categorically assign counts of sediment particles to different ranges of sizes. This technique mirrors sieve-analysis techniques, wherein square cutouts of specific sizes are used to assign a count of each sediment particle within each given size range. This report provides information based on direct measure of each sediment particle, producing more precise estimates of the sediment-particle size distribution of the reach. Comparison between the two techniques for the Delta reach from this study results in a maximum d_{50} of 64 mm (gravelometer) compared to the measured 79 mm of this study, showing that the gravelometer technique resulted in a d_{50} that is 19 percent smaller than observed. The reader is referred to the methods section of the report under "Streambed-sediment characterization" and "Incipient motion of streambed materials" for further discussion of methods used in this report regarding d_{50} and Shields parameter selection.

For the Delta study reach, bank-top survey and direct observation of water-surface slope produced different estimates of the energy-grade line. Pitlick and others (1999) estimated a bankfull energy slope of 0.0019 from a bank-top survey at RM 57. In general, the estimated energy slope performed by Pitlick and others (1999) relies on channel form (bank-top heights) as an indicator of energy gradient in the reach. In this study, the energy slope of 0.0016 for 13,300 ft^3/s was based on a survey of high-water marks between cross-sections 2 and 4, which encompass RM 57 (fig. 21, table 8). The smaller d_{50} and steeper "bankfull" energy slope used by Pitlick and others (1999) indicates potential bed-material entrainment at 13,300 ft^3/s streamflow conditions; whereas, the calculations in this study, using a coarser-sediment-particle size and lesser energy slope, indicate only limited bed-material entrainment for the same streamflow.

Gunnison at Whitewater

A study reach was established near the Gunnison River near Grand Junction, Colorado (09152500), streamflow-gaging station. The reach was 450 ft long and began at the cableway that is colocated with the streamflow-gaging station. Water surfaces were flagged when streamflow was 11,000 ft^3/s (05/25/2005); 1,950 ft^3/s (07/08/2005); 14,000 ft^3/s (05/23/2008); 7,700 ft^3/s (06/18/2008); and 3,750 ft^3/s (07/01/2008). Four cross sections were surveyed on October 9, 2007: (1) at the cableway, (2) 150 ft upstream from the cableway, (3) 300 ft upstream from the cableway, and (4) 450 ft upstream from the cableway (fig. 24). Sediment characteristics were sampled at two locations upstream from the cableway and one location downstream from the cableway (fig. 4). The median sediment-particle size (d_{50}) of the streambed sediment ranged from 71 to 77 mm, with a mean of 74 mm determined in this investitgation (table 6). The critical shear stress to move this particle within a gravel-framework bed is 0.88 and 1.25 lb/ft^2 using the Shields parameter values of 0.035 and 0.050, respectively (table 8).

Three of the four cross sections were relatively symmetrical whereas the fourth cross section, 450 ft upstream from the cableway, has an exposed bar along the right side (viewed looking downstream) of the channel (figs. 25 and 26). The cross-channel calculated boundary shear stresses do not approach the minimum critical shear stress for any cross section or any streamflow. This indicates that the d_{50} particle is not moving at streamflows of 14,000 ft^3/s or less in this study reach (figs. 25 and 26). The critical shear stress calculated with the more conservative Shields parameter (0.050) is not attained in any of these cross sections or streamflows.

The mean boundary shear stress was highest for all cross sections for the peak streamflow of 14,000 ft^3/s (table 7). Yet, it was still no more than 76 percent of the minimum critical shear stress for the d_{50} in the GUNNISON study reach (table 8) and represents a peak streamflow with a 5- to 10-year recurrence interval and streamflow values of 12,800 and 16,300 ft^3/s, respectively (table 9).

The median sediment-particle size (d_{50}) of the streambed sediment was characterized by Pitlick and others (1999) as 50 mm near this study reach. The cross-channel calculated shear stresses approach or exceed the minimum critical shear stress for 50 mm particles at some locations in some cross sections for streamflows of 7,700 ft^3/s or greater (figs. 25 and 26). This indicates that the d_{50} determined by Pitlick and others

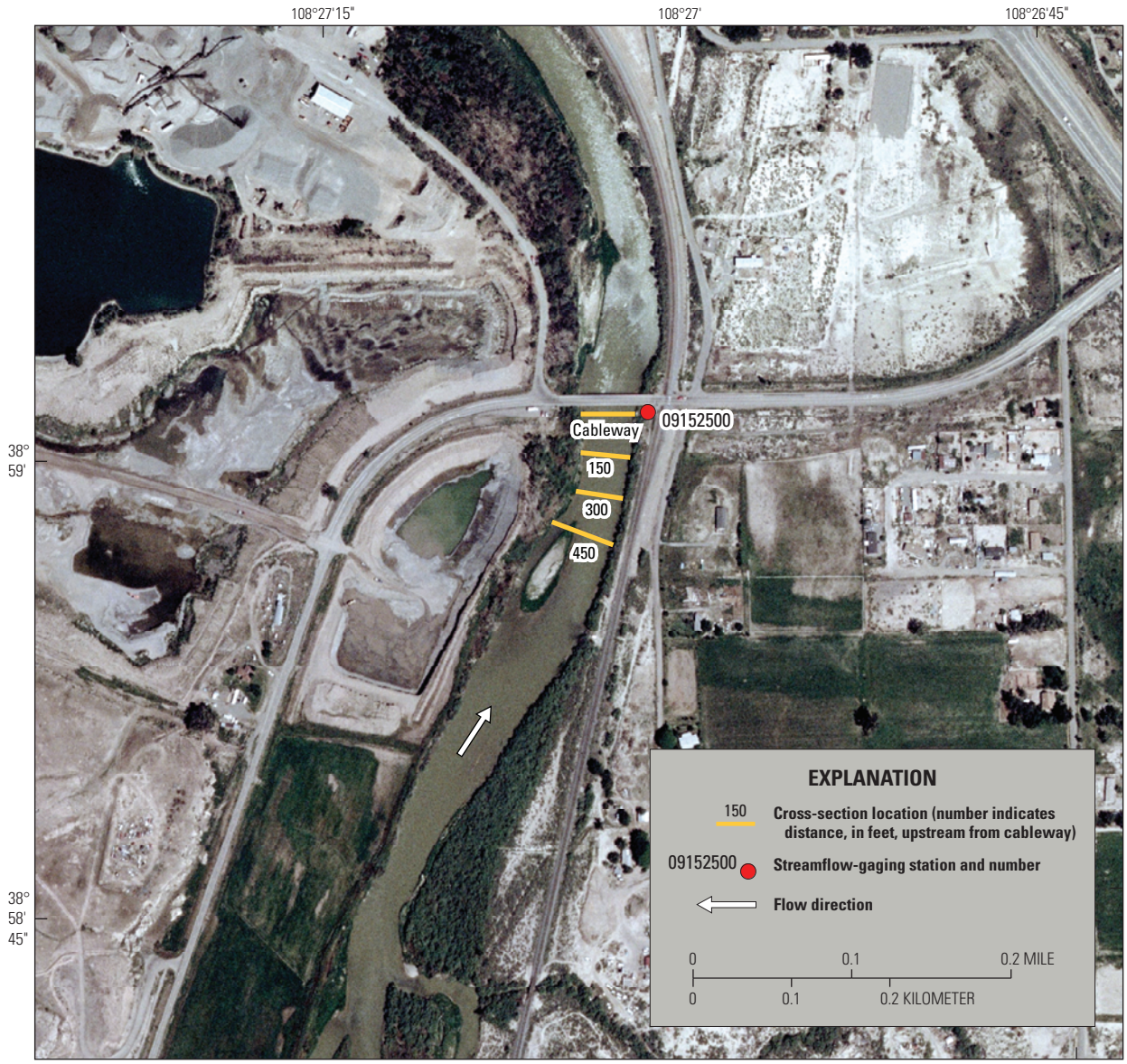

Orthoimages from U.S. Department of Agriculture National Agriculture Imagery Program (2007)
Universal Transverse Mercator North American Datum 1983, Zone 12 North
Scale 1:6,500

Figure 24. Map showing locations of the four cross sections of the study reach on the Gunnison River near Grand Junction, Colorado.

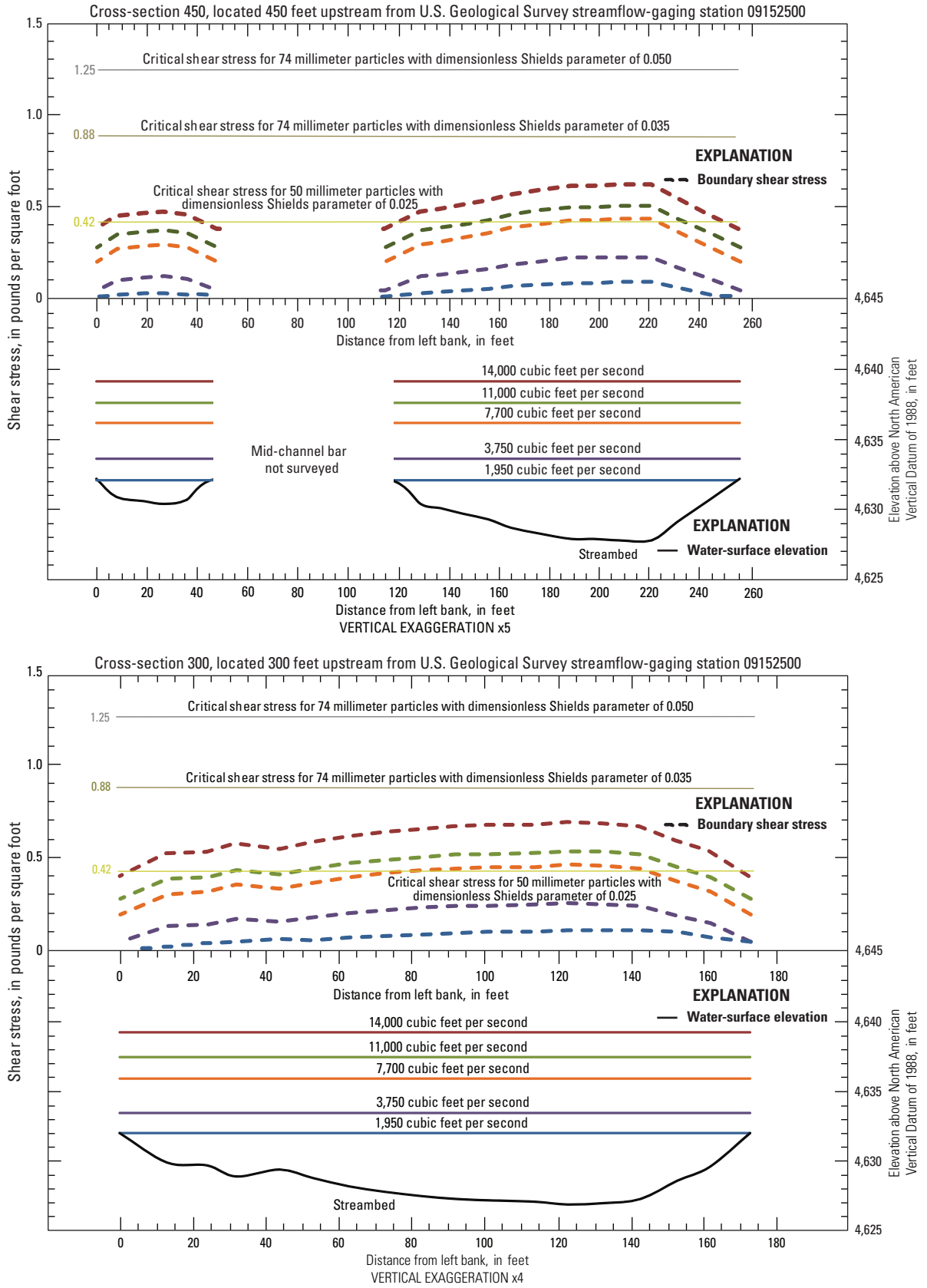

Figure 25. Graphs showing boundary shear stresses, water-surface elevations, and streambed elevations for selected streamflows at the cross sections located 450 and 300 feet upstream from U.S. Geological Survey streamflow-gaging station, 09152500, Gunnison River near Grand Junction, Colorado.

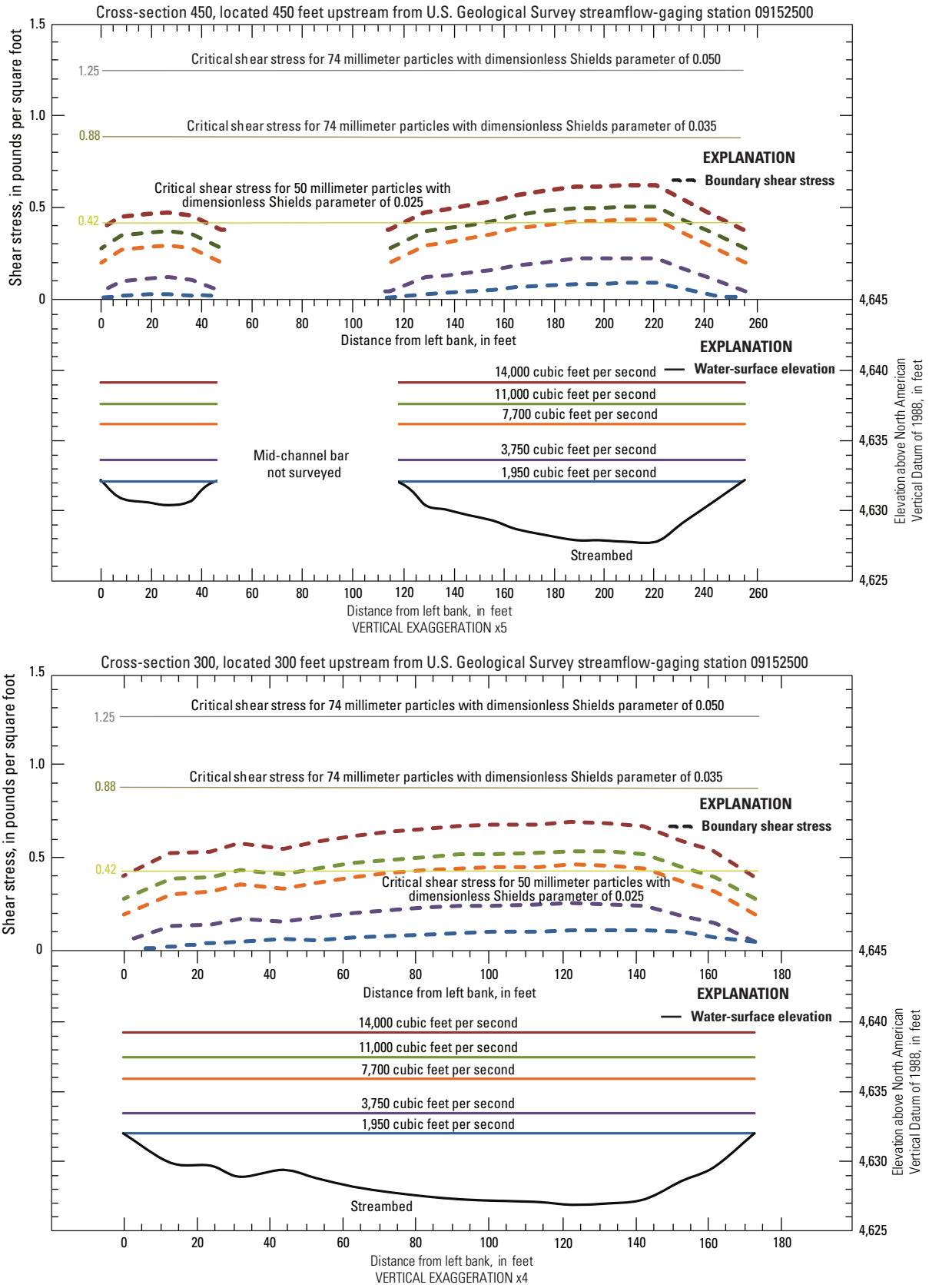

Figure 26. Graphs showing shear stresses, water-surface elevations, and streambed elevations for selected streamflows at the cross sections located 150 feet upstream from and along the cableway of U.S. Geological Survey streamflow-gaging station, 09152500, Gunnison River near Grand Junction, Colorado.

(1999) is potentially moving at streamflows of 7,700 ft^3/s or greater in this study reach (figs. 25 and 26). However, the critical shear stress calculated with the more conservative Shields parameter (0.050) cannot be attained in any of these cross sections or streamflows. Widespread entrainment (or "significant motion") of the streambed likely occurs only at discharges greater than 14,000 ft^3/s. These comparisons are for the Gunnison at Whitewater reach only; no analysis was performed near the other cross sections surveyed by Pitlick and others (1999) for this river reach.

Green River near Jensen

The study reach on the Green River 5 miles downstream from the Green River near Jensen, Utah, streamflow-gaging station (09261000) was 10,000 ft long, began about 2,000 ft upstream from the meander bend where the first cross section was located, and ended about 3,800 ft downstream from an island that sits in the middle of the study reach. Water surfaces and boundary shear-stress values were obtained from the calibrated two-dimensional streamflow and sediment-transport models developed for this area representing streamflows of 9,000, 10,600, 14,100, 17,700, and 19,000 ft^3/s. Six cross sections were surveyed (1) at the meander bend, (2) upstream from the island, (3) in the first half of the portion of the channel that flows along the left side of the island, (4) in the second half of the portion of the channel that flows along the left side of the island, (5) in the portion of the channel that flows on the right side of the channel, and (6) downstream from the island (fig. 27).

Streambed conditions within the study reach can be characterized by two dominant sediment-particle size distributions, which vary spatially and temporally within the system. There is a gravel-dominated pavement layer, which is intermittently exposed within the channel with varying thicknesses of a sand veneer along the surface. Within the study reach, flow velocities and water depths prevented direct sampling of the gravelly bed material so sediment-particle-size analysis was based on pebble-count data from exposed bars and channel margins in the vicinity of the gaging station located 5 mi upstream. Dredge samples of the sand veneer also were characterized at multiple locations within the reach (fig. 4). Evaluation of transport characteristics of each of the two sediment-particle-size distributions were used to produce the end members of a continuum that represent the characteristics of the channel. In the areas best characterized as gravel-framework beds (less than 20–30 percent sand), incipient motion of the gravels and sands are represented by the gravel critical shear stress. For the areas with larger portions of sand (typically expressed as a sand veneer overlaying the gravel-framework bed), incipient motion of the sand is represented by the sand critical shear stress and may decrease the shear stress needed for incipient motion of the gravels.

In the sand-matrix framework, the d_{50} of the sand veneer of the streambed sediment ranged from 0.25 to 2.0 mm, and 1.4 mm was used for the analysis of incipient-motion calculations (table 6). The critical shear stress needed to move the sand-sized particles was 0.01 and 0.02 lb/ft^2 using Shields parameter values of 0.035 and 0.050, respectively (table 8). The median d_{50} of the bed material 5 mi upstream from the study reach was 56 to 64 mm, and 56 mm was used for the incipient-motion calculations (table 6). The critical shear stress to move the cobble-sized particles within the gravel-framework bed was 0.66 and 0.95 lb/ft^2 using Shields parameter values of 0.035 and 0.050, respectively (table 8).

For all streamflows at all cross sections the boundary shear stress exceeded the critical shear stress to move the sand-sized particles (d_{50} from 0.4 to 1.4 mm); however, the boundary shear stress does not reach the critical shear stress to move the cobble-sized particles (d_{50} from 56 to 64 mm) for any modeled streamflow at these cross sections (figs. 28–32). At cross-section 1 (upstream end of reach) boundary shear stress generally is symmetrical and increases slightly with increasing streamflow (fig. 28). The shear stress at cross-section 2 has the opposite pattern; the boundary shear stress decreases as streamflow increases, indicative of a backwater effect from the island (figs. 28 and 29). At cross-section 3, the boundary shear stress does not have a consistent pattern with increasing streamflow, which may indicate that the island continues to influence the boundary shear stress with either backwater or other eddy effects at this location (fig. 30). Moving downstream, cross-sections 4 and 5 have relatively constant boundary shear stress regardless of streamflow (figs. 30 and 31). Cross-section 6 has a pattern similar to cross-section 1 where boundary shear stress generally increases with increasing streamflow (figs. 31 and 32).

The mean boundary shear stress was greatest at all cross sections at 17,700 ft^3/s (table 7) and was greatest within the reach at cross-section 1 (the upstream-most cross section), located at the meander bend. Even the maximum was less than the minimum critical shear stress necessary to move the d_{50} of the cobble-sized particles that were sampled (table 8) and represents a peak streamflow with a 2- to 2.3-year recurrence interval (streamflow values of 17,000 and 18,100 ft^3/s, respectively) (table 9). The maximum modeled streamflow of 19,000 ft^3/s represents a peak streamflow with a 2.3- to 5-year recurrence interval (streamflow values of 18,100 and 22,800 ft^3/s, respectively) (table 9).

Figure 27 (following page). Map showing shear stress cross-section locations, 5 miles downstream from the Green River near Jensen, Utah, streamflow-gaging station.

Orthoimages from U.S. Department of Agriculture National Agriculture Imagery Program (2007)
Universal Transverse Mercator North American Datum 1983, Zone 13 North
Scale 1:10,000

EXPLANATION

1 **Cross-section location and identification**

Flow direction

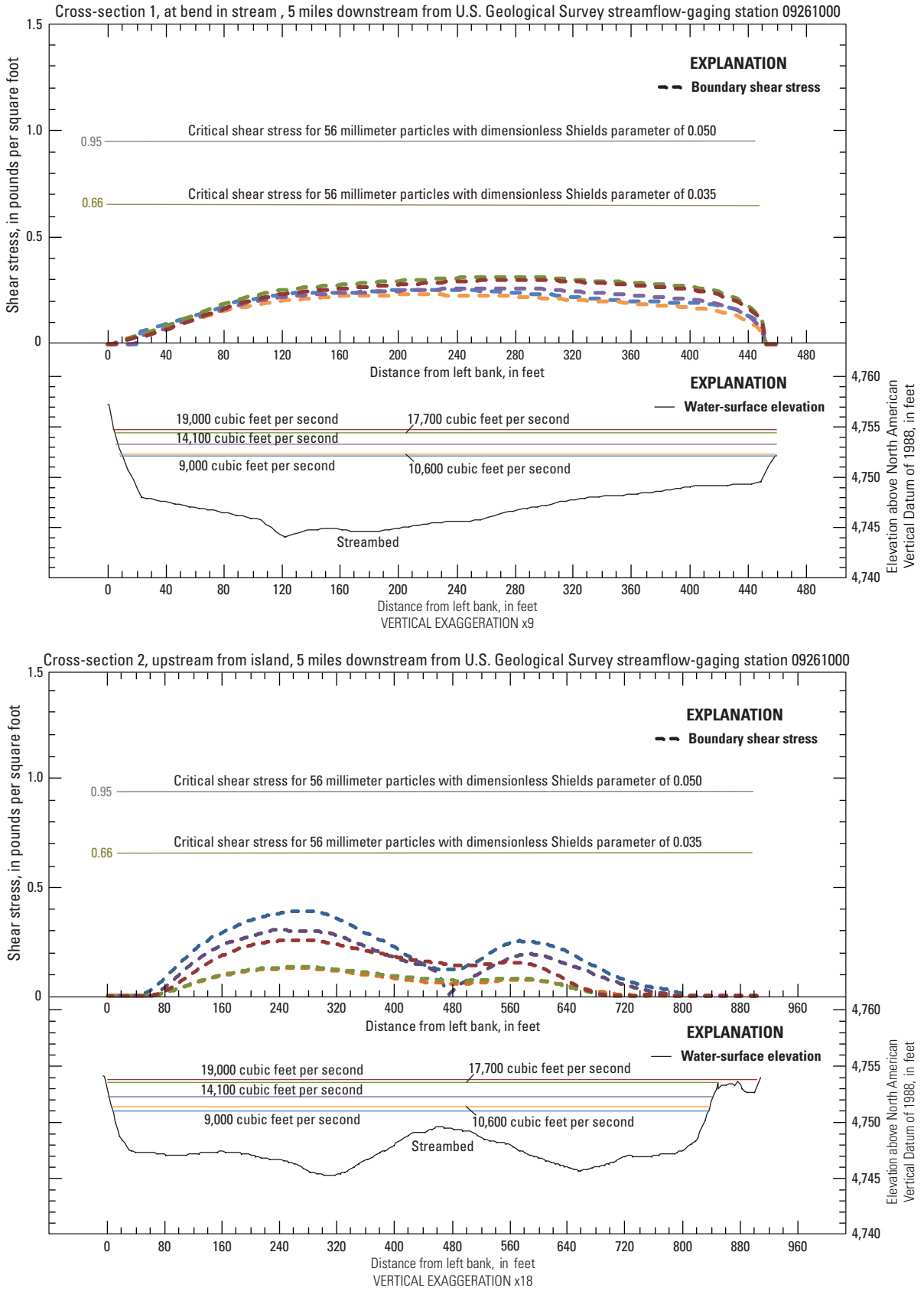

Figure 28. Graphs showing cross-sections 1 and 2 boundary shear stresses for the median particle size of 56 millimeters, water-surface elevations, and streambed elevations for selected streamflows at U.S. Geological Survey streamflow-gaging station, 09261000, Green River near Jensen, Utah.

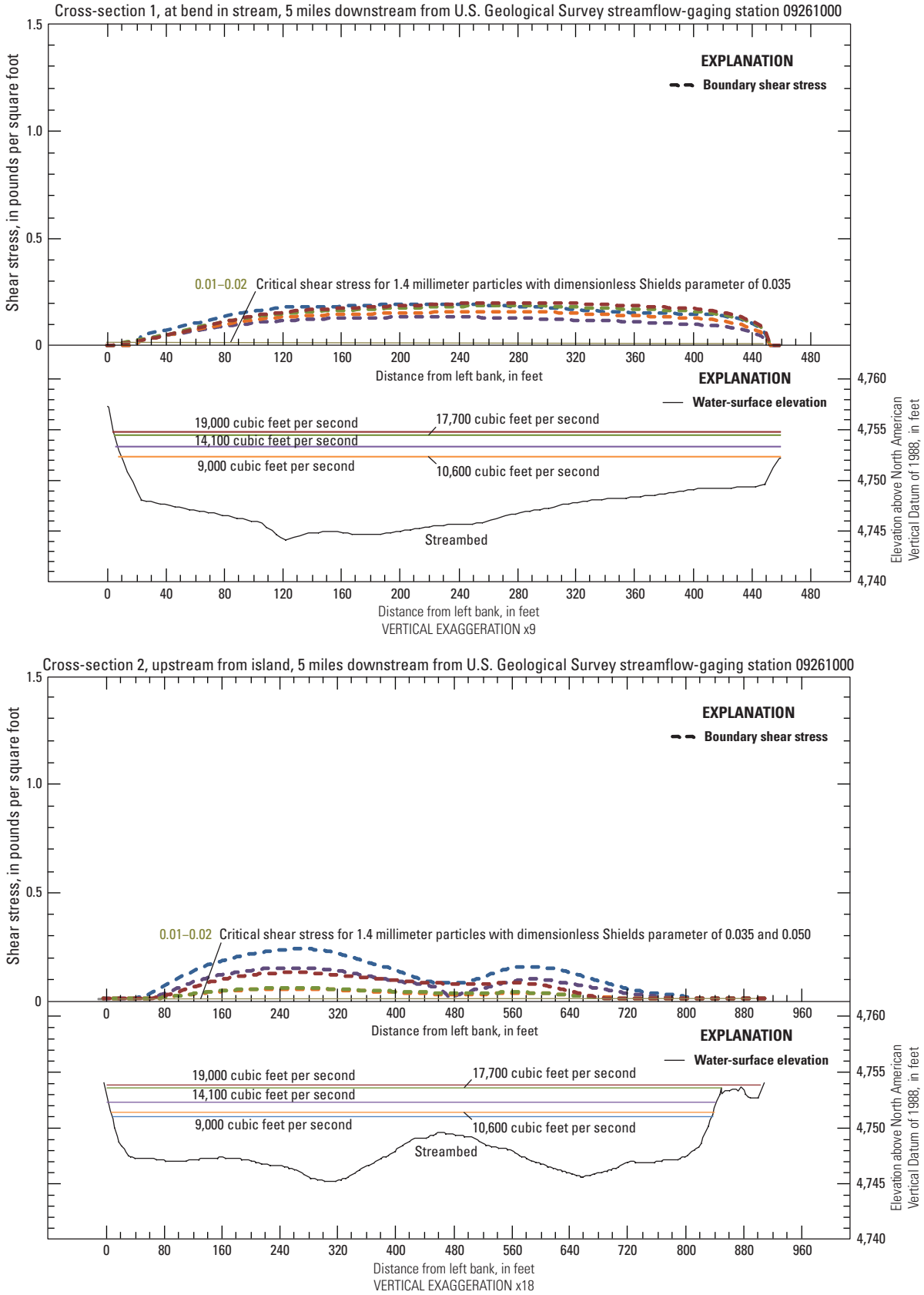

Figure 29. Graphs showing cross-sections 1 and 2 boundary shear stresses for the median particle size of 1.4 millimeters, water-surface elevations, and streambed elevations for selected streamflows at U.S. Geological Survey streamflow-gaging station, 09261000, Green River near Jensen, Utah.

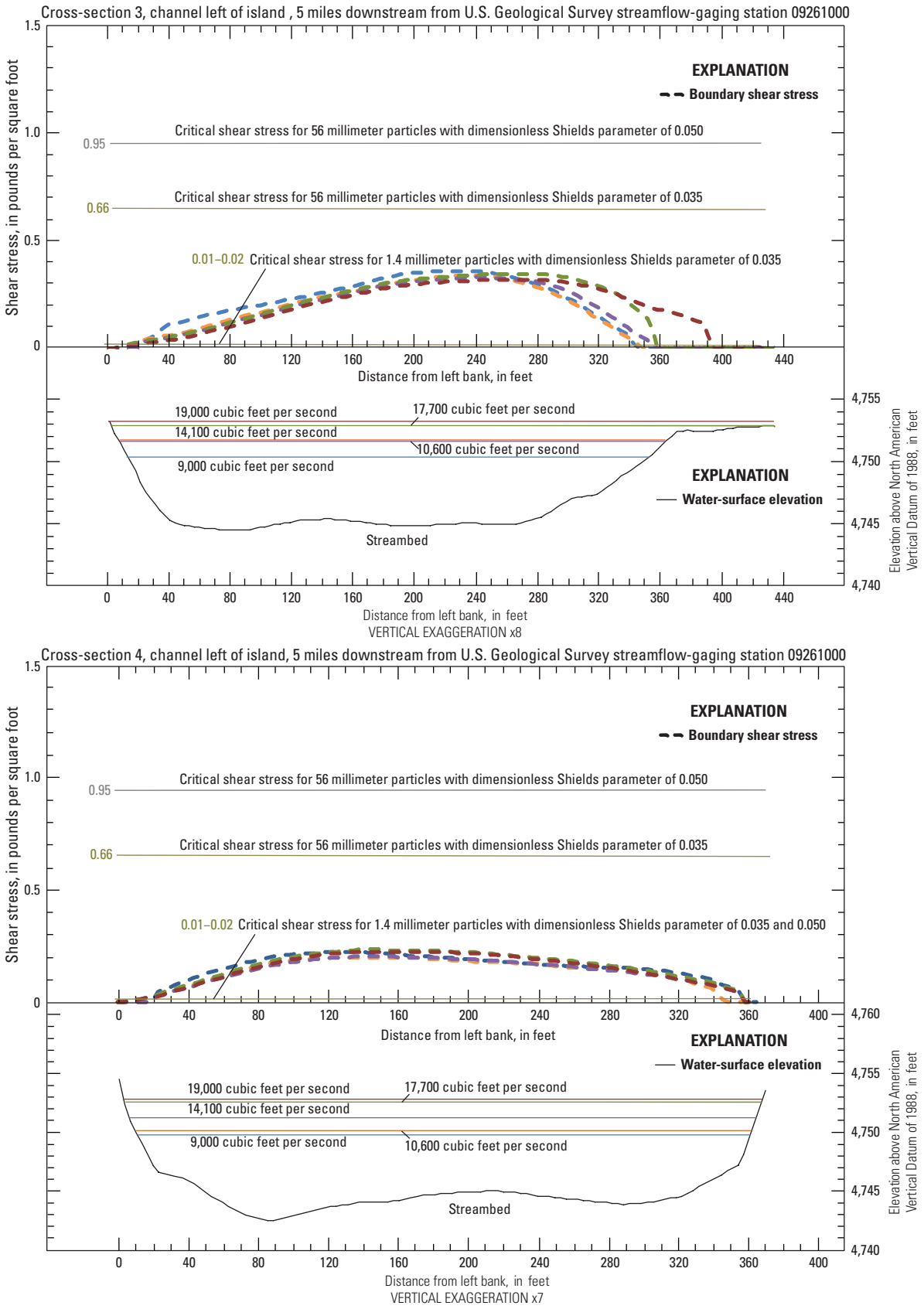

Figure 30. Graphs showing cross-sections 3 and 4 boundary shear stresses for the median particle sizes of 1.4 and 56 millimeters, water-surface elevations, and streambed elevations for selected streamflows at U.S. Geological Survey streamflow-gaging station, 09261000, Green River near Jensen, Utah.

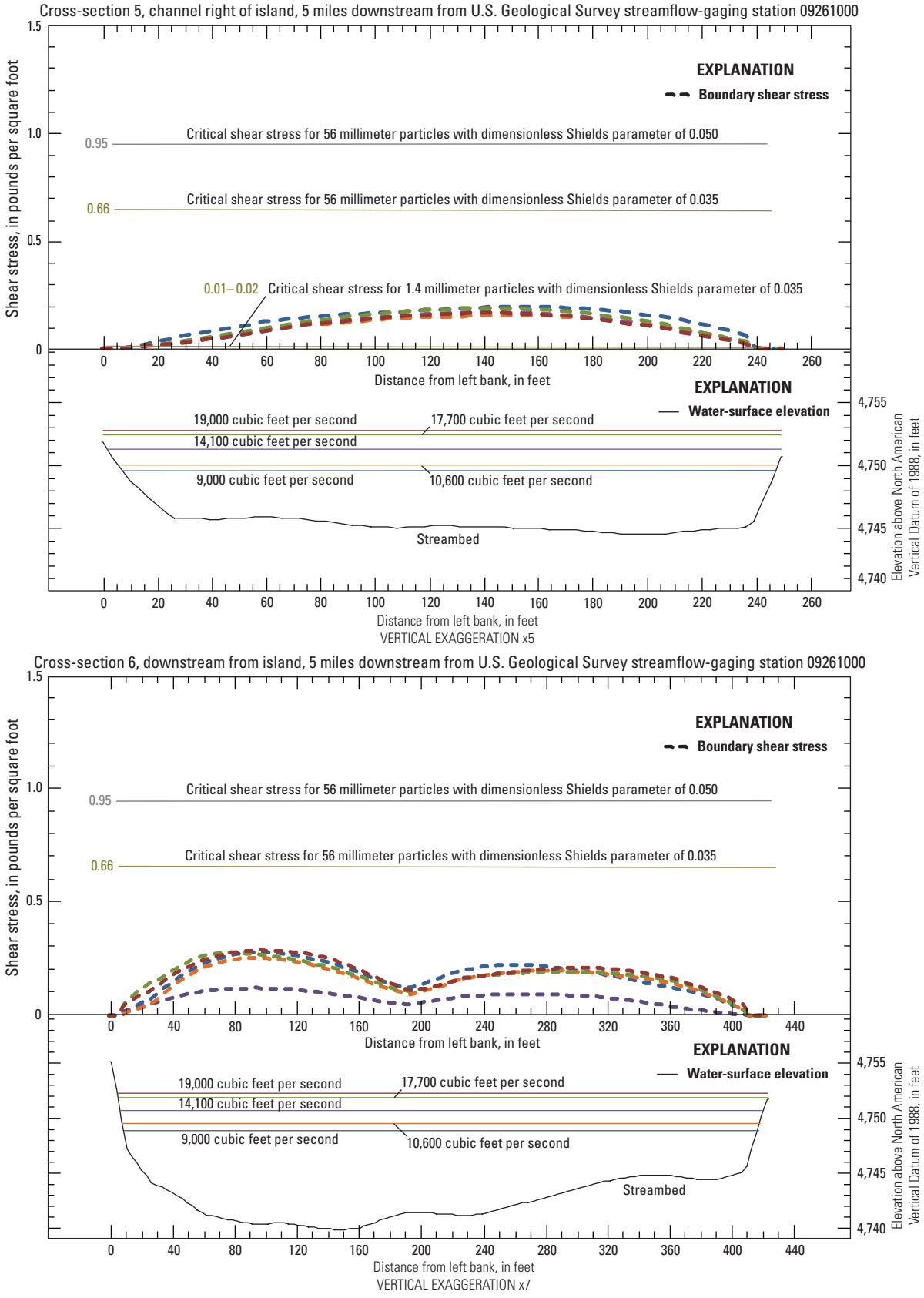

Figure 31. Graphs showing cross-sections 5 and 6 boundary shear stresses for the median particle sizes of 1.4 and (or) 56 millimeters, water-surface elevations, and streambed elevations for selected streamflows at U.S. Geological Survey streamflow-gaging station, 09261000, Green River near Jensen, Utah.

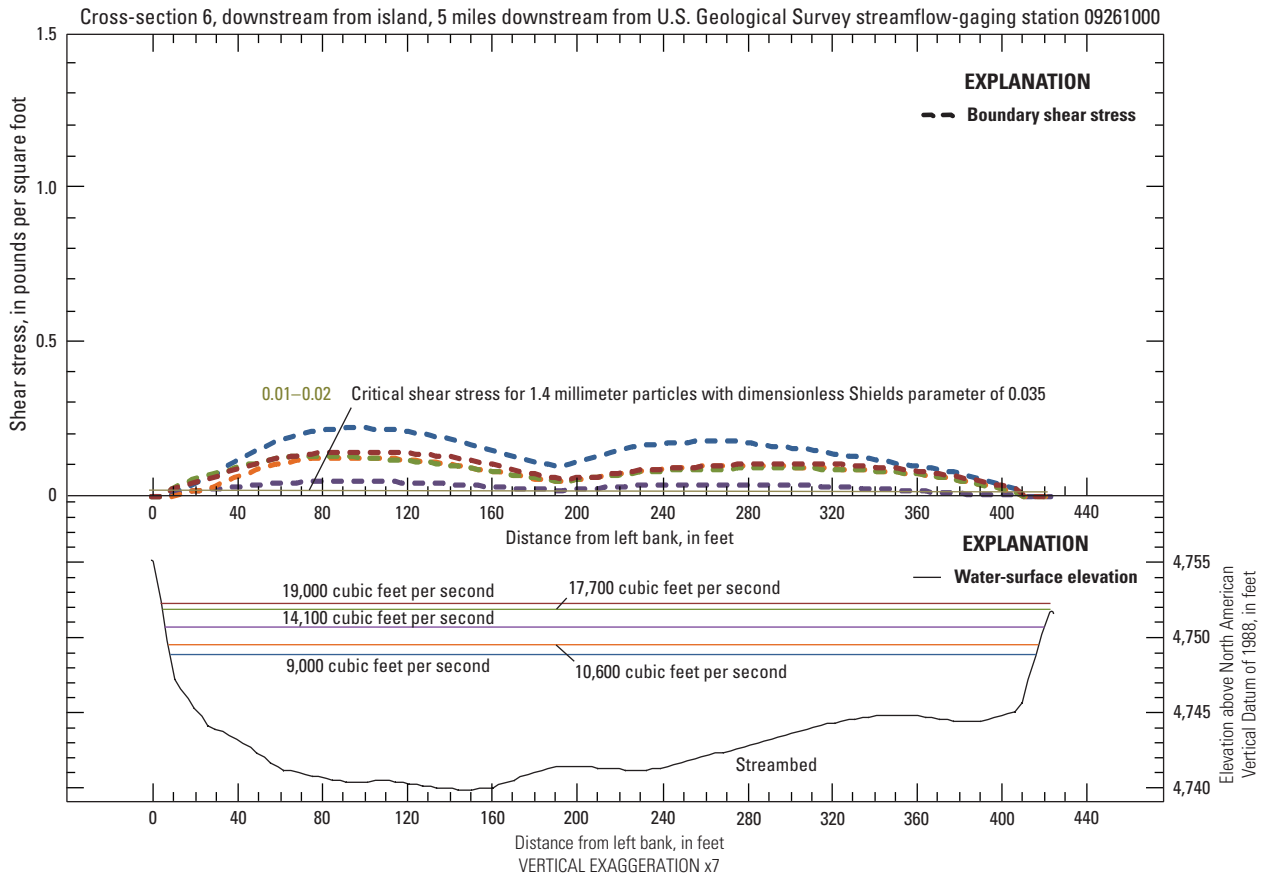

Figure 32. Graph showing cross-section 6 boundary shear stresses for the median particle size of 1.4 millimeters, water-surface elevations, and streambed elevations for selected streamflows at U.S. Geological Survey streamflow-gaging station, 09261000, Green River near Jensen, Utah.

Sediment-Transport Applications to Resource Management

The native fishes of the Upper Colorado River Basin have adapted to the diverse and unique habitat characteristics and geomorphic features found within the Colorado River. The streams that provide this habitat are characterized by larger channel gradients, high levels of water turbidity and salinity, and extreme seasonal variation in water temperature and streamflow. As a result, the native fishes are highly susceptible to the ecological changes that result from anthropogenic activities including streamflow regulation, habitat destruction and alteration, introduction of non-native fishes, and degraded water quality (Valdez and Muth, 2005). Habitat for endangered fishes in these rivers includes both gravel-bed reaches (spawning-habitat and food-source locations), backwater areas, and overbank habitat (juvenile habitat) formed along the banks of sand-bed reaches (Andrews, 1986; McAda, 2003). The formation and maintenance of these habitats historically (pre-reservoir) were assumed to be in equilibrium with streamflow conditions and sediment supplies (Andrews, 1986).

Creation and operation of large reservoirs and other anthropogenic water uses (irrigation and municipal diversions) within these river systems have resulted in reductions of peak streamflows and reduced effective discharge (where effective discharge is defined as the flow responsible for the majority of geomorphic work done by a stream over a period of several years) (Andrews, 1986; Elliott and Parker, 1997; McAda, 2003). Effective discharge has been reduced by as much as one-half in the Green River and has resulted in a 10-percent reduction in stream widths, which has lead to vegetation encroachment (Andrews, 1986). Channel narrowing and vegetation encroachment also has been observed in the Gunnison River (Elliott and Parker, 1997) and in the Colorado River near Grand Junction, Colorado (Osmundson and Kaeding, 1991; Pitlick, 2005). Understanding how stream conditions

and habitat change in response to alterations in streamflow is important for water administrators and wildlife managers and can be determined with an understanding of sediment transport (both bed- and suspended-sediment load).

Alteration of historic channel characteristics through streamflow regulation has resulted in observable changes in the range and number of multiple native and endangered species (Valdez and Muth, 2005; U.S. Fish and Wildlife Service, 2011a). Separation and identification of the processes and sediment characteristics that support important physical (channel morphology) and biological (habitat) stream attributes within priority reaches of this system allows for better applied water-management strategies and aids recovery of the endangered fishes. Determination of the processes that control sediment transport within this system is a key step in identifying streamflow conditions responsible for restored channel morphology and habitat. Restored channel morphology and habitat is needed in conjunction with other non-native fish management for sustained recovery of endangered fishes within these river systems. This report demonstrates that sediment-transport conditions at selected locations within the system have significant dependence on the magnitude and timing of streamflows and water management within the system. The following section will present findings from this report that can aid resource management within the study area.

Suspended-Sediment Transport

Suspended-sediment transport can be a large part of the total-sediment flux within the rivers of this study and as such is strongly related to the geomorphology and habitat conditions found in these reaches. Suspended-sediment transport affects the channel form, bank and bar development, and the availability and quality of habitat for multiple life-stages of aquatic species. Regression analysis was used in this report to estimate suspended-sediment transport as a function of streamflow, seasonality, and temporal trends. Estimates of SS flux can be helpful in determining total flux of sediments within the river at a station or to evaluate sediment budgets between stations. Understanding the processes that explain the variability of SS concentration also can provide information needed to better manage water resources within these rivers (related to the timing and magnitude of flow releases and withdrawal from reservoirs and diversion structures) and to evaluate temporal and spatial changes at a station and within river reaches.

The particle-size range of transported sediments plays a strong role in many processes related to channel form and habitat. The primary effect of sediment transported as wash load is related to the clarity or turbidity of the water column, though wash load also effects transient depositional features within the stream. Wash load has limited longstanding (more than a few months to a year) influence on processes controlling the channel form or streambed habitat within the active channel. Sand-sized particles can be transported as wash load and as suspended load and, relative to silt/clay-sized particles, will interact with the streambeds at greater frequencies over the majority of the wetted-channel area. Thus, sand SS flux (and sand SS concentration) may be more strongly related to channel-forming fluvial processes and habitat conditions than silt/clay SS flux (and silt/clay SS concentration).

Suspended-sediment transport equations using regression analysis were generated for the six stations that had sufficient data within the study area: three stations on the main-stem Colorado River between Cameo, Colorado, and the confluence with the Green River (CAMEO, STATELINE, and CISCO); one station on the Gunnison River downstream from the Aspinall Storage Unit (GUNNISON); and two stations on the Green River below Flaming Gorge Reservoir, and downstream from the confluence of the Yampa River (JENSEN and GREEN) (table 5). Interpretations of the variables used within the regression analysis aid in identification and quantification of the processes or mechanisms that are important controls on suspended-sediment transport within the system and to provide information on the timing of sediment inputs (supply changes) to the system.

Regression analysis of the suspended-sediment data show that streamflow explains 40 percent or less of the variability in natural logarithm SS concentration and 72 percent or less of the variability in natural logarithm sand SS concentration (fig. 14). For each station, natural logarithm streamflow including y-intercept, explained 26–40 percent of the observed variability in natural logarithm SS concentration (39–72 percent for natural logarithm sand SS concentration); seasonality (time within the year) explained 13–16 percent of the observed variability in natural logarithm SS concentration (2.1–14 percent for natural logarithm sand SS concentration); and temporal trends (time over mulitple years) explained 1.5–8.9 percent of the observed variability in natural logarithm SS concentration (0–6.2 percent for natural logarithm sand SS concentration).

Identified patterns in SS concentration related to seasonal variations (time within year, fig. 16); temporal trends (time over multiple years, figs. 17 and 18); and climatic effects (differences between wet and dry years, fig. 19) influence sediment-transport conditions and have a significant effect on the shape, slope, and intercept of the streamflow sediment-transport relation (Glysson, 1987). Depictions of the typical (median) relation between streamflow and SS concetration is provided for each station in figure 15 with additional depiction of seasonal differences between SS concentration and streamflow shown in figures 16–19, as previously indicated.

Figure 16 shows the annual cycle of SS concentration derived from each transport equation for an average year (artificial hydrograph produced from mean daily streamflows). Differences in the slopes and shapes of each plot when compared between stations or between SS concentration and sand SS concentration show seasonal differences in the relation between SS concentration and streamflow, also known as hysteresis (see section “Seasonal and Temporal Effects on Suspended-Sediment Transport” for further discussion on hystereisis effects) (fig. 16). Examination of the chronological sequences within the plots shows that the SS

concentration for a given streamflow is seasonally dependent; that is, for a specific streamflow there can be multiple predicted SS concentrations depending on the time of year.

For the stations in this study where the combination of streamflow and seasonality terms explains a smaller portion of the overall variability, sediment supply to these systems is inherently more variable and complex. Those stations are not as well characterized by the transport equations and continued sediment monitoring through daily data collection (in place of transport equations) may be warranted depending on the monitoring objectives. The systems associated with those stations may have increased variability owing to streamflow conditions in tributary areas or owing to spatial variations in geology (erosivity) within contributing areas.

Consistent temporal patterns in the dataset may represent adjustments to multi-season processes within the basin. The trends in natural logarithm SS concentration at the GUNNISON and Green River stations (GREEN and JENSEN) may be a continued response to channel adjustments that have been underway following completion of the Aspinall Storage Unit and the Flaming Gorge Reservoir. Previous investigations have documented the effects of reductions of peak streamflow and reduced effective discharge on the balance of sediment storage and transport within these river systems (Andrews, 1986; Elliott and Parker, 1997; McAda, 2003). Relative occurrence of the trend-direction reversal (progression through time from upstream to downstream) is consistent with a basin response to an upstream alteration of flow regime and sediment supply. In general, the upstream stations (the stations closer to the location of the alteration) will respond more quickly to the alteration and reach a new equilibrium ahead of downstream locations, although multiple oscillations may occur within the system before equilibrium is achieved. The trend-direction reversal clearly evident on the Green River where JENSEN reached a trend minimum in 1992, may be followed by a trend reversal at GREEN, but the lack of recent data (last sample was collected in 2000) precludes an assessment of the last decade (fig. 17). Trends in sand SS concentration at JENSEN may be an effect of bank stabilization, vegetation encroachment, or other anthropogenic changes (water management or land use) or climatic effects within the basin that have reduced fine-sediment (less than 0.0625 mm) entrainment (fig. 18). The Colorado (CAMEO) and Gunnison River (GUNNISON) have no evidence of reaching equilibrium conditions in SS concentration. This indicates that larger time scales may be needed to reach stable conditions within this system or that the observed trends are in response to more temporally continuous anthropogenic changes or climatic effects within the basin (fig. 17). The reversal in natural logarithm sand SS concentration at STATELINE and GUNNISON may indicate that a similar reduction in fine-sediment (less than 0.0625 mm) entrainment is occurring in the Colorado River from bank stabilization, vegetation encroachment, or land-use changes (fig. 18).

Significant differences (p-value less than 0.05) in the slope and intercept between natural logarithm streamflow and natural logarithm SS concentration were tested for at all stations, based on classification as wet and dry years, and were determined at five of the six stations (rising-limb: CAMEO, CISCO, JENSEN, and GREEN; falling-limb: GUNNISON) (fig. 19). No statistically significant differences were determined between any multi-year cycle comparison and may be indicative of the smaller dataset available for such comparisons. The natural logarithm SS concentration during wet years is typically higher than during dry years for the same streamflow (rising-limb) and is less strongly controlled (flatter slopes) by streamflow magnitude. For GUNNISON (falling-limb), differences in natural logarithm SS concentration at smaller streamflow values (less than 7,000 ft^3/s) show that dry years have higher concentrations than wet years, and at larger streamflows the concentrations are lower than wet years. Differences in sediment-transport processes or water management on the Gunnison River (Aspinall Storage Unit and (or) Ridgeway Reservoir) may be causing the inconsistency between GUNNISON and nearby CAMEO and CISCO.

Some of the differences determined between wet and dry years (rising-limb) may be affected by the sediment continuity between reaches and the size and location of reservoirs. Areas that are downstream from large main-stem reservoirs may not show as strong an influence between wet and dry years. This may be because the reservoirs act effectively as sediment traps, resulting in reduced downstream transport of sediment, thus lessening the effect that wet and dry years have on sediment-transport dynamics. As such, stations unaffected by large main-stem reservoirs, like CAMEO, have stronger effects from wet and dry years because reservoirs are located distally within the watershed. Reduced effects of wet and dry years occur at GUNNISON and STATELINE and are likely related to the effects from sediment traps on the Gunnison River (Aspinall Storage Unit and Ridgeway Reservoir). The effect of these reservoirs is no longer observable at CISCO, potentially in response to sediment inputs from the Dolores River. The sediment-rich Yampa River Basin may alleviate the effects from sediment storage in Flaming Gorge Reservoir for stations on the Green River below the Yampa River confluence (JENSEN and GREEN) such that differences in sediment-transport conditions between wet and dry years are significant. Future sediment monitoring at locations in reaches on the Green River below Flaming Gorge and upstream from the Yampa River confluence could be used for confirmation of this hypothesis.

Incipient Motion and Bed-Load Transport

Incipient motion of streambed material (often occurring as bed-load transport) and the sorting of bed materials are important controls on channel form and habitat and are strongly related to the channel morphology and habitat conditions within these rivers (Knighton, 1998). The characteristics of bed material strongly control the down-cutting and transport of sediments especially in basins with modifications to flow regimes resulting from water management. To prevent further channel narrowing and loss of functioning side channel- and backwater-habitat, it may be necessary to break up the layer of gravels and cobbles

that have created a pavement layer in the streambeds of these channels through armoring. When the pavement layer is broken up and possibly entrained, the finer gravels and sands that underlie the pavement layer, or are trapped between the cobbles, also are entrained allowing for adjustment and maintenance of channel dimensions (Milhous, 1982). Encroaching vegetation in the riparian areas can be eradicated when the alluvial banks and bars are regularly inundated and when significant entrainment of the d_{50} occurs (Friedman and Auble, 1999). The composition of streambeds also relates to aquatic ecosystem food supply (benthic invertebrates) as well as spawning conditions (McAda, 2003). Deposition of fine sediment on top of benthic or spawning habitat (seasonally dependent) can reduce habitat quality and require stream conditions capable of (1) removal of fine sediments (flushing of fines) from gravel-bed reaches or (2) entrainment of the gravel-bed material to expose and transport fine materials, which are sheltered by the larger gravels, in order to restore the habitat quality. Characterization of bed-material sediment-particle sizes and forces needed to initiate motion of these particles can provide information to better manage water resources within these rivers.

Comparison between boundary shear stresses of multiple streamflows and the relative mobility of bed material (d_{50}, median sediment-particle sizes) characterizes the effects of flow magnitude on mobilization of framework grains within the streambed. Observations at multiple cross sections within two reaches of the Gunnison River downstream from the Aspinall Storage Unit (09144250, Gunnison River at Delta, Colorado, figs. 21–23; and 09152500, Gunnison River at Grand Junction, Colorado, figs. 24–26) show ineffectual mobilization of most, if not all, areas within the surveyed cross sections. The largest surveyed streamflow exceeded bankfull conditions at the Gunnison River at Delta, Colorado, with a peak streamflow magnitude of 13,300 ft^3/s (recurrence interval of 5 to 10 years, table 9). At the Gunnison River near Grand Junction, Colorado, the largest surveyed peak streamflow was 14,000 ft^3/s (recurrence interval of 5 to 10 years, table 9).

Observations at multiple cross sections within a study reach of the Green River downstream from Flaming Gorge Reservoir (09261000, Green River near Jensen, Utah, figs. 27–32) show a range of potential transport conditions. Streambed conditions within the study reach on the Green River can be characterized by two dominant-size distributions that vary spatially and temporally within the system. A gravel-dominated pavement layer was exposed intermittently within the channel with varying thicknesses of a sand veneer along the surface. Evaluation of transport characteristics of each of the two size distributions was used to produce the end members of a continuum that represent the characteristics of the channel. Incipient motion of specific particles within this area may occur along a continuum that is defined by the proportion of sand within a given gravel mixture (gravel critical shear stresses were less than 20–30 percent sand; sand critical shear stress for sand veneer with reduction in the gravel critical shear possible). Incipient-motion analysis shows ineffectual mobilization of most, if not all, areas within the surveyed cross sections of the larger bed material (based on gravel d_{50}) including peak streamflows of as much as 19,000 ft^3/s (recurrence interval of 2.3 to 5 years, table 9). However, when the sand veneer is present at these cross sections, or where the portion of sand within the bed material exceeds 20–30 percent of the total, mobilization of the bed material (based on sand d_{50}) will occur at most locations within the surveyed cross sections for peak streamflows of 9,000–19,000 ft^3/s (recurrence intervals ranging from 1 to 5 years, table 9) with mobilization of gravels possible in some areas. Further sediment-particle-size classification and determination of the portions of sands throughout the reach would be needed to quantify the portion of the gravel bed that is mobilized within the reach.

Case Study: Evaluation of Sand Transport in the Green River near Jensen, Utah

Application of the two-dimensional stream hydraulics and sediment-transport models provides enhanced capabilities for evaluations of dynamic reach-scale processes that affect habitat suitability. An evaluation of the sediment-transport conditions for sand-sized particles in spawning habitat can be used to determine streambed conditions and provide enhancement to conceptual models within these systems. Identification of processes that limit sediment transport within these systems is necessary to correctly identify proper streamflow targets that create and maintain habitat within these systems. Linking physical measurements of critical habitat to conceptual and process-based models can define critical relations between habitat and streamflow conditions. Those links provide a better understanding of the processes that affect the sediment-transport characteristics, which are important to the maintenance of endangered fish spawning habitat, and can be used to inform the flow-recommendations process that currently (2012) guides water management of Flaming Gorge Reservoir (fig. 3). Razorback sucker spawning occurs over cobble- or gravel-sized streambed material, with streamflow velocities less than 3.3 ft/s and flow depths of less than 3.3 ft (Valdez and Muth, 2005). Spawning occurs during the rising-limb of the snowmelt-runoff hydrograph when water temperatures are approximately 15°C, typically mid-April to June (Valdez and Muth, 2005). The eggs are a sticky mass laid down by the females, and when gravels are present and flushed of finer sediments (sands) the egg-mass adheres to the surface of the gravels and remains in place. When sands overlay the gravels along the streambed, the egg-mass adheres to the sands instead of the gravels. Without the added weight of the gravels, the egg-mass can be transported downstream where predation and scattering of the eggs is more likely to occur. During spawning seasons, female razorback suckers have been reported to remove thin layers of sands in order to expose the covered gravels along the spawning habitat (Wick, 1997). If changes in sediment transport within the reach result in the migration of sands along the streambed (transported as bed load), deposits of eggs that have adhered to the gravel bed can become smothered by sand preventing successful emergence of the larvae (Wick, 1997).

Evaluation of Sediment-Transport and Spawning-Habitat Conditions

Transport conditions for two selected sizes of sands were compared within the Green River study reach (fig. 27). Sand-sized particles ranging from 0.5 to 1.4 mm represent the range in sediment-particle size that is commonly present in the reach upstream from the spawning habitat and are consistent with sediment-particle sizes found in previous investigations (Wick, 1997). These two sediment-particle sizes represent the d_{16} through the d_{84} sizes for sediments sampled at selected locations within the reach using dredge samplers (Williams and others, 2009). Using this range of sand-sized particles provides representative measures of how most sands are moving within the system.

Variations in sediment mobility and transport mode can be characterized within the study reach over the range of streamflows typical of the spawning seasons (mid-April to June, post-Flaming Gorge Reservoir, WY 1965–2008). Streamflow conditions ranged from 5,030 to 13,500 ft^3/s and typically were between 7,310 and 12,250 ft^3/s, based on the 25th and 75th percentiles of mean daily streamflows at USGS streamflow-gaging station, 09261000, Green River near Jensen, Utah (April 15–May 31 for WY 1965–2008) (U.S. Geological Survey, 2011). Characterizations of sand transport for a reach of the Green River containing identified razorback sucker spawning habitat were evaluated using the output from modeled stream hydraulics representative of 9,000; 10,600; 14,100; 17,700; and 19,000 ft^3/s (figs. 33–37, respectively).

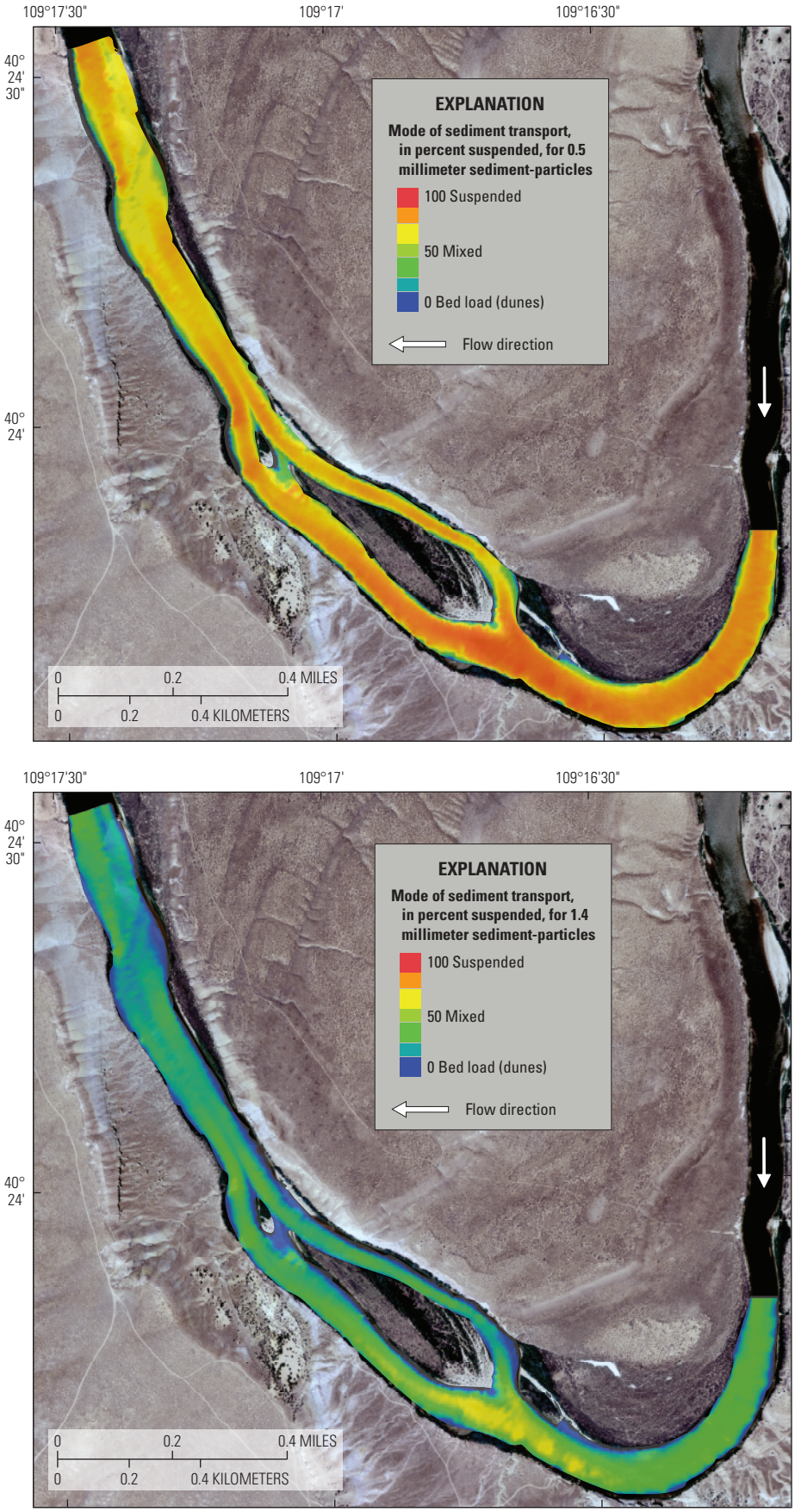

Orthoimages from U.S. Department of Agriculture National Agriculture Imagery Program (2007)
Universal Transverse Mercator North American Datum 1983, Zone 13 North

Figure 33. Maps showing comparison of the modes of sediment transport for sands in a reach of the Green River near identified razorback sucker spawning habitat at a modeled streamflow of 9,000 cubic feet per second.

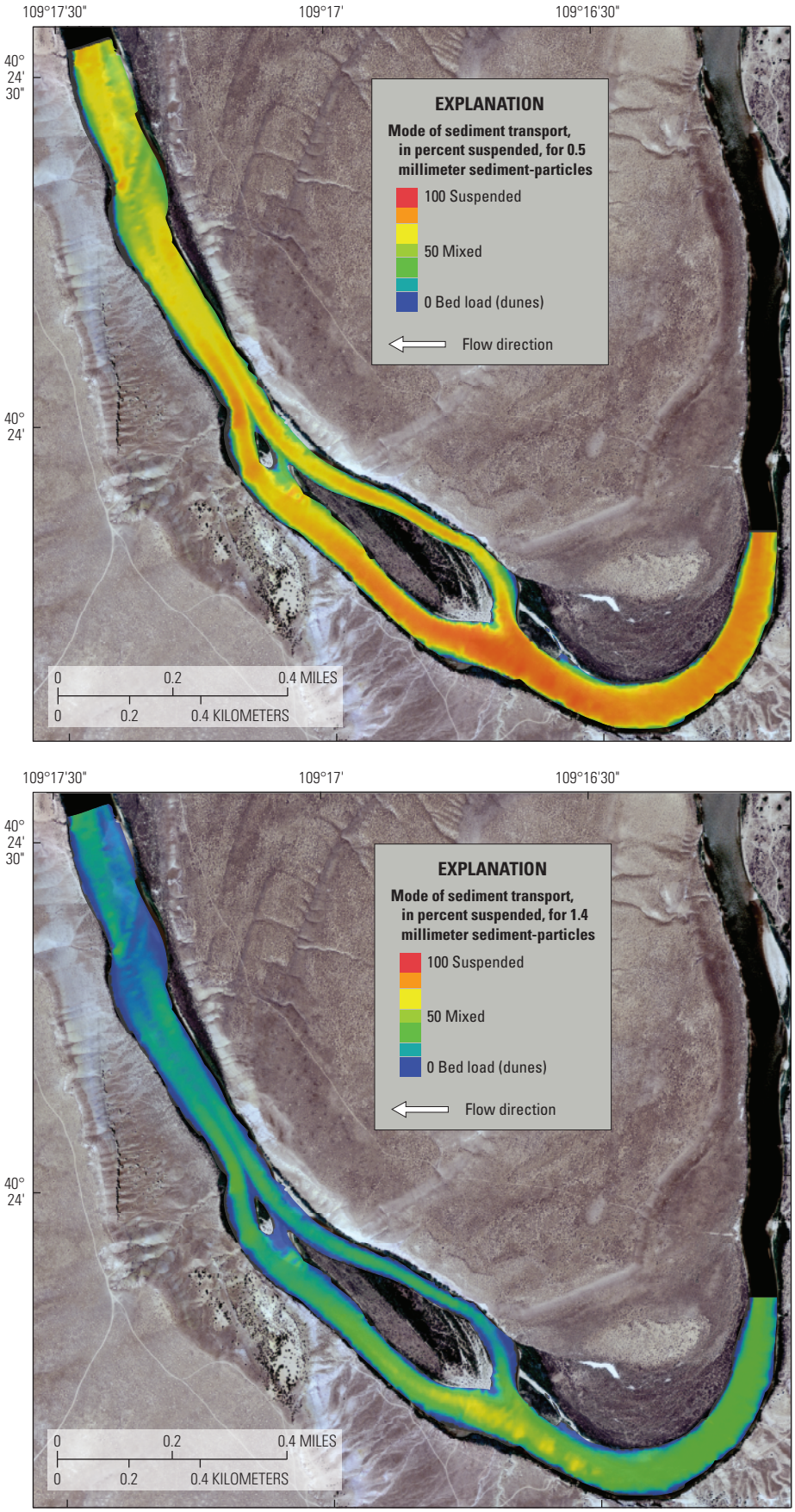

Orthoimages from U.S. Department of Agriculture National Agriculture Imagery Program (2007)
Universal Transverse Mercator North American Datum 1983, Zone 13 North

Figure 34. Maps showing comparison of the modes of sediment transport for sands in a reach of the Green River near identified razorback sucker spawning habitat at a modeled streamflow of 10,600 cubic feet per second.

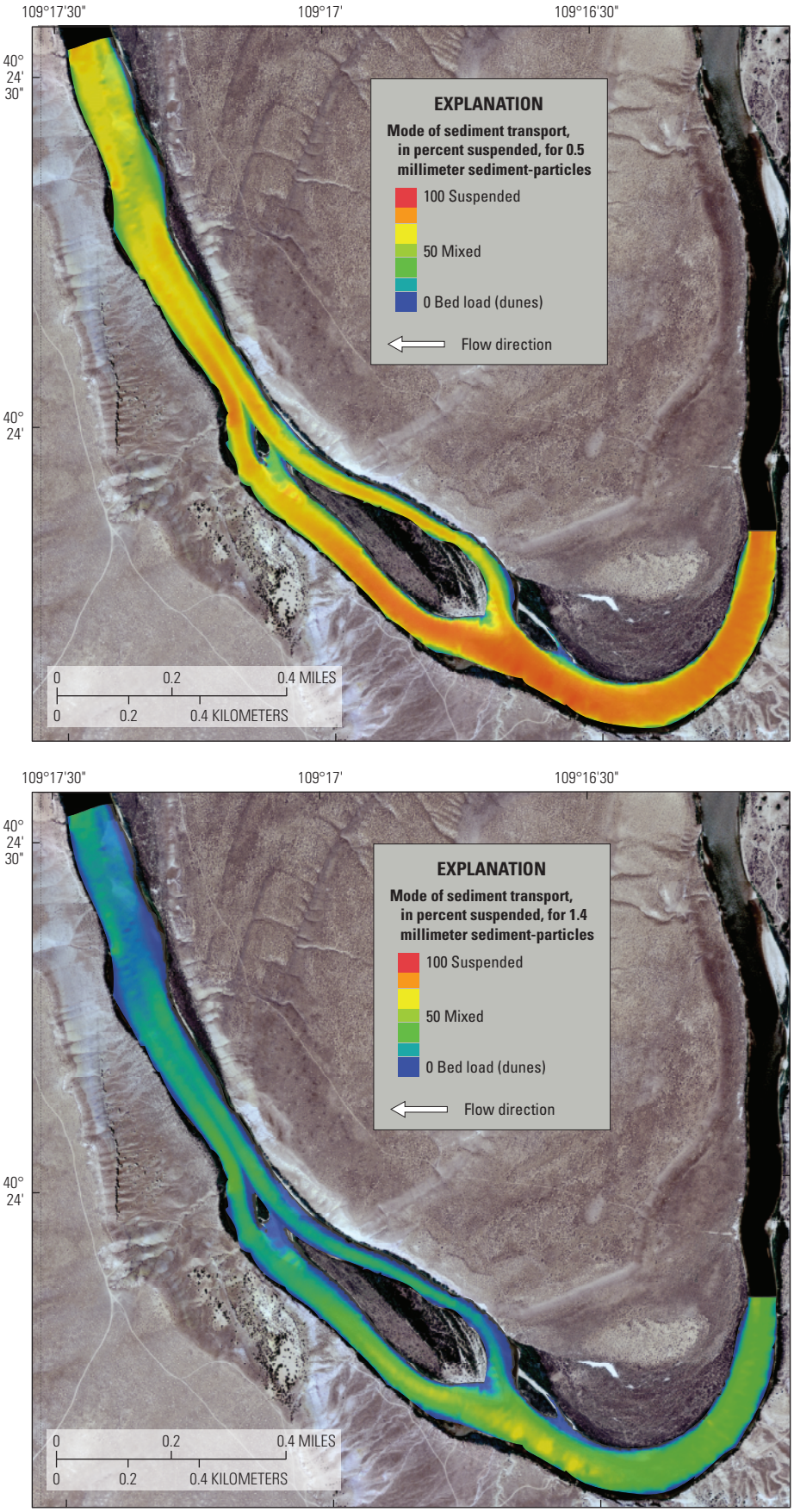

Orthoimages from U.S. Department of Agriculture National Agriculture Imagery Program (2007)
Universal Transverse Mercator North American Datum 1983, Zone 13 North

Figure 35. Maps showing comparison of the modes of sediment transport for sands in a reach of the Green River near identified razorback sucker spawning habitat at a modeled streamflow of 14,100 cubic feet per second.

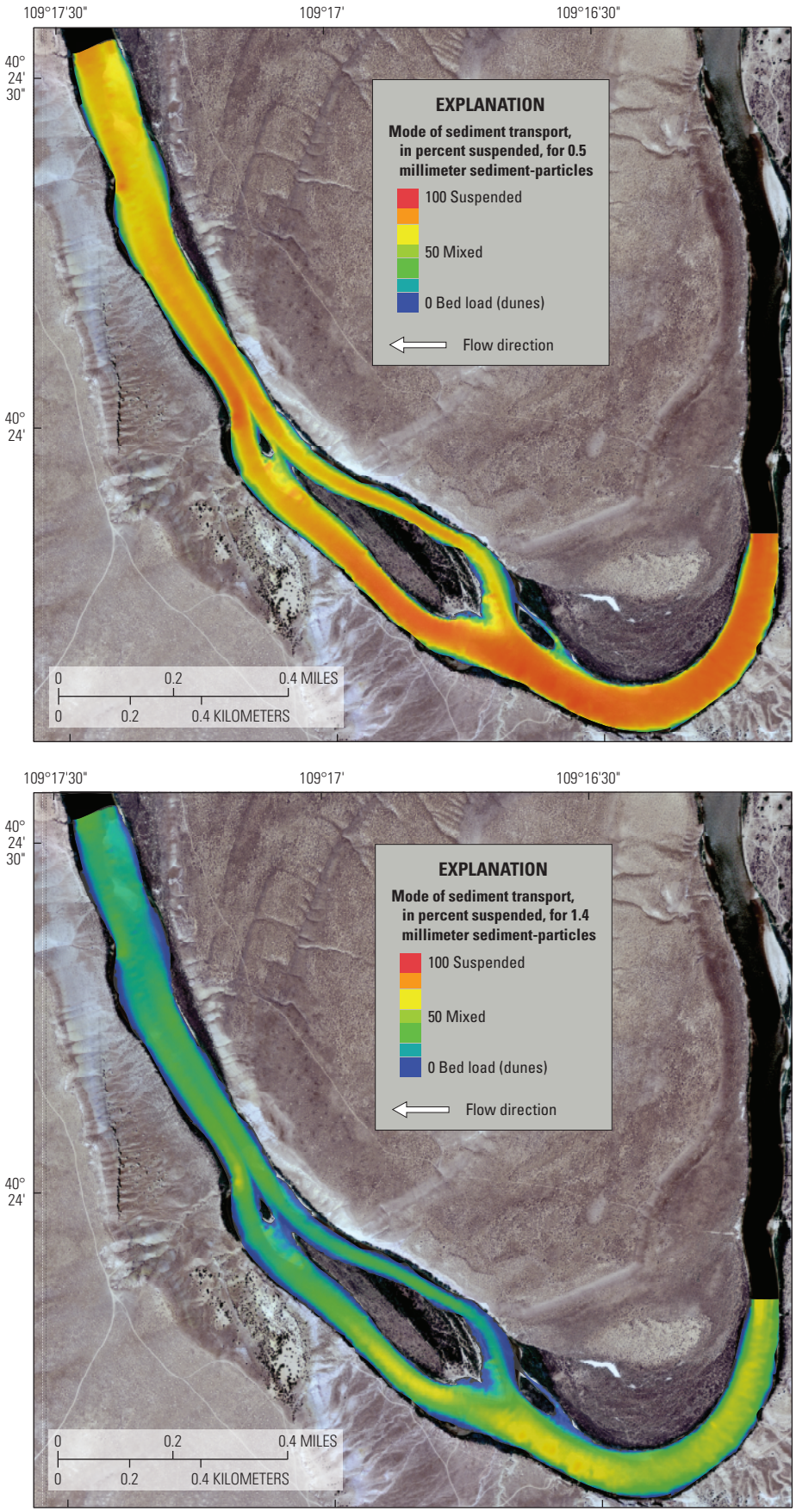

Orthoimages from U.S. Department of Agriculture National Agriculture Imagery Program (2007)
Universal Transverse Mercator North American Datum 1983, Zone 13 North

Figure 36. Maps showing comparison of the modes of sediment transport for sands in a reach of the Green River near identified razorback sucker spawning habitat at a modeled streamflow of 17,700 cubic feet per second.

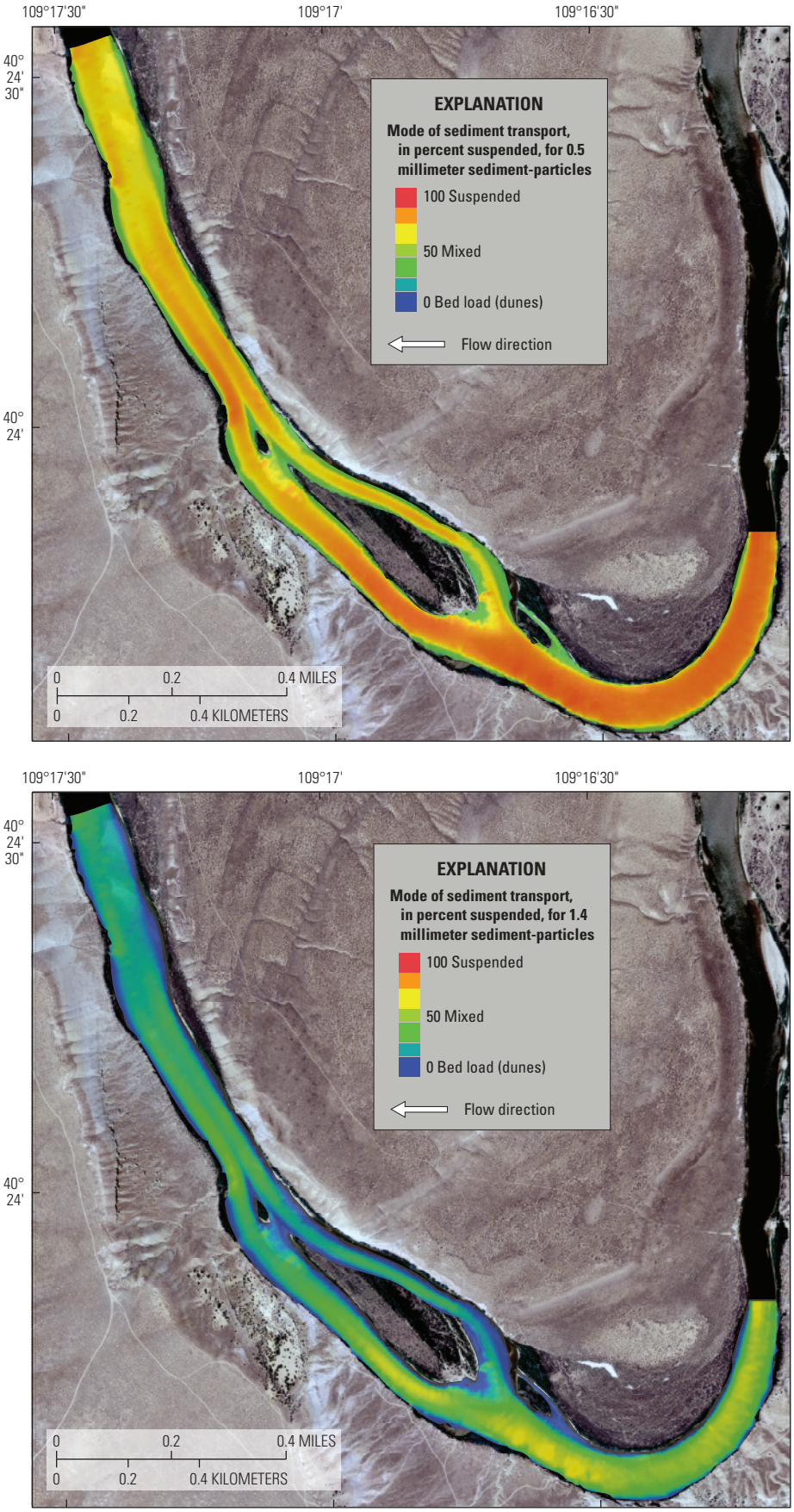

Orthoimages from U.S. Department of Agriculture National Agriculture Imagery Program (2007)
Universal Transverse Mercator North American Datum 1983, Zone 13 North

Figure 37. Maps showing comparison of the modes of sediment transport for sands in a reach of the Green River near identified razorback sucker spawning habitat at a modeled streamflow of 19,000 cubic feet per second.

Characterization of the Sand-Transport Conditions within the Study Reach

Increasing streamflow within the study reach has variable effects on sand-transport conditions (figs. 27, and 33–37). Transport of both sand sizes occurs throughout the main channel of the reach over all modeled streamflows (9,000–19,000 ft^3/s). Along and upstream from the meander bend for modeled streamflows up to 14,100 ft^3/s, increases in streamflow results in increases in the proportion of sands carried in suspension (based on calculations of the Rouse numbers and reference to table 2); increases in streamflow between the largest modeled streamflows (17,700 and 19,000 ft^3/s) results in a reduction in the percentage of sand transported in suspension. The areas immediately upstream from the mid-channel bar generally show decreases in the percentage of sand transported in suspension as streamflow increases. The small secondary channel along river-right (right side of the river, as viewed looking downstream) just upstream from the mid-channel bar becomes inundated at 9,000 ft^3/s and begins transporting 0.5 and 1.4 mm sands into the main channel at a streamflow of 17,700 ft^3/s. Flow along river-left of the mid-channel bar shows reductions in the percentage of sand transported in suspension between streamflows 9,000 and 14,100 ft^3/s followed by marked increase in the percentage of sand transported in suspension at larger streamflows (17,700 and 19,000 ft^3/s). The percentage of sand transported in suspension is relatively consistent over the entire range of modeled streamflows river-right of the mid-channel bar (between cross-sections 2, 5, and 6; fig. 27). Transport conditions downstream from the mid-channel bar show a decrease in the percentage of sand transported in suspension with increases in streamflow between 9,000 and 17,700 ft^3/s. However, the percentage of sand transported in suspension increases at larger streamflows (17,700 and 19,000 ft^3/s) and is greatest at modeled streamflows of 17,700 ft^3/s.

Identification of Processes Controlling Sediment Transport in the Study Reach

The constraints on sand transport within the study reach can be shown in comparisons of boundary shear stress for the five modeled streamflows. Evaluation of model conditions along a longitudinal profile (fig. 38) was done to compare changes in transport conditions along the study reach from upstream to downstream. Boundary shear stress for all modeled streamflows generally was greater upstream and decreased downstream from the mid-channel bar, with the reductions occurring just upstream from or along the mid-channel bar (fig. 39). In areas river-right of the mid-channel bar, there is a sudden reduction in boundary shear stress of approximately 50 percent (relative to conditions just-upstream-from the bar), which is maintained downstream from the mid-channel bar. Along river-left of the mid-channel bar there is a similar reduction in boundary shear stress, which is quickly regained and then gradually reduced to levels similar to river-right of the mid-channel bar.

Comparisons between the modeled streamflows show that in areas upstream from the mid-channel bar, increases in streamflow generally correspond to increases in boundary shear stress (fig. 40). In areas just upstream from the mid-channel bar there is a reversal in the relation between boundary shear stress and streamflow and increases in streamflow result in decreases in boundary shear stress. Within areas river-right of and downstream from the mid-channel bar, the boundary shear stress tends to be largest for the 9,000 and 17,700 ft^3/s streamflows and smallest for the 10,600 and 14,100 ft^3/s streamflows. Along areas river-left of the mid-channel bar, larger streamflows (17,700 and 19,000 ft^3/s) have increased boundary shear stresses and smaller streamflows have decreased boundary shear stresses.

Comparisons were done among water-surface elevations for the five modeled streamflows and the effects on sand transport to investigate causality. Increases in streamflow result in changes in flow depth and changes to water-surface slopes, though, these changes may not always be unidirectional within a channel. Water-surface elevations for the streamflow models show that in the reach upstream from the mid-channel bar, water-surface slope remains nearly constant (fig. 40). For areas along and downstream from the mid-channel bar, as streamflow increases water-surface slopes decrease (fig. 40). Along the mid-channel bar, water-surface slopes decrease from 0.00069 (9,000 ft^3/s) to 0.00043 (19,000 ft^3/s), and downstream from the mid-channel bar they decrease from 0.00038 (9,000 ft^3/s) to 0.00024 (19,000 ft^3/s). This is approximately a 37-percent reduction in water-surface slope between 9,000 and 19,000 ft^3/s for areas along and downstream from the mid-channel bar.

A previous investigation (Wick, 1997) reported that sediment deposition on the spawning habitat (figs. 38–40) may result from backwater effects (decreases in water-surface slope) produced in the areas along the mid-channel bar at streamflows above 14,500 ft^3/s. The backwater effect is reported to arise from a channel constriction (reduction in flow area) just downstream from the mid-channel bar (Wick, 1997). Reductions in water-surface slope are observed within the simulations of this analysis along the mid-channel bar (at the downstream end) and are consistent with findings from Wick (1997), although backwater effects appear more substantial along river-left (fig. 40). A small secondary channel (identified in figs. 27 and 38) also was identified as a locally important source area for sands that are deposited on the spawning habitat at streamflows of 11,500 ft^3/s and greater. Comparisons of model simulations from this analysis showed limited transport of sands in isolated locations within the secondary channel at streamflow of 10,600 ft^3/s with more extensive continuous transport at streamflows of 14,100 ft^3/s and greater (figs. 33–37).

Figure 38 (following page). Map showing longitudinal profile for modeled output, 5 miles downstream from the Green River near Jensen, Utah, streamflow-gaging station.

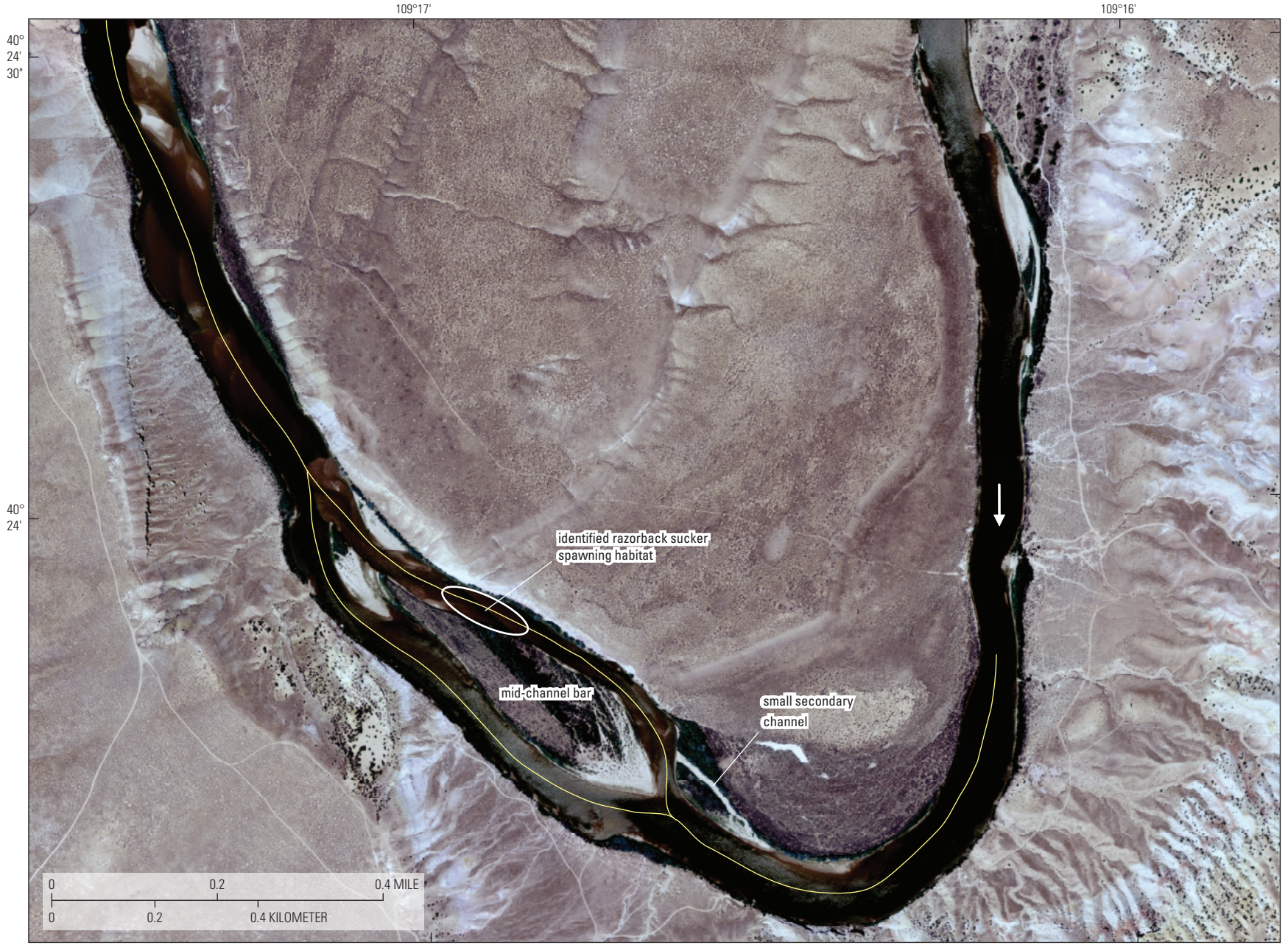

Orthoimages from U.S. Department of Agriculture National Agriculture Imagery Program (2007)
Universal Transverse Mercator North American Datum 1983, Zone 13 North
Scale 1:10,000

EXPLANATION

Longitudinal profile of modeled output

Flow direction

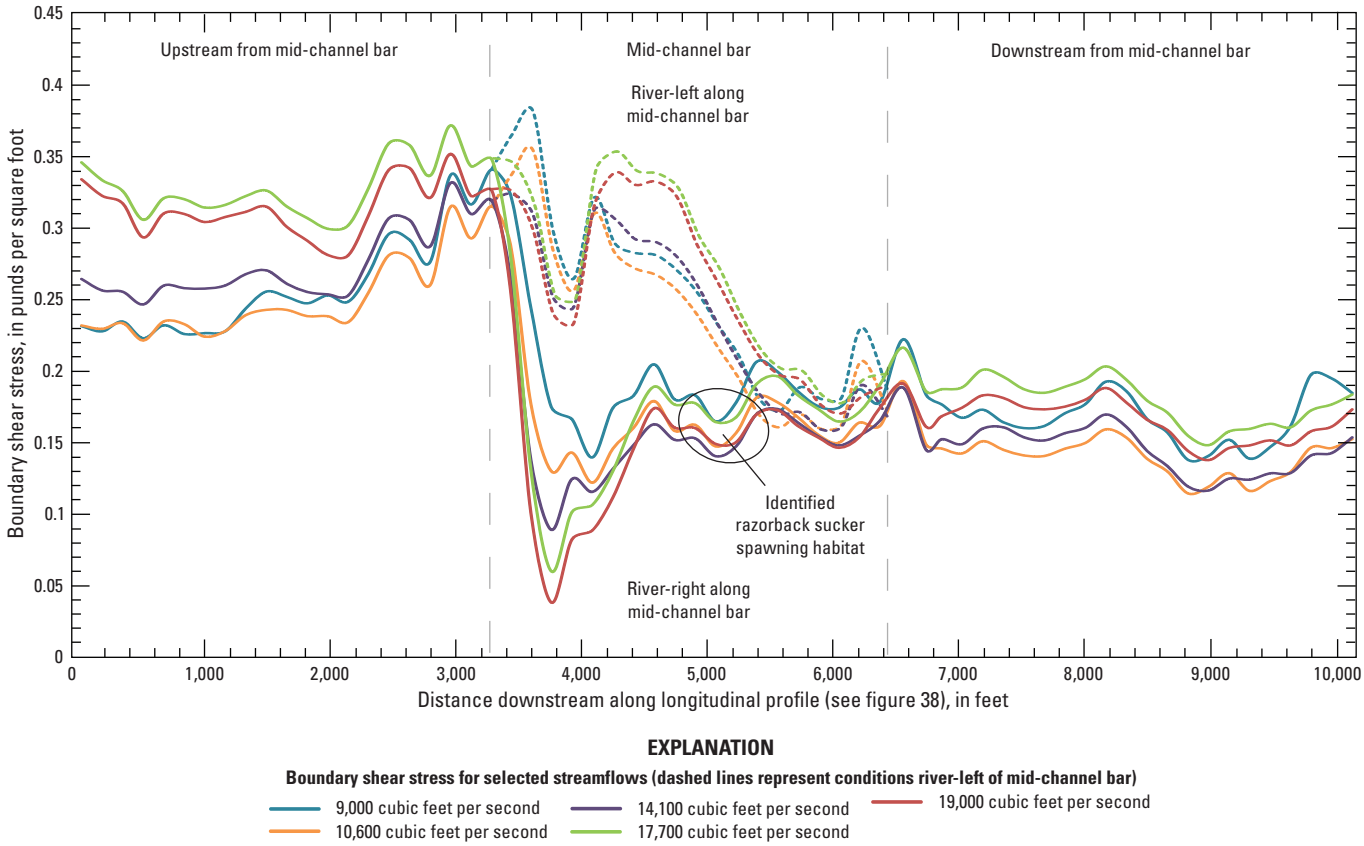

Figure 39. Graph showing boundary shear stress along longitudinal profile of a reach 5 miles downstream from the Green River near Jensen, Utah, streamflow-gaging station.

Evaluations of the processes that are important in understanding sediment deposition on the spawning habitat near the mid-channel bar are not limited to stream-transport conditions within the spawning-habitat reach. Considerations of sediment availability and net changes in sediment transport between upstream reaches and the spawning habitat are important. As previously mentioned, sands are mobile throughout the main channel for all modeled streamflows (9,000–19,000 ft^3/s), but in areas upstream from the mid-channel bar (and spawning habitat) increases in streamflow tend to increase boundary shear stress and the percentage of sediment transported in suspension. Increases in boundary shear stress increase the percentage of sediment transported in suspension resulting in increased transport rates (bed-load transport tends to occur in sporadic starts and stops and suspended transport moves at rates closer to water velocities).

Within the spawning habitat, increases in streamflow result in decreases in water-surface slope and varied responses to boundary shear stress, although the percentage of sand transported in suspension is relatively unchanged. Recall that Wick (1997) reported that deposition of sand on the spawning habitat does not occur at streamflows less than 14,500 ft^3/s, which corresponds to a difference in boundary shear stress between the upstream reach and the spawning areas of 0.06 lb/ft^2 or 33 percent. At larger streamflows where depositions are reported to occur, the difference in boundary shear stress between the upstream reach and the spawning-habitat areas increases to 0.13 lb/ft^2 or 68 percent.

At larger streamflows (14,100–17,700 ft^3/s), sediment upstream from the mid-channel bar is transported in greater amounts and likely at greater rates than can be transported by the conditions at the spawning-habitat reach. This may exceed a threshold between the two areas, thus resulting in a disequilibrium and net deposition of sands on the spawning habitat at higher streamflows (14,100–17,700 ft^3/s). Spawning habitat may be less suitable at these higher streamflows owing to deposition of sands on the spawning habitat under these conditions.

Figure 40 (following page). Graphs showing *A*, relative water-surface slopes and *B*, water-surface elevations along longitudinal profile of a reach 5 miles downstream from the Green River near Jensen, Utah, streamflow-gaging station.

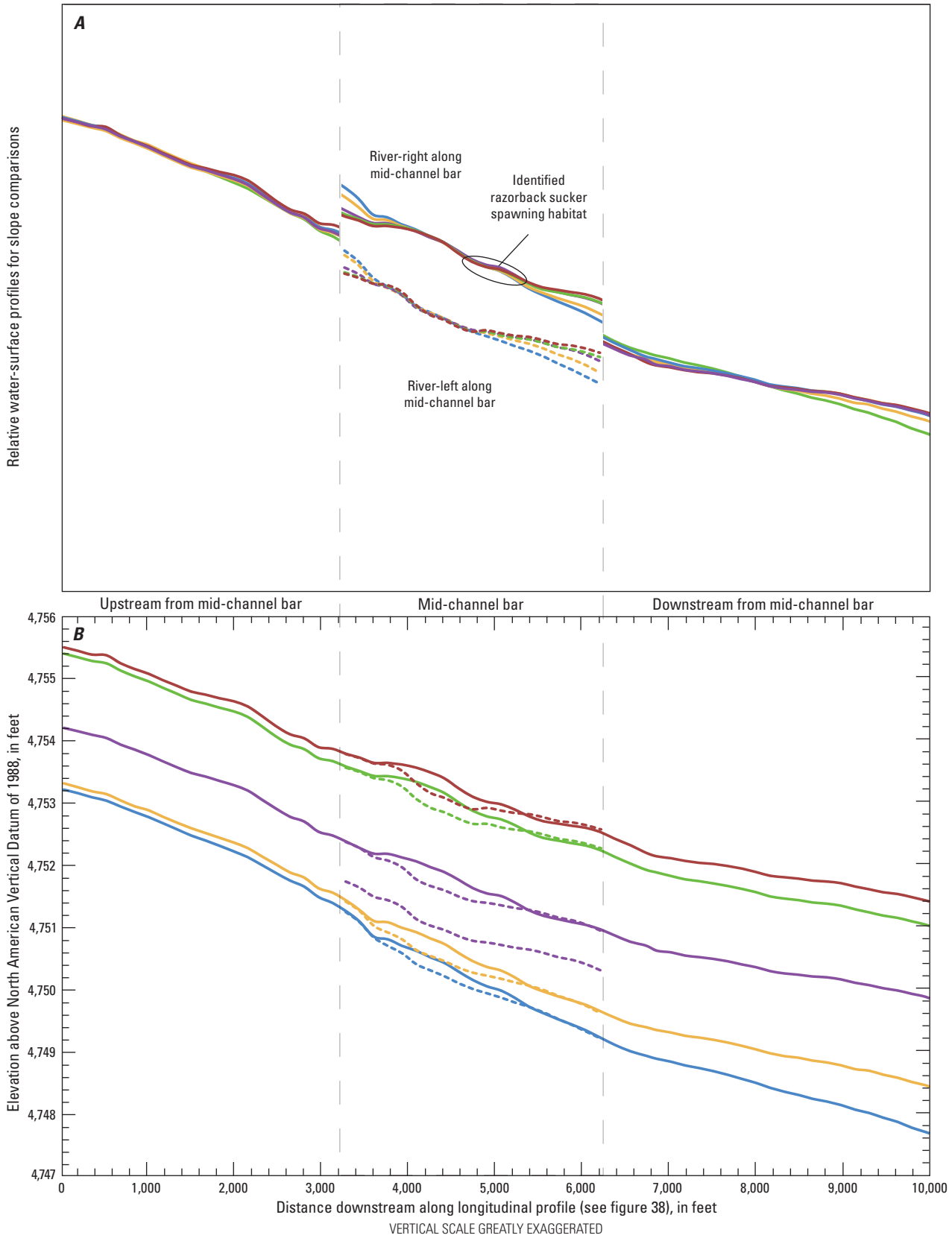
A
Relative water-surface profiles for slope comparisons
River-right along mid-channel bar
Identified razorback sucker spawning habitat
River-left along mid-channel bar
Upstream from mid-channel bar
Mid-channel bar
Downstream from mid-channel bar
B
Elevation above North American Vertical Datum of 1988, in feet
4,756
4,755
4,754
4,753
4,752
4,751
4,750
4,749
4,748
4,747
0
1,000
2,000
3,000
4,000
5,000
6,000
7,000
8,000
9,000
10,000
Distance downstream along longitudinal profile (see figure 38), in feet
VERTICAL SCALE GREATLY EXAGGERATED
EXPLANATION
Water-surface elevations for selected streamflows (dashed lines represent conditions river-left of mid-channel bar)
9,000 cubic feet per second
10,600 cubic feet per second
14,100 cubic feet per second
17,700 cubic feet per second
19,000 cubic feet per second

Summary

The Colorado River Basin provides habitat for 14 native fish, including 4 endangered species protected under the Federal Endangered Species Act of 1973. These endangered fish species once thrived in the Colorado River system, but water-resource development, including the building of numerous diversion dams and several large reservoirs, and the introduction of non-native fish, resulted in large reductions in the numbers and range of the four species through loss of habitat and stream function. Understanding how stream conditions and habitat change in response to alterations in streamflow is important for water administrators and wildlife managers and can be determined from an understanding of sediment transport. Characterization of the processes that are controlling sediment transport is an important first step in identifying flow regimes needed for restored channel morphology and the sustained recovery of endangered fishes within these river systems. The U.S. Geological Survey, in cooperation with the Upper Colorado River Endangered Fish Recovery Program, Bureau of Reclamation, U.S. Fish and Wildlife Service, Argonne National Laboratory, Western Area Power Administration, and Wyoming State Engineer's Office, began a study in 2004 to characterize sediment transport at selected locations on the Colorado, Gunnison, and Green Rivers to begin addressing gaps in existing datasets and conceptual models of the river systems.

This report identifies and characterizes the relation between streamflow (magnitude and timing) and sediment transport and presents the findings through discussions of (1) suspended-sediment transport, (2) incipient motion of streambed material, and (3) a case study of sediment-transport conditions for a reach of the Green River identified as a razorback sucker spawning habitat.

Estimation of suspended sediment (SS) flux can be accomplished using sediment-transport curves, which define the relation between SS flux and relevant explanatory variables such as streamflow, seasonality, and time. Understanding the relation between streamflow and suspended-sediment transport can aid in the evaluation of physical and temporal processes that affect sediment transport. Inter-annual conditions can be important in sediment supply and storage. The sediment-streamflow relation may change following a hydrological 'wet' or 'dry' year or period. Comparisons were made between differing annual cycles (1-year periods) and between multi-year cycles (1-year periods following specific multi-year periods). This analysis was designed to identify antecedent conditions that produced discernable changes in the slope and intercept of the streamflow sediment-transport relation.

Suspended-sediment transport can be a large part of the total-sediment flux within the rivers of this study and as such is strongly related to the geomorphology and habitat conditions found in these reaches. Suspended-sediment transport affects the channel form, bank and bar development, and the availability and quality of habitat for multiple life-stages of aquatic species. Regression analysis was used in this report to estimate SS transport as a function of streamflow, seasonality, and temporal trends. Estimates of SS flux can be helpful in determining total flux of sediments within the river at a station or to evaluate sediment budgets between stations. Understanding the processes that explain the variability of SS concentration also can provide information needed to better manage water resources within these rivers (related to the timing and magnitude of flow releases and withdrawal from reservoirs and diversion structures) and to evaluate temporal and spatial changes at a station and within river reaches.

The sediment-particle-size range of transported sediments plays a strong role in many processes related to channel form and habitat. The primary effect of sediment transported as wash load is related to the clarity or turbidity of the water column, though wash load also effects transient depositional features within the stream. Wash load has limited longstanding (more than a few months to a year) influence on processes controlling the channel form or streambed habitat within the active channel. Sand-sized particles can be transported as wash load and as suspended load and, relative to silt/clay-sized particles, will interact with the streambeds at greater frequencies over the majority of the wetted-channel area. Thus, sand SS flux (and sand SS concentration) may be more strongly related to channel-forming fluvial processes and habitat conditions than silt/clay SS flux (and silt/clay SS concentration).

Suspended-sediment transport equations using regression analysis were generated for the six stations that had sufficient data within the study area: three stations on the main-stem Colorado River between Cameo, Colorado, and the confluence with the Green River; one station on the Gunnison River downstream from the Aspinall Storage Unit; and two stations on the Green River below Flaming Gorge Reservoir, and downstream from the confluence of the Yampa River. Interpretations of the variables used within the regression analysis aid in identification and quantification of the processes or mechanisms that are important controls on suspended-sediment transport within the system and to provide information on the timing of sediment inputs (supply changes) to the system.

Regression analysis of the suspended-sediment data show that streamflow explains 40 percent or less of the variability in natural logarithm SS concentration and 72 percent or less of the variability in natural logarithm sand SS concentration. For each station, natural logarithm streamflow including y-intercept, explained 26–40 percent of the observed variability in natural logarithm SS concentration (39–72 percent for natural logarithm sand SS concentration); seasonality (time within the year) explained 13–16 percent of the observed variability in natural logarithm SS concentration (2.1–14 (Wick, 1997) percent for natural logarithm sand SS concentration); and temporal trends (time over mulitple years) explained 1.5–8.9 percent of the observed variability in natural logarithm SS concentration (0–6.2 percent for natural logarithm sand SS concentration).

Identified patterns in SS concentration related to seasonal variations (time within year); temporal trends (time over multiple years) and climatic effects (differences

between wet and dry years) influence sediment-transport conditions and have a significant effect on the shape, slope, and intercept of the streamflow sediment-transport relation. Depictions of the typical (median) relation between streamflow and SS concentration shows that the SS concentration for a given streamflow is seasonally dependent; that is, for a specific streamflow there can be multiple predicted SS concentrations depending on the time of year. For the stations in this study where the combination of streamflow and seasonality terms explains a smaller portion of the overall variability, sediment supply to these systems is inherently more variable and complex. Those stations are not as well characterized by the transport equations and continued sediment monitoring through daily data collection (in place of transport equations) may be warranted depending on the monitoring objectives. The systems associated with those stations may have increased variability owing to streamflow conditions in tributary areas or owing to spatial variations in geology (erosivity) within contributing areas.

Consistent temporal patterns in the dataset may represent adjustments to multi-season processes within the basin. The trends in natural logarithm SS concentration at the Gunnison and Green River stations may be a continued response to channel adjustments that have been underway following completion of the Aspinall Storage Unit and the Flaming Gorge Reservoir, respectivley. Previous investigations have documented the effects of reductions of peak streamflow and reduced effective discharge on the balance of sediment storage and transport within these river systems. Relative occurrence of the trend-direction reversal (progression through time from upstream to downstream) is consistent with a basin response to an upstream alteration of flow regime and sediment supply. The Colorado and Gunnison River stations have no evidence of reaching equilibrium conditions in SS concentration. This indicates that larger time scales may be needed to reach stable conditions within this system or that the observed trends are in response to more temporally continuous anthropogenic changes or climatic effects within the basin.

Significant differences (p-value less than 0.05) in the slope and intercept between natural logarithm streamflow and natural logarithm SS concentration were tested for at all stations, based on classification as wet and dry years, and were determined at five of the six stations. No statistically significant differences were determined between any multi-year cycle comparison and may be indicative of the smaller dataset available for such comparisons. The natural logarithm SS concentration during wet years is higher than during dry years for the same streamflow (rising-limb) and is less strongly controlled (flatter slopes) by streamflow magnitude. Some of the differences determined between wet and dry years (rising-limb) may be affected by the sediment continuity between reaches and the size and location of reservoirs. Areas that are downstream from large main-stem reservoirs may not show as strong an influence between wet and dry years. This may be because the reservoirs act effectively as sediment traps, resulting in reduced downstream transport of sediment, thus lessening the effect that wet and dry years have on sediment-transport dynamics.

Incipient motion of streambed material (often occurring as bed-load transport) and the sorting of bed materials are important controls on channel form and habitat and are strongly related to the channel morphology and habitat conditions within these rivers. Comparison between boundary shear stresses of multiple streamflows and the relative mobility of bed material (d_{50}, median sediment-particle sizes) characterizes the effects of flow magnitude on mobilization of framework grains within the streambed. Observations at multiple cross sections within two reaches of the Gunnison River downstream from the Aspinall Storage Unit show ineffectual mobilization of most, if not all, areas within the surveyed cross sections. The largest surveyed streamflow exceeded bankfull conditions at the Gunnison River at Delta, Colorado, with a peak streamflow magnitude of 13,300 cubic feet per second (ft^3/s) (recurrence interval of 5 to 10 years). At the Gunnison River near Grand Junction, Colorado, the largest surveyed peak streamflow was 14,000 ft^3/s (recurrence interval of 5 to 10 years).

Observations at multiple cross sections within a study reach of the Green River downstream from Flaming Gorge Reservoir show a range of potential transport conditions. Streambed conditions within the study reach on the Green River can be characterized by two dominant-size distributions that vary spatially and temporally within the system. A gravel-dominated pavement layer was exposed intermittently within the channel with varying thicknesses of a sand veneer along the surface. Evaluation of transport characteristics of each of the two size distributions was used to produce the end members of a continuum that represent the characteristics of the channel. Incipient motion of specific particles within this area may occur along a continuum that is defined by the proportion of sand within a given gravel mixture. Incipient-motion analysis shows ineffectual mobilization of most, if not all, areas within the surveyed cross sections of the larger bed material including peak streamflows of as much as 19,000 ft^3/s (recurrence interval of 2.3 to 5 years). However, when the sand veneer is present at these cross sections, or where the portion of sand within the bed material exceeds 20–30 percent of the total, mobilization of the bed material will occur at most locations within the surveyed cross sections for peak streamflows of 9,000–19,000 ft^3/s (recurrence intervals ranging from 1 to 5 years) with mobilization of gravels possible in some areas. Further sediment-particle-size classification and determination of the portions of sands throughout the reach would be needed to quantify the portion of the gravel bed that is mobilized within the reach.

Application of the two-dimensional stream hydraulics and sediment-transport models provides enhanced capabilities for evaluations of dynamic reach-scale processes that affect habitat suitability. Understanding the processes that affect the sediment-transport characteristics, which are important to the maintenance of endangered fish spawning habitat, can be used to inform the flow-recommendations process that currently (2012) guides water management of Flaming Gorge Reservoir.

Evaluations of the processes controlling sediment deposition on the spawning habitat near the mid-channel bar are not limited to stream-transport conditions within the spawning-habitat reach. Considerations of sediment availability and net changes in sediment transport between upstream reaches and the spawning habitat are important. Sands are mobile throughout the main channel for all modeled streamflows (9,000–19,000 ft^3/s), but in areas upstream from the mid-channel bar (and spawning habitat) increases in streamflow tend to increase transport rates. Within the spawning habitat, increases in streamflow result in decreases in water-surface slope and varied responses to boundary shear stress. At larger streamflows (14,100–17,700 ft^3/s), sediment upstream from the mid-channel bar is transported in greater amounts and likely at greater rates than can be transported by the conditions at the spawning-habitat reach. This may exceed a threshold between the two areas resulting in a disequilibrium and net deposition of sands on the spawning habitat at higher streamflows (14,100–17,700 ft^3/s). Spawning habitat may be less suitable at these higher streamflows owing to deposition of sands on the spawning habitat under these conditions.

References Cited

American Geological Institute, 1976, Dictionary of geological terms (revised ed.): Garden City, N.Y., Anchor Books.

Andrews, E.D., 1978, Present and potential sediment yields in the Yampa River Basin, Colorado and Wyoming: U.S. Geological Survey Water-Resources Investigations Report 78–105, 33 p.

Andrews, E.D., 1980, Effective and bankfull discharges of streams in the Yampa River Basin, Colorado and Wyoming: Journal of Hydrology, v. 46, p. 311–330.

Andrews, E.D., 1983, Entrainment of gravel from naturally sorted riverbed material: Geological Society of America Bulletin, v. 94, p. 1225–1231.

Andrews, E.D., 1986, Downstream effects of Flaming Gorge Reservoir on the Green River, Colorado and Utah: Geological Society of America Bulletin, v. 97, p. 1012–1023.

Apodaca, L.E., Stephens, V.C., and Driver, N.E., 1996, What affects water quality in the Upper Colorado River Basin?: U.S. Geological Survey Fact Sheet 109–96, 4 p.

Asselman, N.E.M., 2000, Fitting and interpretation of sediment rating curves: Journal of Hydrology, v. 234, p. 228–248.

Barton, G.J., McDonald, R.R., Nelson, J.M., and Dinehart, R.L., 2005, Simulation of flow and sediment mobility using a multidimensional flow model for the white sturgeon critical-habitat reach, Kootenai River near Bonners Ferry, Idaho: U.S. Geological Survey Scientific Investigations Report 2005–5230, 54 p.

Benson, M.A., and Dalrymple, Tate, 1967, General field and office procedures for indirect discharge measurements: U.S. Geological Survey Techniques of Water-Resources Investigation, book 3, chap. CA1, 30 p.

Bowen, Z.H., Bovee, K.D., Waddle, T.J., Modde, T., and Kitcheyan, C., 2001, Habitat measurement and modeling in the Green and Yampa Rivers, Fort Collins, Colorado: U.S. Geological Survey Project Report to Natural Resource Preservation Program, December 2001, 181 p., accessed April 5, 2011, at *http://www.fort.usgs.gov/Products/Publications/4012/4012.pdf*.

Bradu, Dan, and Mundlak, Yair, 1970, Estimation in log-normal linear models: Journal of the American Statistical Association, v. 65, no. 329, p. 198–211.

Butler, D.L., and Leib, K.L., 2002, Characterization of selenium in the lower Gunnison River Basin, Colorado, 1998–2000: U.S. Geological Survey Water-Resources Investigations Report 2002–4151, 26 p.

Butler, D.L., Wright, W.G., and Stewart, K.C., 1996, Detailed study of selenium, alfalfa, and biota associated with irrigation drainage in the Uncompahgre Project Area and in the Grand Valley, West-Central Colorado, 1991–93: U.S. Geological Survey Water-Resources Investigations Report 96–4138, 136 p.

Carling, P.A., 1983, Threshold of coarse sediment transport in broad and narrow natural streams: Earth Surface and Landform Processes, v. 8, p. 1–18.

Cohn, T.A., 1995, Recent advances in statistical methods for the estimation of sediment and nutrient transport in rivers: Reviews in Geophysics, v. 33 (Supplement), p. 1117–1124.

Cohn, T.A., 2005, Estimating contaminant loads in rivers—An application of adjusted maximum likelihood to type 1 censored data: Water Resources Research, v. 41, no. 7, 13 p.

Cohn, T.A., Caulder, D.L., Gilroy, E.J., Zynjuk, L.D., and Summers, R.M., 1992, The validity of a simple statistical model for estimating fluvial constituent loads—An empirical study involving nutrient loads entering Chesapeake Bay: Water Resources Research, v. 28, no. 9, p. 2353–2363.

Cohn, T.A., Delong, L.L., Gilroy, E.J., Hirsh, R.M., and Wells, D.K., 1989, Estimating constituent loads: Water Resources Research, v. 25, no. 5, p. 937–942.

Chow, V.T., 1959, Open-channel hydraulics: New York, McGraw–Hill, 680 p.

Curtis, J.A., Flint, L.E., Alpers, C.N., Wright, S.A., and, Snyder, N.P., 2005, Use of sediment rating curves and optical backscatter data to characterize sediment transport in the Upper Yuba River Watershed, California, 2001–03: U.S. Geological Survey Scientific Investigations Report 2005–5246, 74 p.

Dalby, C.E., 2006, Use of regression and time-series methods to estimate a sediment budget for Nevada Creek Reservoir, Montana: Proceedings of the 2006 AWRA Summer Specialty Conference, Adaptive Management of Water Resources, June 26–28, 2006, Missoula, Mont., 10 p.

Deacon, J.R., Mize, S.V., and Spahr, N.E., 1999, Characterization of selected biological, chemical, and physical conditions at fixed sites in the Upper Colorado River Basin, Colorado, 1995–98: U.S. Geological Survey Water-Resources Investigations Report 99–4181, 71 p.

Edwards, T.K., and Glysson, G.D., 1999, Field methods for measurement of fluvial sediment (revised): U.S. Geological Survey Techniques of Water-Resources Investigation, book 3, chap. C2, 89 p.

Elliott, J.G., and Anders, S.P., 2005, Summary of sediment data from the Yampa River and Upper Green River Basins, Colorado and Utah, 1993–2002: U.S. Geological Survey Scientific Investigations Report 2004–5242, 35 p.

Elliott, J.G., and Hammack, L.A., 1999, Geomorphic and sedimentologic characteristics of alluvial reaches in the Black Canyon of the Gunnison National Monument, Colorado: U.S. Geological Survey Water-Resources Investigations Report 99–4082, 67 p.

Elliott, J.G., and Hammack, L.A., 2000, Entrainment of riparian gravel and cobbles in an alluvial reach of a regulated canyon river: Regulated Rivers—Research & Management, v. 16, no. 1, p. 37–50.

Elliott, J.G., and Parker, R.S., 1997, Altered streamflow and sediment entrainment in the Gunnison Gorge: Journal of the American Water Resources Association, v. 33, no. 5, p. 1041–1054.

Fahnestock, R.K., 1963, Morphology and hydrology of a glacial stream—White River, Mount Rainier, Washington: U.S. Geological Survey Professional Paper 422-A, 70 p.

Ferguson, R.I., 1986, River loads underestimated by rating curves: Water Resources Research, v. 22, no. 1, p. 74–76.

Flynn, K.M., Kirby, W.H., and Hummel, P.R., 2006, User's manual for program PeakFQ, Annual Flood Frequency Analysis Using Bulletin 17B Guidelines: U.S. Geological Survey Techniques and Methods book 4, chap. B4, 42 p.

Friedman, J.M., and Auble, G.T., 1999, Mortality of riparian box elder from sediment mobilization and extended inundation: Regulated Rivers—Research & Management, v. 15, no. 5, p. 463–476.

Glysson, G.D., 1987, Sediment-transport curves: U.S. Geological Survey Open-File Report 87–218, 47 p.

Graf, W.H., 1971, The hydraulics of sediment transport: New York, McGraw–Hill, 513 p.

Guy, Harold P., 1977, Laboratory theory and methods for sediment analysis: U.S. Geological Survey Techniques of Water-Resources Investigation, book 5, chap. C1, 59 p.

Hansen, David, and Bray, D.I., 1993, Single-stations estimates of suspended sediment loads using sediment rating curves: Canadian Journal of Civil Engineering, v. 20, p. 133–143.

Helsel, D.R., and Hirsch, R.M., 2002, Statistical methods in water resources: U.S. Geological Survey Techniques of Water-Resources Investigation, book 4, chap. A3, 523 p.

Horowitz, A.J., 2003, An evaluation of sediment rating curves for estimating suspended sediment concentrations for subsequent flux calculations: Hydrological Processes, v. 17, p. 3387–3409.

Julien, P.Y., 1998, Erosion and sedimentation: Cambridge, United Kingdom, The Cambridge University Press, 304 p.

Julien, P.Y., 2010, Erosion and sedimentation (2d ed.): Cambridge, United Kingdom, The Cambridge University Press, 371 p.

Knighton, David, 1998, Fluvial forms and processes: A new perspective: London, Great Britian, Hodder Education, 383 p.

Komar, P.D, 1987, Selective gravel entrainment and the empirical evaluation of flow competence: Sedimentology, v. 34, p. 1165–1176.

Kuhn, Gerhard, and Williams, C.A., 2004, Evaluation of streamflow losses along the Gunnison River from Whitewater downstream to the Redlands Canal Diversion Dam, near Grand Junction, Colorado, 1995–2003: U.S. Geological Survey Scientific Investigations Report 2004–5095, 22 p.

Lane, E.W., 1955, Design of stable channels: Transactions of the American Society of Civil Engineers, v. 120, p. 1234–1260.

Langley, D.E., 2006, Calculation of scour depth at the Parks Highway Bridge on the Tanana River at Nenana, Alaska, using one- and two-dimensional hydraulic models: U.S. Geological Survey Scientific Investigations Report 2006–5023, 19 p.

Likes, Jiri, 1980, Variance of the MVUE for lognormal variance: Technometrics, v. 22, no. 2, p. 253–258.

Lisle, T.E., Nelson, J.M., Pitlick, John, Madej, M.A., and Barkett, B.L., 2000, Variability of bed mobility in natural, gravel-bed channels and adjustments to sediment load at local and reach scales: Water Resources Research, v. 26, no. 12, p. 3743–3755.

McAda, C.W., 2003, Flow recommendations to benefit endangered fishes in the Colorado and Gunnison Rivers (Final Report): Grand Junction, Colo., Upper Colorado River Endangered Fish Recovery Program Project Number 54, 237 p., accessed April 5, 2011, at *http://www.usbr.gov/uc/wcao/rm/aspeis/pdfs/GunnCoFlowRec.pdf*.

McDonald, R.R., Bennett, J.P., and Nelson, J.M., 2001, The USGS Multi-Dimensional Surface Water Modeling System, *in* Proceedings of the Seventh Federal Interagency Sedimentation Conference, March 25–29, 2001, Reno, Nev.: p. I161–I-167, accessed April 5, 2011, at *http://pubs.usgs.gov/misc/FISC_1947-2006/pdf/1st-7thFISCs-CD/7thFISC/7Fisc-V1/7FISC1-1.pdf*.

McDonald, R.R., Nelson, J.M., Kinzel, P.J., and Conaway, J., 2006, Modeling surface-water flow and sediment mobility with the Multi-Dimensional Surface Water Modeling System (MD_SWMS): U.S. Geological Survey Fact Sheet 2005–3078, 6 p.

Milhous, R.T., 1982, Effect of sediment transport and flow regulation on the ecology of gravel-bed rivers, *in* Hey, R.D., Bathurst, J.C., and Thorne, C.R., eds., Gravel-bed rivers: Chichester, England, Wiley, p. 819–842.

National Atlas, 2010, Land cover 200 meter resolution, accessed January 29, 2010, at *http://nationalatlas.gov/mld/lancovi.html*.

Nelson, J.M., Bennett, J.P., and Wiele, S.M., 2003, Flow and sediment-transport modeling, *in* Kondolf, G.M., and Piegay, H., eds., Tools in fluvial geomorphology: Chichester, England, Wiley, p. 539–576.

Nelson, J.M., and McDonald, R.R., 1997, Mechanics and modeling of flow and bed evolution in lateral separation eddies: Bureau of Reclamation, Glen Canyon Environmental Studies Report, 69 p.

Osmundson, D.B., and Kaeding, L.R., 1991, Recommendations for flows in the 15-mile reach during October-June for maintenance and enhancement of endangered fish populations in the upper Colorado River—Final Report: Grand Junction, Colo., U.S. Fish and Wildlife Service, 82 p.

Osmundson, D.B, Nelson, P., Fenton, K., and Ryden, D.W., 1995, Relationships between flow and rare fish habitat in the 15-mile reach of the Upper Colorado River: Denver, Colo., U.S. Fish and Wildlife Service, Final Report to the Colorado River Recovery Implementation Program, 67 p.

Osterkamp, W.R., 2008, Annotated definitions of selected geomorphic terms and related terms of hydrology, sedimentology, soil science and ecology: U.S. Geological Survey Open-File Report 2008–1217, 49 p.

Ott, R.L., and Longnecker, M.T., 2001, An introduction to statistical methods and data analysis (5th ed.): Pacific Grove, Calif., Duxbury Press, 1,184 p.

Oxford University Press, 2010, Dictionary of science (6th ed.): New York.

Parker, Gary, Klingman, P.C., and McLean, D.G., 1982, Bedload and size distribution in paved gravel-bed streams: American Society of Civil Engineers, Journal of the Hydraulics Division 108(HY4), p. 544–571.

Pitlick, John, 2005, Channel monitoring to evaluate geomorphic changes on the main stem of the Colorado River—Final Report: Grand Junction, Colo., U.S. Fish and Wildlife Service, 54 p.

Pitlick, John, Van Steeter, M.M., Cress, R., Barkett, B., and Franseen, M., 1999, Geomorphology and hydrology of the Colorado and Gunnison Rivers and implications for habitats used by endangered fishes—Final Report: Grand Junction, Colo., U.S. Fish and Wildlife Service, 64 p.

Porterfield, George, 1972, Computation of fluvial-sediment discharge: U.S. Geological Survey Techniques of Water-Resources Investigation, book 3, chap. C3, 66 p.

Powell, D.M., and Ashworth, P.J., 1995, Spatial pattern of flow competence in bed load transport in a divided gravel bed river: Water Resources Research, v. 31, no. 3, p. 741–752.

PRISM Climate Group, 2008, Precipitation normals (1971–2000): Oregon State University, accessed January 29, 2010, at *http://prism.oregonstate.edu/*.

Rantz, S.E., and others, 1982, Measurement and computation of streamflow—Volume 1, Measurement of stage and discharge: U.S. Geological Survey Water Supply Paper 2175, v. 1, p. 1–284.

R Development Core Team, 2008, R—A language and environment for statistical computing: Vienna, Austria, R Foundation for Statistical Computing, ISBN 3-9000051-07-0, accessed April 5, 2011, at *http://www.r-project.org*.

Runkel, R.L., Crawford, C.G., and Cohn, T.A., 2004, Load estimator (LOADEST)—A fortran program for estimating constituent loads in streams and rivers: U.S. Geological Survey Techniques and Methods, book 4, chap. A5, 69 p.

Schruben, P.G., Arndt, R.E., and Bawlec, W.J., 1974, Geology of the conterminous United States at 1:2,5000,000—A digital representation of the 1974 P.B. King and H.M. Beikman map: U.S. Geological Survey Digital Data Series, DDS-11, on CD-ROM.

Seaber, P.R., Kapinos, F.P., and Knapp, G.L., 1987, Hydrologic unit maps: U.S. Geological Survey Water Supply Paper 2294, 63 p.

Shields, A., 1936, Application of similarity principles and turbulence research to bedload movement, translated from Anwendung der Aehnlichkeitsmechanik und der Turbulenzforschung auf die Geschiebewegung: Mitteilung Preussischen Versuchanstalt fur Wasserbau und Schiffbau, Berlin, No. 26, by W.P. Ott and J.C. van Uchelen, California Institute of Technology Hydrodynamics, Pasadena, Calif., Report No. 167, 43 p.

Sichingabula, H.M., 1998, Factors controlling variations in suspended sediment concentration for single-valued sediment rating curves: Hydrological Processes, v. 13, p. 1035–1050.

Teledyne RD Instruments, 2006, StreamPro ADCP operation manual: P/N 95B-6003-00, 116 p.

Thompson, D. M., Nelson, J.M., and Wohl, E.E., 1998, Interactions between pool geometry and hydraulics: Water Resources Research, v. 34, no. 12, p. 3673–3681.

Trimble Navigation Limited, 1998, Trimble Survey Controller field guide (ver 7.0): Sunnyvale, Calif.

U.S. Fish and Wildlife Service, 2011a, About the Upper Colorado River Endangered Fish Recovery Program: Upper Colorado River Endangered Fish Recovery Program, accessed July 21, 2011, at *http://www.coloradoriverrecovery.org/general-information/about.html.*

U.S. Fish and Wildlife Service, 2011b, Instream flow identification and protection: Upper Colorado River Endangered Fish Recovery Program, accessed July 21, 2011, at *http://www.coloradoriverrecovery.org/general-information/program-elements/instream-flow-protection.html*.

U.S. Geological Survey, 2007, Water-resources data for the United States—Water year 2007: U.S. Geological Survey Water-Data Report WDR-US-2007, accessed April 5, 2011, at *http://wdr.water.usgs.gov/wy2007/search.jsp*.

U.S. Geological Survey, 2011, National Water Information System: accessed April 5, 2011, at *http://waterdata.usgs.gov/co/nwis*.

U.S. Interagency Advisory Committee on Water Data, 1982, Guidelines for determining flood-flow frequency: Reston, Va., U.S. Geological Survey Office of Water Data Coordination, Bulletin 17B of the Hydrology Subcommittee, 183 p.

Valdez, R.A., and Muth, R.T., 2005, Ecology and conservation of native fishes in the Upper Colorado River Basin: American Fisheries Society Symposium, v. 45, p. 157–204.

Walling, D.E., 1977, Assessing the accuracy of suspended sediment rating curves for a small basin: Water Resources Research, v. 13, no. 3, p. 531–538.

Wick, E.J., 1997, Physical processes and habitat critical to the endangered razorback sucker on the Green River, Utah: Fort Collins, Colo., Colorado State University, Ph.D. Dissertation, 118 p.

Wilcock, Peter, Pitlick, John, and Cui, Yantao, 2009, Sediment transport primer—Estimating bed-material transport in gravel-bed rivers: Fort Collins, Colo., U.S. Department of Agriculture, Forest Service, Rocky Mountain Research Station, General Technical Report RMRS-GTR-226, 78 p.

Wilcock, P.R., 1992, Experimental investigation of the effect of mixture properties on transport dynamics, *in* Billi, P., Hey, R.D., Thorne, C.R., and Tacconi, P., eds., Dynamics of gravel-bed rivers: Chichester, England, Wiley, p. 109–139.

Wilcock, P.R., 1998, Two-fraction model of initial sediment motion in gravel-bed rivers: Science, v. 280, no. 5362, p. 410–412.

Wilcock, P.R., and McArdell, B.W., 1993, Surface-based fractional transport rates—Mobilization thresholds and partial transport of a sand-gravel sediment: Water Resources Research, v. 29, no. 4, p. 1297–1312.

Wilcox, D.C., 2007, Basic fluid mechanics (3d ed.): DCW Industries, Inc., 856 p.

Williams, C.A., Gerner, S.J., and Elliott, J.G., 2009, Summary of fluvial sediment collected at selected sites on the Gunnison River in Colorado and the Green and Duchesne Rivers in Utah, water years 2005–2008: U.S. Geological Survey Data Series 409, 123 p.

Williams, G.P., 1978, Bank-full discharge of rivers: Water Resources Research, v. 14, no 6, p. 1141–1154.

Wolman, M.G., 1954, A method of sampling coarse river-bed material: American Geophysical Union Transactions, v. 35, p. 951–956.

Yalin, M.S., 1977, Mechanics of sediment transport (2d ed.): Oxford, Pergamon Press, 298 p.

Publishing support provided by:
Denver Publishing Service Center

For more information concerning this publication, contact:
Director, USGS Colorado Water Science Center
Box 25046, Mail Stop 415
Denver, CO 80225
(303) 236-4882

Or visit the Colorado Water Science Center Web site at:
http://co.water.usgs.gov/
(303) 236-2000

Glossary

ADCP Acoustic Doppler Current Profiler; An instrument that obtains profiles of water velocity by transmitting sound of known frequency into the water and measuring the Doppler shift of reflections from scatterers, which are assumed to be passively moving with the water (Teledyne RD Instruments, 2006).

Antecedent conditions Preceding conditions or conditions found prior to an event (American Geological Institute, 1976, p. 16).

Boundary shear stress Density of water multiplied by the shear velocity squared or the shear stress along channel margin (streambed and banks) (Julien, 2010, p. 117).

Critical shear stress The lowest required value of shear stress applied by flowing water to initiate motion of individual particles of specified size (diameter) along the bed of a stream (Osterkamp, 2008, p. 14).

Coefficient of determination Proportional reduction in the squared error of the response variable (Ott and Longnecker, 2001, p. 646).

Decimal years A mathematical manipulation of a calendar date which represents the date as the sum of the year and decimal portion of the year.

d_{50} Particle diameter, as determined from a size-distribution analysis, in which 50 percent of the sediment sample, by weight or count, is finer than the total sample weight or count (Osterkamp, 2008, p. 42).

Effective discharge The increment of discharge that transports the largest fraction of the annual sediment load over a period of years (Andrews, 1980, p. 311).

Entrainment The process by flowing water or air, or by the mixing of water or air between opposing currents, of mobilizing sediment by picking up particles and transporting them in suspension, as suspended load, and along the channel or other surface of transfer, as bed (or traction) load; rates of hydrologic entrainment depend on stream power (the product of discharge and water-surface slope) and the sizes of the sediment particles (Osterkamp, 2008, p. 19).

Estimated residual variance The sum of the squared deviations (deviations of the measurements from their mean) divided by the sample size minus the degrees of freedom, or the number of estimated slope coefficients plus the intercept (simple linear regression has two degrees of freedom for the estimation of the intercept and one slope coefficient). This quantity is often thought of as the variance (measure of variability) around the regression line. Some textbooks refer to this as mean-square error (Ott and Longnecker, 2001, p. 546).

Fourier series An expansion of a periodic function as a series of trigonometric functions. In Fourier analysis, a function f(x), which is periodic in x, is represented as an infinite series of sine and cosine functions (Oxford University Press, 2010, p. 332).

Grain shear stress A component of shear stress that acts on individual sediment particles (Julien, 2010, p. 184).

Incipient motion The threshold condition when the hydrodynamic moments of force acting on a single particle balance the resisting moments of force (Julien, 2010, p. 146).

Natural logarithm Logarithm is the power to which a number, called the base, must be raised to give another number. Any number y can be written in the form of y = xn where n is then the logarithm to the base x of y, that is, n = logxy. Natural logarithms are to the base e = 2.71828 and are written logey or more commonly in this report lny (Oxford University Press, 2010, p. 486).

Rouse number Ratio of the sediment properties to the hydraulic characteristics of the flow (Julien, 2010, p. 231)

Seasonality Seasonal variations in evapotranspiration rates, precipitation volume, or type that results in seasonal variations in discharge. Many surface-water concentrations (sediment and water chemistry) show strong seasonal patterns due to the seasonal variations in discharge (Helsel and Hirsch, 2002, p. 337).

Sediment transport flux The rate at which a dry weight of sediment passes a section of a stream in a given time (Osterkamp, 2008, p. 39).

Shear stress That portion of stress acting tangentially as a tearing action (as opposed to that portion that acts as a normal stress) to a plane or surface; thus, a sediment particle resting on a channel bed is affected by the shear stress created by water moving on the bed (Osterkamp, 2008, p. 40).

Shields parameter Dimensionless shear stress, is defined as the ratio of fluid forces acting on a non-cohesive sediment particle and the submerged weight of the particle (Julien, 2010, p. 146).

Slope coefficient The expected change in the response variable for a unit increase in the explanatory variable associated with the slope coefficient when all other explanatory variables are held constant (Ott and Longnecker, 2001, p. 621). Examples of explanatory variables from this report include time, streamflow, and the seasonality variables.

Temporal trends Whether the probability distribution from which a series of observations of a random variable has arisen has changed over time (Helsel and Hirsch, 2002, p. 324).

Two-dimensional stream model Model that solves for flow properties for two-dimensional elements (downstream and cross-stream directions), rather than for entire cross-sections as does a one-dimensional model. This produces a spatially distributed grid of data points where the downstream and cross-stream components of the governing equations of open-channel flow are solved separately, which assumes that the flow components in the vertical direction are negligible (Wilcox, 2007, p. 555; Langley, 2005, p. 4).